

Evaluation and Improvement of Heat Treat Furnace Model

by

Radhakrishnan Purushothaman

A Dissertation

Submitted to the Faculty

of the

WORCESTER POLYTECHNIC INSTITUTE

in partial fulfillment of the requirements for the

Degree of Doctor of Philosophy

in

Manufacturing Engineering

June 2008

APPROVED:

Yiming (Kevin) Rong

Advisor and Associate Director of Manufacturing and Materials Engineering

ABSTRACT

Heat treating is the controlled heating and cooling of a material to achieve certain mechanical properties, such as hardness, strength and the reduction of residual stresses. Many heat treating processes require the precise control of temperature over the heating cycle. Typically, the energy used for process heating accounts for 2% to 15% of the total production cost. The objective of this work is to develop a comprehensive furnace model by improving the current Computerized Heat Treatment Planning System (CHT) based furnace model to accurately simulate the thermal profile of load inside the furnace. The research methodology was based on both experimental work and theoretical developments including modeling different types of heat treat furnaces. More than 50 experimental validations through case studies using the current CHT model were conducted in 11 manufacturing locations to identify the specific problems in the current model. An enhanced furnace model based on Knowledge Data Discovery (KDD) technique and neural network is developed and validated. The new model takes into account the real time furnace parameters determined from the experimental data and accounts for furnace deterioration and some of the complex gradients and heating patterns that exist inside the furnace that is difficult to model.

ACKNOWLEDGEMENT

This dissertation describes the research I conducted at the Worcester Polytechnic Institute (WPI) from 2003 after obtaining my Master of Science in Manufacturing Engineering also at WPI. This work would not have been possible without the support and help of many people here at WPI and from outside. First of all I want to thank my advisor Prof. Kevin Rong who is also my mentor. He was always available and provided me with guidance, advice, support and inspiration. I'm thankful to everyone in the Manufacturing and Materials Engineering Program here at WPI. And over the years I had opportunity to interact, share, learn and rejoice with almost everyone in the program. I would like to take this opportunity to thank Prof. Richard Sisson, Prof. Diran Apelian, Prof. Satya Shivkumar, Prof. Chris Brown, Ms. Sue Milkman, Ms. Carol Garofoli, and Ms. Maureen Plunket for the support over the years.

I would like to thank CAMLAB at WPI and the members for their help and support during my stay here in WPI and in CHT Software Development and also support in other projects. I would also like to thank Prof. Jinwu Kang, Tshingua University, Dr. Zhang Lei and Dr. Xubing Chen.

The unique opportunity to meet the leaders in the industry, learn and solve technical problems along with them at Center for Heat Treating Excellence (CHTE) was the most valuable learning experience for me at WPI. I would like to thank Metal Processing Institute, CHTE and CAT for this opportunity and support. I would also like to thank all the member companies who helped this research by providing the resources and facilities for this research. I like to thank American Heat Treating, CT; Sousa Corporation, CT; Bodycote (Waterbury, CT; Berlin, CT; South Windsor, CT and Worcester, MA); Caterpillar, Peoria, IL; Queen city steel, Cincinnati, OH; Ipsen, Rockford, IL; and . I would like to thank Mr. Max Heotzl of Surface Combustion who was an advisor and a champion for this project. Who spent numerous hours with the research group assisting us solve several technical challenges. I also thank Advanced Materials Technology Division at Caterpillar for the research internship opportunity at Peoria. I would like to thank my colleagues at Caterpillar Mr. Tom Clements, Mr. Randall Conklen, Mr. Harold Placher and Mr. Don Benckendorf for their help and insight for this project.

Last, but not least, I want to thank my fiancée Neha Chandra for all her love and support and my parents for their continuous encouragement.

TABLE OF CONTENTS

<u>CHAPTER</u>	<u>Page</u>
ABSTRACT	i
ACKNOWLEDGMENTS	ii
TABLE OF CONTENTS	iii
LIST OF FIGURES.....	vi
LIST OF TABLES.....	xi
CHAPTER 1 – Introduction	1
1.1 Objectives and scope of study	
1.2 Dissertation organization	
CHAPTER 2 – Background and literature review	4
2.1 Heat treating process overview	4
2.2 Types of furnaces	8
2.3 Furnace heat input.....	12
2.4 Furnace control.....	17
2.5 The need to model furnaces.....	18
2.6 Current research.....	19
2.7 Current software tools.....	19
2.8 The Summary	22
CHAPTER 3 – CHT furnace model.....	23
3.1 Overview of current CHT furnace model	23
3.2 Furnace Energy Balance Model	26
3.3 Heat Transfer model.....	35
3.4 Furnace temperature control.....	42
3.5 Summary	47
CHAPTER 4 – Furnace model analysis	48
4.1 Furnace model study	49
4.2 Problem identification in the current CHT furnace model	52
4.3 Summary & Conclusions	54

CHAPTER 5 – Improved furnace model	55
5.1 Introduction	55
5.2 The door open model.....	57
5.3 The furnace gradient model.....	69
5.4 Virtual load design and calibration	86
5.5 Conclusion	91
CHAPTER 6 – Knowledge data discovery based furnace model.....	92
6.1 Furnace calibration model	98
6.2 User defined item.....	105
6.3 KDD auto-learning classification model	105
6.4 Tuning model and procedure	108
6.5 Summary & Conclusions	108
CHAPTER 7 – Summary	109
REFERENCES	111
Appendix A – Case Studies.....	117

LIST OF FIGURES

Page No

2.1 - Energy Source Breakdown for Key Industrial Process Heating Applications	5
2.2 – A typical heat treatment cycle for a typical carburizing process with a reheat cycle	5
2.3 – Furnace Classification	8
2.4 - A schematic of Batch–Integral furnace	10
2.5 - Pusher-type and rotary-hearth heat-treat system	11
2.6 - Schematic of the indirect-fired section of the Inland Steel annealing furnace ..	12
2.7 - Variations in the furnace thermal efficiencies with load and refractory emissivities (left) & Variations in the load and roof surface temperatures with distance for varying load emissivities (right)	13
2.8 - Variations in the load and crown surface temperatures with distance for different radiant-tube designs in the furnace	14
2.9 - A typical pusher-type direct fired furnace: (a) longitudinal section, (b) transverse section	15
2.10 – (a) A comparison of model predictions for steel temperature and plant data at between-skid thermocouple locations. (b) A comparison of model predictions for steel temperature and plant data at over-skid thermocouple locations	16
2.11 – Comparison of the thermocouples with the thermal imaging system and the thermal gradient inside the box type furnace	17
2.12 - Impact of production rate on energy consumption per unit of production	18
2.13 - The load pattern for continuous belt in FurnXpert software	20
2.14 - The result illustration of FurnXpert software	21
3.1 - Key components of a process heating system	23
3.2 - Flowchart for temperature calculation of loaded furnace	25
3.3 - Schematic of a heat balance in a batch furnace.	27

3.4 - Schematic of a heat balance in a continuous furnace	31
3.5 - Factors that affect the furnace temperature.....	36
3.6 - Loads in a heat treating furnace	36
3.7 - The factors affecting the workpiece temperature.....	37
3.8 – The equivalent workpiece	39
3.9 - Schematic of the Temperature controller in a radiant tube type furnace	42
3.10 - On/Off & Proportional type controllers commonly used in furnaces	43
3.11 - Control feedback loop of PID control	45
5.1a - The thermal gradients inside a Continuous Pusher Furnace, experimental data from continuous datapak with 6 thermocouples.	55
5.1b - The thermal profile of the CHT calculated and measured workpiece temperature at 6 different locations in a Continuous Furnace	57
5.2 - Pusher type Continuous Furnace Model.....	58
5.3 - Door open/ Push sequence in a Continuous Furnace Model	60
5.4 - Empirical data used by a furnace manufacturer based on experiments and experience to predict the loss of atmosphere during the door operation in a continuous furnace.....	61
5.5 - The pressure in two different final zones in a Continuous Pusher Furnace.....	62
5.6 - The pressure variations as a function of different door operations events Holding Chamber (left) & Quench Chamber (right)	63
5.7 - The door open schedule based on the furnace layout represented in the time domain.....	64
5.8 - The screen shot of the furnace thermal profile computed by CHT-c/f software using the improved furnace model	66
5.9 - The comparison of the furnace thermal profile computed using improved furnace model and measurement results.	67

5.10 - The thermal gradients inside a batch type heat treating furnace	69
5.11 - Furnace temperature gradients and gradient variations in a fully loaded furnace over a period of 40 minutes in a Continuous Pusher type. Carburizing Furnace with a push cycle time of 16 minutes.	70
5.12a - Experimental setup showing the datapak and thermocouple locations inside the Pusher Furnace.	72
5.12b - The thermal gradients inside a Continuous Pusher Furnace, experimental data from continuous datapak with 6 thermocouples.	72
5.13 - Temperature gradient between the set point temperature and the work area (center of furnace) at 3 different zones and locations in a Rotary type Continuous Furnace.....	73
5.14 - Different burner patterns / schemes commonly used in the Pusher Type Continuous Furnaces.....	75
5.15 - Thermal gradients measured at different locations in a Pusher type Continuous Furnace with different zones marked.	76
5.16 – The top view of boost zone with thermocouple locations and the corresponding shim port locations for the data gathered.	77
5.17a – The measured temperature gradient pattern inside furnace – Holding Chamber (Burner layout – I)	78
5.17b – The measured temperature gradient pattern inside furnace (Burner layout – II)	78
5.17c – The measured temperature gradient pattern inside furnace (Burner layout –III)	79
5.18 – The gradient generated across the entire furnace using the static experiments.....	79
5.19 - Calculation domain of the represented in the space domain and	

the location of i,j,k and zone in a Continues Pusher Furnace.	80
5.20 - Experimental setup to determine	81
5.21 - Trilinear interpolation scheme to populate the thermal gradients from the experimental data	81
5.22 - Plot of workspace inside the furnace showing locations of the 6 points measured using the experiments and 3 interpolated points (P3, P4 & P5)	82
5.23(a) - Interpolated at point P3	83
5.23(b) - Interpolated at point P4	83
5.23(c) - Interpolated at point P5	83
5.23 - Plots of calculated at points P3, P4 & P5 (refer Fig.5.22 for locations)	83
5.24 - Comparison of the measured and improved CHT model calculated results in a Pusher type Continuous Furnace. (Top figure - calculated near top of the load, Bottom figure- calculated near bottom of load)	84
5.25 - Spalled and corroded furnace refractory walls.....	87
6.1 - Heat distribution and balance in the furnace.....	93
6.2 - Error of predicted furnace temperature (Illustration)	95
6.3 - Strategy logic of KDD furnace model solution	97
6.4 - Neural Network based calibration furnace model	99
6.5 - Two layer feed forward neural network.....	100
6.6 - CHT-bf Temperature prediction with KDD model	102
6.7 - Arrangement of workpieces in the basket and thermocouple placements.....	103
6.8 - Comparison of CHT-bf & KDD Temperature prediction with measured results.....	104
6.9 - Classification Illustration of loads with same As	106

LIST OF TABLES

3.1 - Energy terms and their definitions 26

3.2 - Heat loss for different furnace walls construction (Btu/hr-ft²) 29

3.3 - Combustion properties of typical commercial fuel gases 30

4.1 - List of case studies in different furnaces and locations 49

CHAPTER - 1

Introduction

Heat treating is the controlled heating and cooling of a material to achieve certain mechanical properties, such as hardness, strength, flexibility, and the reduction of residual stresses. Many heat treating processes require the precise control of temperature over the heating cycle. Heat treating is used extensively in metals production, and in the tempering and annealing of glass and ceramics products. Typically, the energy used for process heating accounts for 2% to 15% of the total production cost. The US industrial sector consumes 32.6 quadrillion Btu per year, over 1/3 of the total energy use in the US with a value of \$100 billion. Of that amount, 60% is consumed in fossil-fired systems such as furnaces, boilers, and lehrs, with varying energy losses. Thermal efficiencies can range from over 90% for condensing boilers to under 10% for small, batch operated, high temperature furnaces like heat treat furnaces [1]. In order to improve the energy efficiency and optimize the load throughput, it's vital to have numerical modeling capability to accurately simulate the heat treatment processes. Currently there are plenty of commercial solutions for modeling the heat transfer and material properties for a single workpiece but none of them have a furnace model for simulating the thermal profile of the entire load. A comprehensive furnace model for different kinds of furnaces is crucial to accurately simulate the temperature of the load.

1.1 Objectives and scope of study

The objective of this work is to develop a comprehensive furnace model by improving the current Computerized Heat Treatment Planning System (CHT) based furnace model. The research methodology was based on both experimental work and theoretical developments including modeling different types of heat treat furnaces. More than 40 experimental validations through case studies using the current CHT model were conducted in 11 manufacturing locations to identify the specific problems in the current model. From the experimental data and knowledge from the experiments several improvements to the current furnace model are implemented and a new furnace model

based on Knowledge Data Discovery (KDD) technique is also developed and validated. A furnace tuning and calibration procedure is developed based on a virtual load design.

The main improvements include modeling thermal gradients present inside the furnace and accounting for heat loss arising due to the furnace door openings during loading and unloading of the furnaces. Also a virtual load is design procedure is developed for different loads and the reverse calculation for determining the furnace emissivity that accounts the wear and tear. Several constants are added to the current heat balance equation and they are determined using the experimental data and neural network. This KDD based model is used to optimize the load pattern using maximum entropy.

It is possible to accurately predict the thermal profile of the load inside a furnace using the improved furnace model. The new model enables us to improve the furnace efficiency by maximizing the load throughputs and save energy by accurately predicting the cycle time. The new model takes into account all the real time furnace parameters determined from the experimental data and accounts for some of the complex gradients and heating patterns that exist inside the furnace that is difficult to model. Based on experimental results the model is trained using neural network and the new improved KDD based model is validated with case studies at different production facilities.

1.2 Dissertation organization

This dissertation is organized into six parts:

Part I - (Chapter 1 – 2) Introduction and Review

Chapter 1. Introduction (this chapter). Introduces the background, specific problem, objectives, solution and results of this research.

Chapter 2. Literature Review. Gives a review of earlier studies related to the furnace models and softwares.

Part II - (Chapter 3) Current Furnace Model & (Chapter 4 & Appendix - A) Furnace Model Analysis

The current model furnace model for both batch and continuous furnaces are studied in detail. It studies the different heat terms in the furnace model and how they are calculated. A detailed analysis is conducted through experimental case studies at different industries (Appendix –A) The furnace model analysis is done to identify the areas for improvement to the current model.

Part IV- (Chapter 5) Furnace model improvements

The furnace model improvements are divided into three sub chapters: Door open model – describes the addition of the heat loss term to the CHT model, Thermal Gradients – describes the approach the model to incorporate the thermal gradients present in the model. Virtual load – describes the virtual load calibration procedure.

Part V (Chapter 6) Knowledge Data Discovery (KDD) based furnace model

A new intelligent furnace model based on Knowledge data discovery is proposed and the model is validated by using industrial case studies

Part VI - (Chapter 7) Summary

The different improvements to the current model and their advantages and limitations are studied in detail.

Appendix A. Analysis of experimental case studies

CHAPTER – 2

Background and literature review

This chapter discusses the various researches done in modeling the heat treat furnaces and different software models available for performing the heat treat thermal simulation and their features and limitations.

2.1 Heat treating process overview

Heat Treatment may be defined as heating and cooling operations applied to metals and alloys in solid state so as to obtain the desired properties. Heat treatment is sometimes done inadvertently due to manufacturing processes that either heat or cool the metal such as welding or forming. Heat treatment is often associated with increasing the strength of material, but it can also be used to refine the grain size, relieve internal stress, to improve machinability and formability and to restore ductility after a cold working process. Some of the objectives of heat treatment are summarized as follows:

- Improvement in ductility
- Relieving internal stresses
- Refinement of grain size
- Increasing hardness or tensile strength
- Improvement in machinability
- Alteration in magnetic properties
- Modification of electrical conductivity
- Improvement in toughness

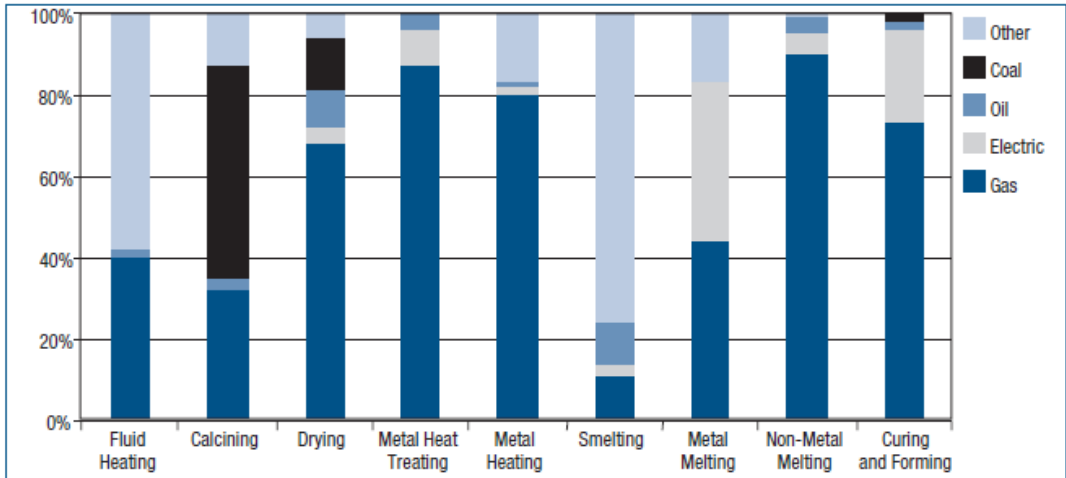


Figure 2.1 - Energy Source Breakdown for Key Industrial Process Heating Applications [2]

The energy source for the heat treating industry is more than 80% from gas. Fig. 2.1 illustrates how fuels are used in several process heating applications. The costs of different fuel types can vary widely, which has a significant impact on the payback period of efficiency improvement projects.

A heated workpiece in a heat-treating furnace will undergo a given thermal schedule, typically, a heating — soaking — cooling cycle. (Fig. 2.2)

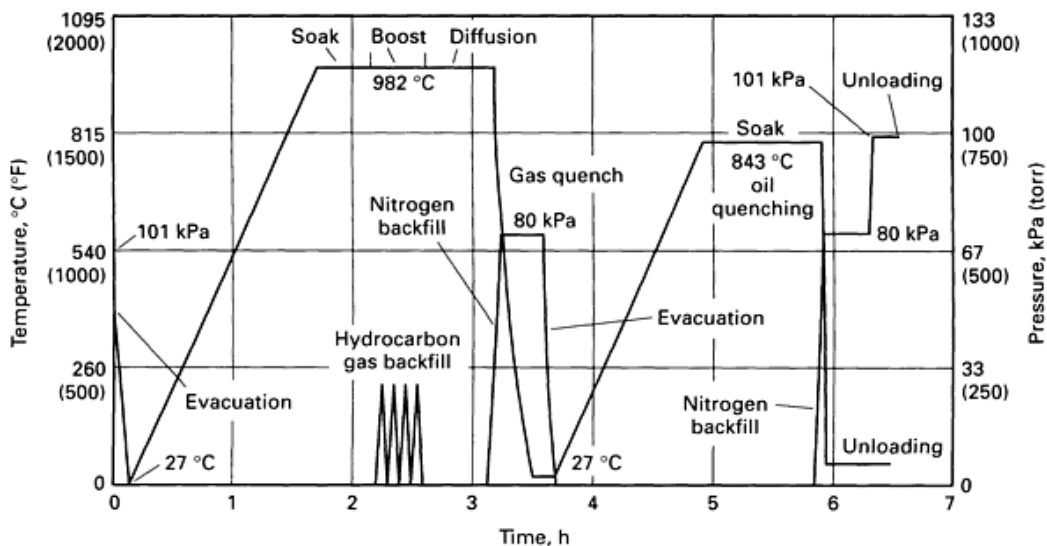


Figure 2.2 – A typical heat treatment cycle for a typical carburizing process with a reheat cycle [3]

2.1.1 Basic requirements of heat treatment process

The main requirement of the heat treatment process is the accurate control of the temperature profile. And also soaking/holding at specified temperature for obtaining uniform cross section temperature across load and workpiece is another basic requirement of the heat treatment process. In processes like carburizing once the load reaches the soaking temperature the enriching hydrocarbon gas is added to the furnace and the load is held at the carburizing temperature for the carbon diffusion to occur until the required case depth is achieved. And the cooling cycle is determined by the required microstructure desired. And the cooling can be either liquid or gas cooling depending on the furnace.

2.1.2 Basic requirements of furnaces

The main requirement of the furnaces in the heat treatment process is to provide the necessary heat input for the load/workpiece. The furnace also requires a control system to control the temperature in the furnace accurately. Also a uniform temperature distribution is desired inside the furnace. Apart from the temperature controller there are also several atmosphere controllers and material handling controllers required based on the type of furnaces.

2.1.3 Heat treatment processes

There are several different types of heat treatment processes. By controlling the soak temperature and the cool down rate of the steel, we can determine the process to be accomplished. Those processes include,

- Annealing
- Normalizing
- Stress relieving
- Hardening
- Tempering

Annealing

Annealing is the process of heating the steel to a particular temperature in the austenite region and cooling down the steel very slowly. There are many derivatives of the annealing process, but generally the process is a slow cool process.

Another derivative of the annealing process is known as sub-critical anneal. This process involves soaking at a temperature below the lower transformation line, in the region of 1,200F to 1,300F, until the steel has equalized across its cross-section in temperature, followed by a slow cool. Slow cooling can mean a cooling rate between 5F per hour up to 50F per hour.

Normalizing

Normalizing is a process that makes the grain size normal. This process is usually carried out after forging, extrusion, drawing or heavy bending operations. When steel is heated to elevated temperatures to complete the above operations, the grain of the steel will grow. In other words, the steel experiences a phenomenon called "grain growth." This leaves the steel with a very coarse and erratic grain structure. Furthermore, when the steel is mechanically deformed by the aforementioned operations, the grain becomes elongated.

There are mechanical property changes that take place as a result of normalizing - inasmuch as the normalized steel is soft, but not as soft as a fully annealed steel. Its grain structure is not as coarse as an annealed steel, simply because the cooling rate is faster than that of annealing. Usually the steel is cooled in still air and free from air drafts. The process temperature is virtually the same as for annealing, but the results are different due to the cooling rate.

Stress relieving

Stress relieving is an intermediate heat treatment procedure to reduce induced residual stresses as a result of machining, fabrication and welding. The application of heat to the steel during its machining or fabrication will assist in removing residual stresses that will,

unless addressed during the manufacturing by stress relieving, manifest themselves at the final heat treatment procedure.

It is a relatively low temperature operation that is done in the ferrite region, which means that there is no phase change in the steel, only the reduction of residual stresses. The temperature region is usually between 800F to 1,300F. However, the higher that one goes in temperature, the greater the risk of surface oxidation there is. It is generally better to keep to the lower temperatures, particularly if the steel is a "pre-hard" steel. The hardness will be reduced if the stress relieve temperature exceeds the tempering temperature of the steel.

2.2 Types of furnaces

The furnaces used in the heat treating process can be classified in several different ways. The most popular classification method is shown in Fig. 2.3.

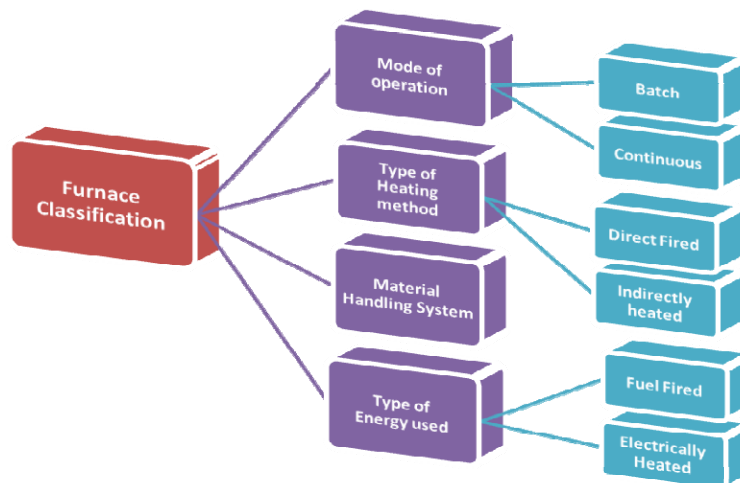


Figure 2.3 – Furnace Classification

2.2.1 Classification based on heating method

One of the popular methods of classifying the furnaces is based upon the heating or energy input method. And it can be divided into combustion based heating and electric heating methods.

Combustion-based (Fuel-based) Process Heating

Heat is generated by the combustion of solid, liquid, or gaseous fuels, and transferred either directly or indirectly to the material. Common fuel types are fossil fuels (e.g. oil, natural gas, coal) The combustion gases can be either in contact with the material (direct heating), or be confined and thus be separated from the material (indirect heating; e.g., radiant burner tube, radiant panel, muffle).

Electric process heating (Electrotechnologies)

Electric currents or electromagnetic fields are used to heat the material. Direct heating methods generate heat within the work piece, by either (1) passing an electrical current through the material, (2) inducing an electrical current (“eddy current”) into the material, or (3) by exciting atoms/molecules within the material with electromagnetic radiation (e.g. microwave). Indirect heating methods use one of these three methods to heat a heating element or susceptor, and transfer the heat either by conduction, convection, radiation or a combination of these to the work piece.

2.2.2 Classification based on mode of operation

Another classification of the furnaces is based on the mode of operation. The classification is either a batch type operation or a continuous operation.

Batch furnaces

The basic batch furnace normally consists of an insulated chamber with an external reinforced steel shell, a heating system for the chamber, and one or more access doors to the heated chamber. Standard batch furnaces such as box, bell, elevator, car-bottom, and pit types are most commonly used when a wide variety of heat-hold-cool temperature cycles are required. Batch furnaces are normally used to heat treat low volumes of parts (in terms of weight per hour). Batch furnaces are also used to carburize parts that require heavy case depths and long cycle times. These furnaces are either electrically heated or gas/oil fired. The gas/oil fired furnaces can further be classified as direct fired and in-direct fired (radiant tube burners)

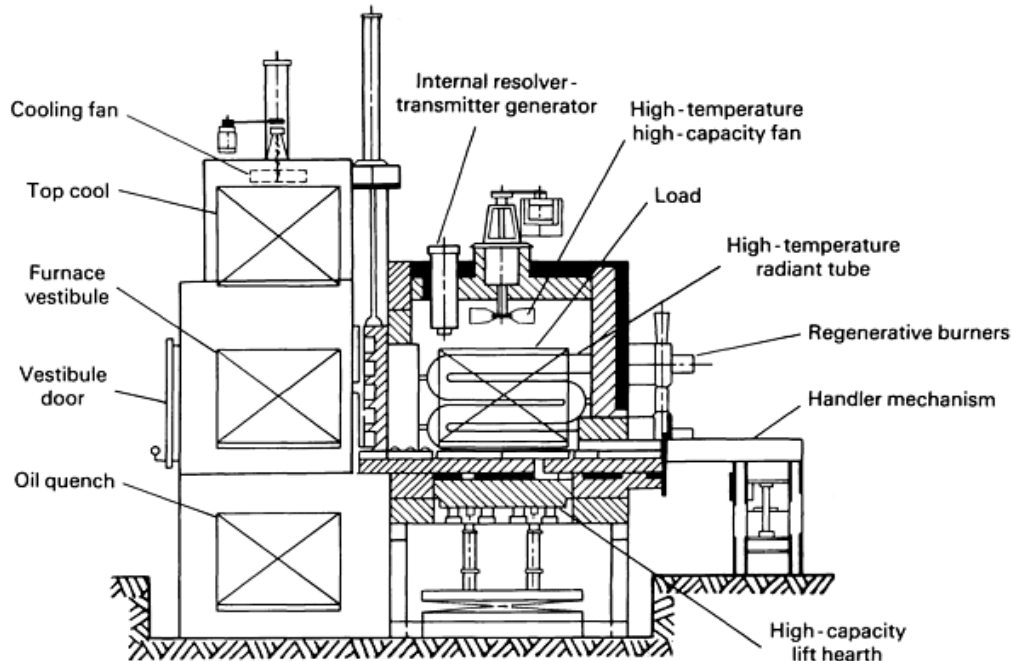


Figure 2.4 - A schematic of Batch-Integral furnace [5]

Vacuum furnaces (Type of batch furnace)

In most heat-treating processes, when materials are heated, they react with atmospheric gases. If this reaction is undesirable, the work must be heated in the presence of some gas or gas mixture other than normal air. This is done in normal atmosphere furnace processing. The gas or gas mixture may be varied to cause desirable reactions with the material being processed or it may be adjusted so that no reactions occur. At different temperatures, different reactions may occur with the work and furnace atmosphere. In most atmosphere furnaces it is not possible to change the atmosphere composition rapidly enough for optimum reactions or to control the atmosphere composition with the degree of precision required for some heat-treating processes. Vacuum furnaces allow gas changes to be made quite rapidly because they contain gases of low weight. Vacuum furnace technology removes most of the components associated with normal atmospheric air before and during the heating of the work. Fig. 2.2 shows a typical vacuum carburizing cycle with time and pressure vs time plot.

Continuous furnaces

Continuous furnaces consist of the same basic components as batch furnaces: an insulated chamber, heating system, and access doors. In continuous furnaces, however, the furnaces operate in uninterrupted cycles as the workpieces move through them. Consequently, continuous furnaces are readily adaptable to automation and thus are generally used for high-volume work. Another advantage of continuous furnaces is the precise repetition of time-temperature cycles, which are a function of the rate of travel through the various furnace zones. A multi chamber pusher-type continuous carburizing furnace system is widely used in industry where the heating, carburizing, and diffusion portions of the cycle are separated.

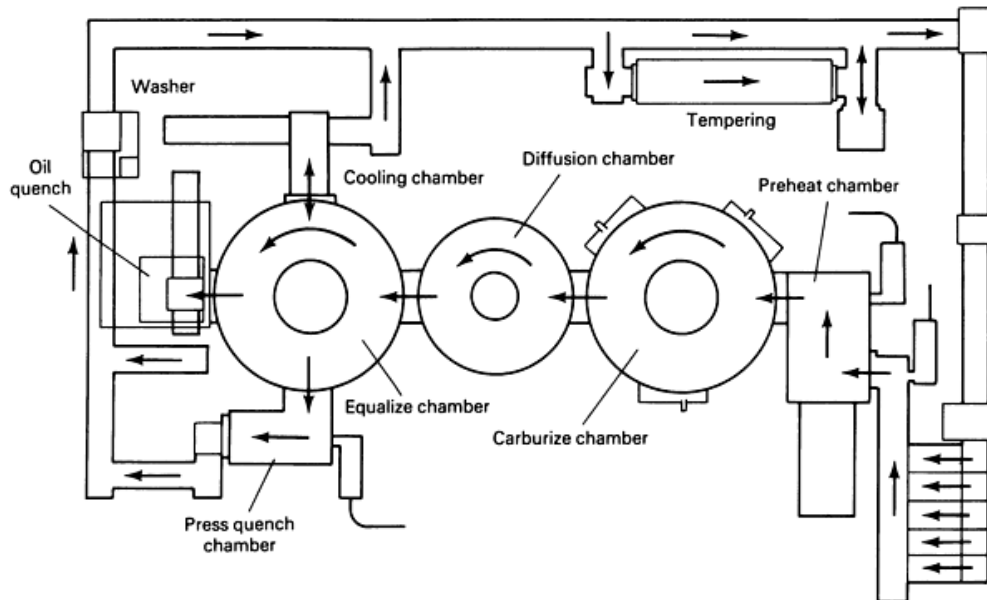


Figure 2.5 - Pusher-type and rotary-hearth heat-treat system [5]

2.2.3 Classification based on material handling system

The selection of the material handling system depends on the properties of the material, the heating method employed, the preferred mode of operation (continuous, batch) and the type of energy used. An important characteristic of process heating equipment is how the load is moved in, handled, and moved out of the system. Several important types of material handling systems are,

- Conveyor, Belts, Buckets, Rollers
- Rotary Hearth Furnaces

- Walking Beam Furnaces
- Pusher Type Furnaces
- Car Bottom Furnaces
- Continuous Strip Furnaces

2.3 Furnace heat input

2.3.1 Indirect fired (Radiant-tube) furnaces

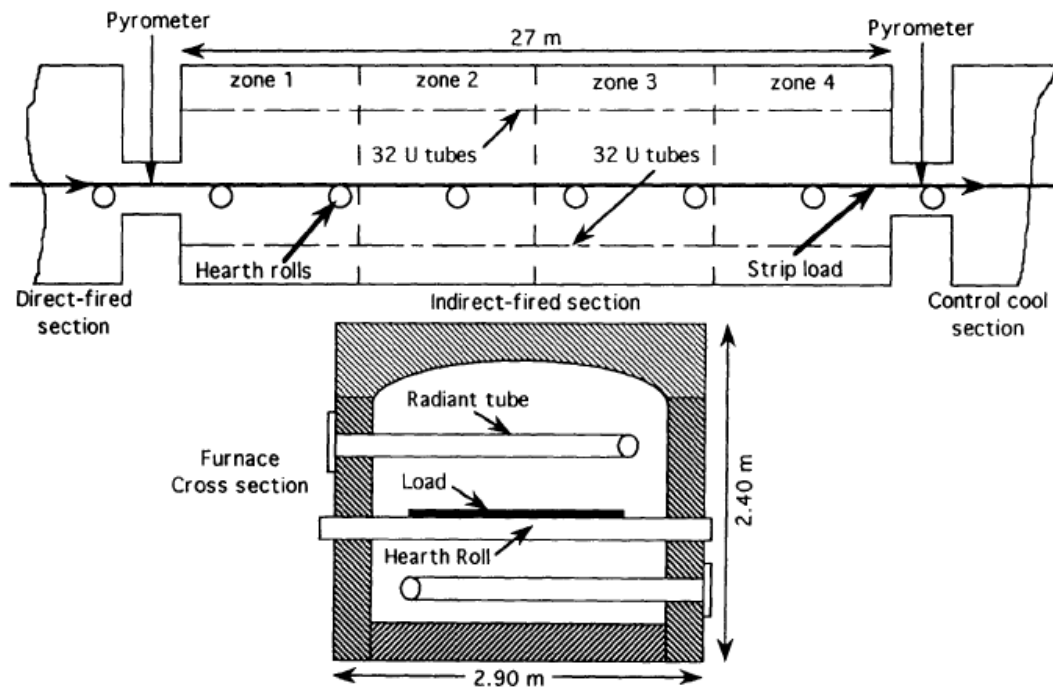


Figure 2.6 - Schematic of the indirect-fired section of the *Inland Steel annealing furnace* [8]

‘A Thermal System Model for a Radiant-Tube Continuous Reheating Furnace’ discusses about a thermal system mathematical model developed for a gas-fired radiant-tube continuous reheating furnace (Fig. 2.6). The mathematical model of the furnace integrates submodels for combustion and heat transfer within the radiant tube with models for the furnace enclosure. The transport processes occurring in the radiant tube are treated using a one-dimensional scheme, and the radiation exchange between the load, the radiant-tube surfaces, and the furnace refractories are analyzed using the radiosity

method. The continuous furnace operation is simulated under steady-state conditions. The scope and flexibility of the model are assessed by performing parametric studies using furnace geometry, material properties, and operating conditions as input parameters in the model and predicting the thermal performance of the furnace. The various parameters studied include the effects of load and refractory emissivities (Fig. 2.7), load velocities, properties of the stock material [8].

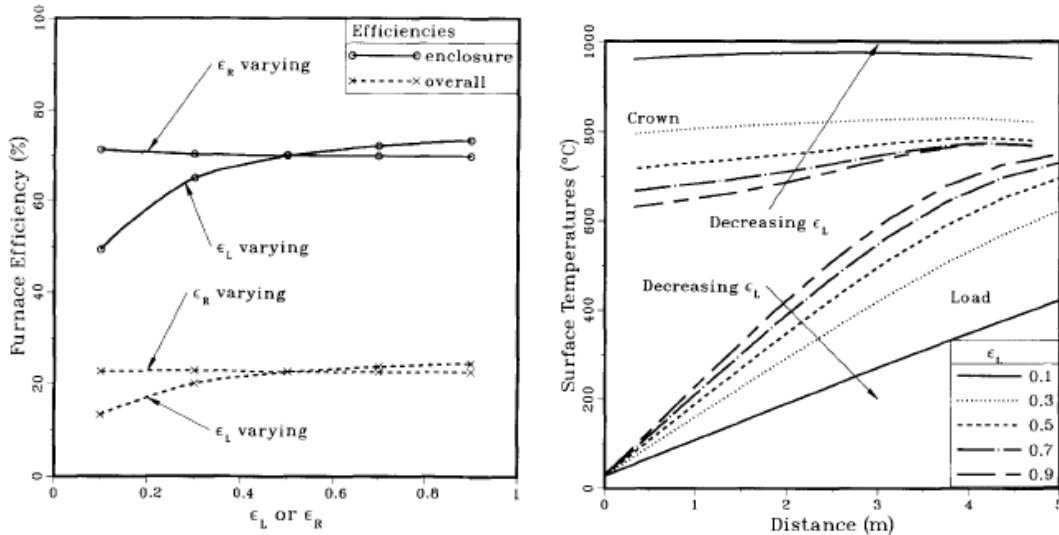


Figure 2.7 - Variations in the furnace thermal efficiencies with load and refractory emissivities (left) & Variations in the load and roof surface temperatures with distance for varying load emissivities (right)[8]

Another study is conducted to access the different types of radiant tube designs. Fig 2.8 which shows the variations in the load surface temperature for the same net fuel firing rate in the radiant tubes, indicates that the load surface temperatures are the highest for the W-type tube design, followed by the U-type and then the straight-through tubes. The lower load surface temperatures for the straight-through tubes in the furnace is due to the incomplete burning of fuel in the radiant tubes. A considerable amount of energy is lost in the form of unburned fuel at the exhaust of the straight-through tube. However, in the U-type and W-type tubes, further burning of the unburned fuel from the first branch takes place, resulting in a higher average tube wall temperature in the successive branches of the tube [8].

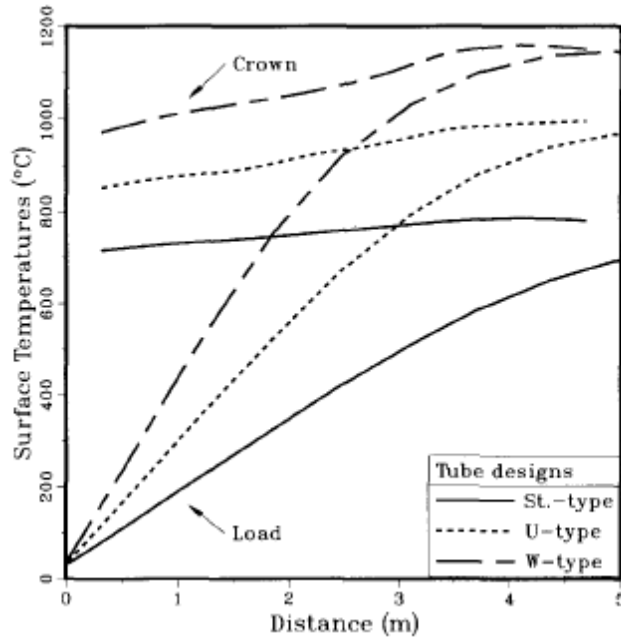
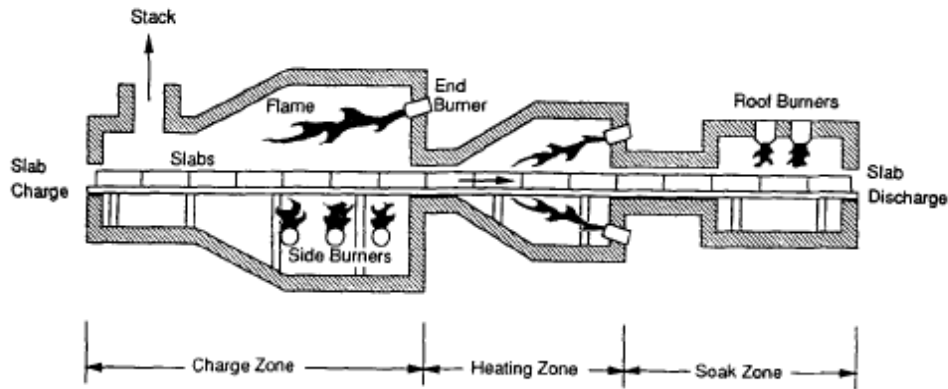


Figure 2.8 - Variations in the load and crown surface temperatures with distance for different radiant-tube designs in the furnace[8]

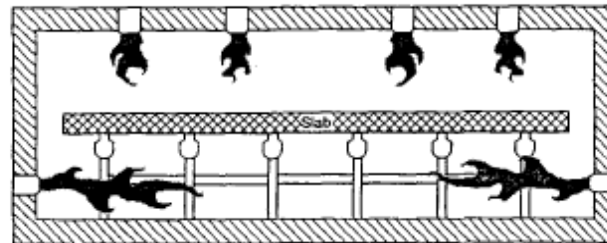
2.3.2 Direct fired furnaces

‘The Development, Verification, and Application of a Steady-State Thermal Model for the Pusher-Type Reheat Furnace’ outlines the development of a steady-state thermal model for the pusher-type steel reheating furnace. (Fig.2.9) Commonly encountered energy consumption are analyzed. The objective of the work is to provide a means by problems with this furnace type like skidmark generation, scale formation, and high which furnace users might assess the effectiveness of changes to current operating practice, proposed furnace modifications, or new furnace designs in controlling these difficulties. The model is verified using data obtained in plant trials on several 32-m furnace reheating slabs, and model predictions for steel temperatures at six locations

within the steel are compared with the experimental results. The inclusion of a hearth in



(a) Longitudinal section



(b) Transverse section

Figure 2.9 - A typical pusher-type direct fired furnace: (a) longitudinal section, (b) transverse section [9].

the furnace soak zone was found to impose the least severe skidmark on the product, reducing the temperature variation over the bottom face from the level of 130 ~ incurred by the best of the soak zone skid configurations examined, to the level of 85 ~ The results suggest that, in the absence of a hearth section, the use of a well-insulated, cold-rider skid system over the majority of the furnace length, followed by a single offset of all skids occurring at the transition to a short section of hot-rider skids near the furnace discharge, is sufficient to suppress the final skidmark to a level very close to the minimum achievable with that particular skid design. When assessed on the basis of minimizing both the final skidmark and the energy loss to the skid system, this configuration was found to be the best of the skid layouts examined

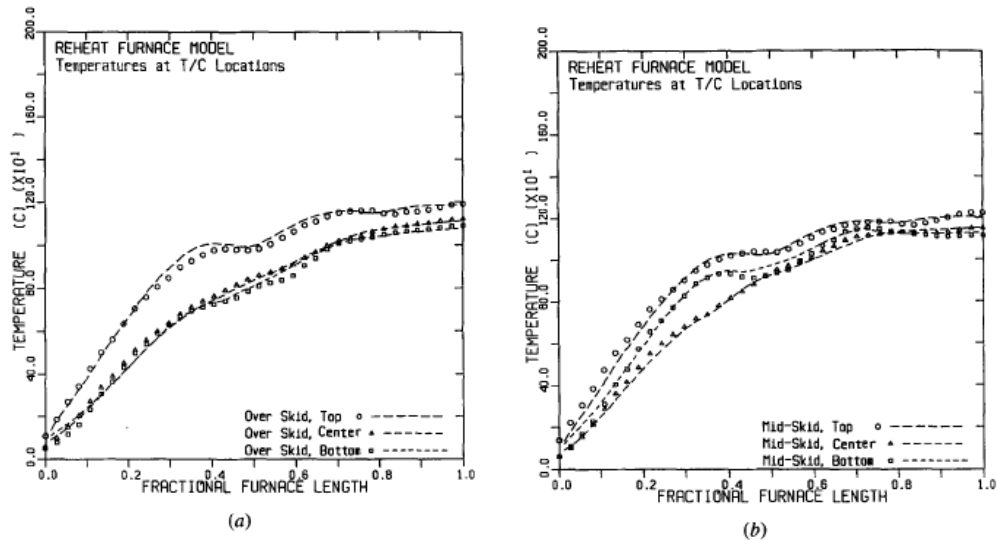


Figure 2.10 – (a) A comparison of model predictions for steel temperature and plant data at between-skid thermocouple locations.
 (b) A comparison of model predictions for steel temperature and plant data at over-skid thermocouple locations[9].

‘Modeling and Parametric Studies of Heat Transfer in a Direct-Fired Continuous Reheating Furnace’ – is a mathematical system model of a direct-fired continuous reheating furnace. The furnace is modeled as several well-stirred gas zones with one-dimensional (1-D) heat conduction in the refractory walls and two-dimensional heat transfer in the load. The convective heat-transfer rate to the load and refractory surfaces are calculated using existing correlations from the literature. Radiative heat exchange within the furnace is calculated using Hottel's zone method by considering the radiant energy exchange between the load, the combustion gases, and the refractories. The nongray characteristics of the combustion gases are considered by using a four-gray gas model to treat the mixture as a radiatively participating medium. The parametric investigations included in this paper study the effects of the load and refractory emissivities and the height of the combustion space on the thermal performance of the furnace.

2.4 Furnace control

Thermal imaging control of furnaces and combustors developed by Gas Technology Institute [6]. The objective of this project is to demonstrate and bring to commercial readiness a near infrared thermal imaging control system for high temperature furnaces and combustors.

The concept used in this project is to provide improved control to high temperature furnaces using a near-IR thermal imaging control system. Initial stages of the Thermal Imaging sensor hardware development were conducted by testing on a laboratory electric furnace. The complete system was then tested on a GTI heat treat furnace. A state-of-the-art control system was installed and accepted input for control from the thermal imaging system.

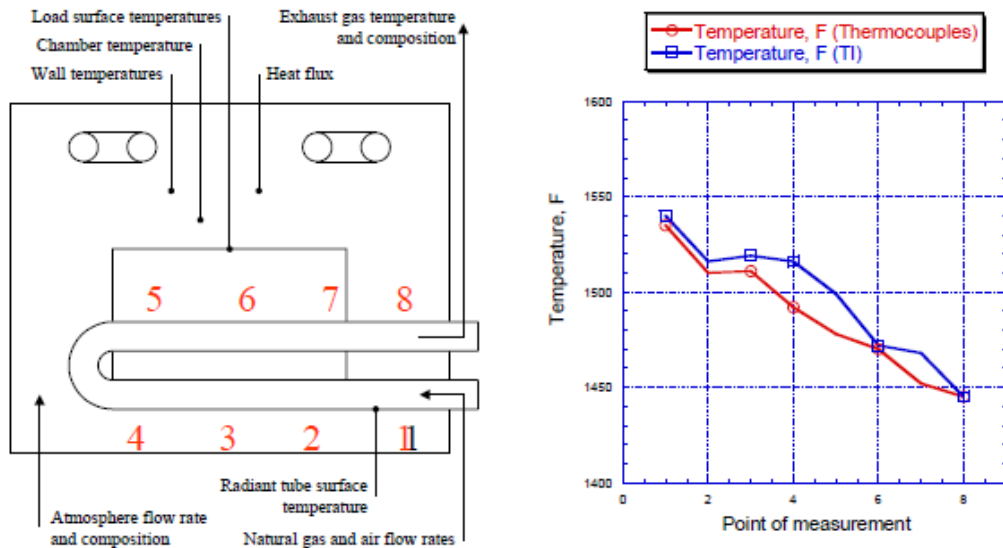


Figure 2.11 – Comparison of the thermocouples with the thermal imaging system and the thermal gradient inside the box type furnace [6]

The project strategy is to input the thermal imaging system data into a set of control system algorithms that would give secondary control instructions to burners (air-fuel ratios, etc.) for tuning control.

2.5 The need to model furnaces

A commonly overlooked factor in energy efficiency is scheduling and loading of the furnace. “Loading” refers to the amount of material processed through the furnace in a given period of time. It can have a significant effect on the furnace's energy consumption when measured as energy used per unit of production (Btu/lb). Certain furnace losses (wall, storage, conveyor and radiation) are essentially constant regardless of production volume; therefore, at reduced throughputs, each unit of production has to carry a higher burden of these fixed losses. Flue gas losses, on the other hand, are variable and tend to increase gradually with production volume. If the furnace is pushed past its design rating, flue gas losses increase more rapidly, because the furnace must be operated at a higher temperature than normal to keep up with production. Total energy consumption per unit of production will follow the curve in Fig. 2.12, which shows the lowest at 100% of furnace capacity and progressively higher the farther throughputs deviate from 100%. Furnace efficiency varies inversely with the total energy consumption. The lesson here is that furnace operating schedules and load sizes should be selected to keep the furnace operating as near to 100% capacity as possible. Idle and partially loaded furnaces are less efficient

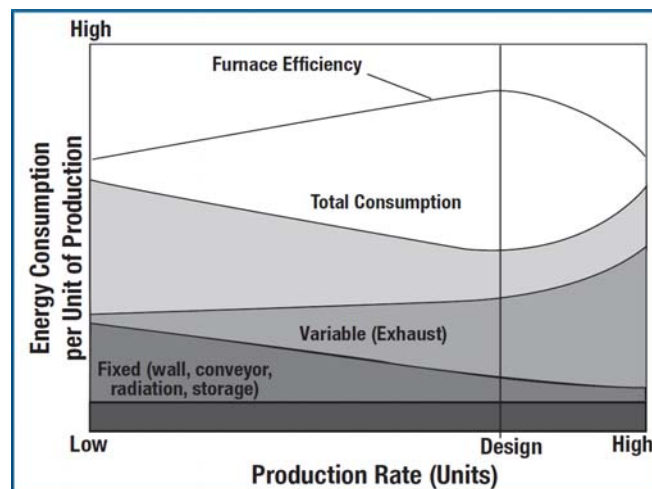


Figure 2.12 - *Impact of production rate on energy consumption per unit of production* [2].

In order to achieve maximum efficiency it is required to design the furnace part load to the maximum furnace capacity. A numerical tool with a furnace model helps to achieve this goal. Also another important quality metric in the heat treatment processes is soak time (amount of time a load stays at a given temperature) A furnace model with workpiece thermal profile prediction can accurately predict the time required to reach the process temperature and the soak time. So the process can be accurately designed eliminating guesses and removing conservative recipes.

2.6 Current research

The current research to model the heat treatment process is focused mostly on a single part model using the commercially available FEM software tools. The topics discussed in chapters 2.3.1 and 2.3.2 are the research conducted by E.S Chapman et al and it focuses on using the FEM method with temperature boundary conditions [9].

Limitations

The major limitations of the single part model and the FEM based model are the determination of the temperature boundary condition. The temperature boundary condition is an important input for the model and the results are dependent on the accuracy of the boundary conditions. Every furnace is unique in the heat treatment industry so it's difficult to determine the boundary condition without a comprehensive furnace model. Currently none of the research is focused on the furnace model. Also FEM based approach is a computation intensive and consumes several hours for calculating results.

2.7 Current software tools

Process Heating Assessment and Survey Tool (PHAST) – is a software tool developed at DOE for identifying methods to improve thermal efficiency of heating equipment. This tool helps industrial users survey process heating equipment that consumes fuel, steam, or electricity, and identifies the most energy-intensive equipment. Use the tool to compare

performance of equipment under various operating conditions and test "what-if" scenarios. PHAST constructs a detailed heat balance for selected pieces of process heating equipment. The process considers all areas of the equipment in which energy is used, lost, or wasted. Results of the heat balance pinpoint areas of the equipment in which energy is wasted or used unproductively.

FurnXpert program is developed to optimize furnace design and operation. The program mainly focuses on the heat balance of the furnace. The load pattern is just aligned load pattern with one layer and it cannot deal with the condition of workpieces loaded in the fixtures. While, in this condition the workpieces inside the fixture are heated by adjacent workpieces, not directly by furnace. Figure 2.13 shows an interface of load pattern specifications in FurnXpert. The result curves are shown in Figure 2.14

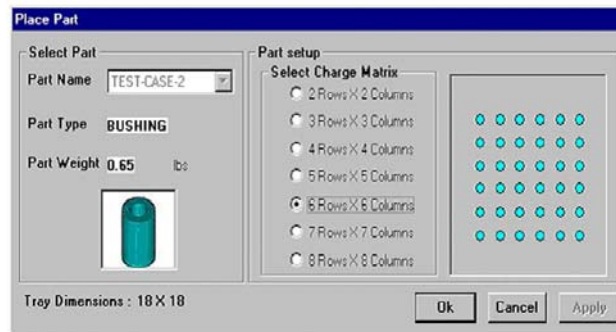


Figure 2.13 - The load pattern for continuous belt in FurnXpert software [10]

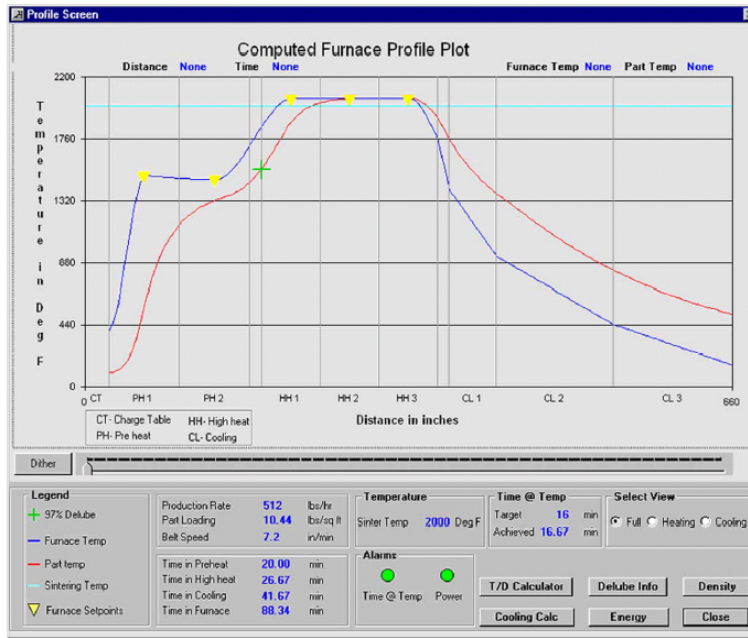


Figure 2.14 - The result illustration of FurnXpert software [10]

SYSWELD, published by the ESI group is another tool for the simulation of heat treatment, welding and welding assembly processes, taking into account all aspects of material behavior, design and process. It can perform FEA on any part geometry that can be modeled through the modeling component, and can be expanded to include additional process data that has already been obtained through experimentation to generate accurate results. SYSWELD simulates all usual heat treatment processes like bulk hardening, tempering and hardening, treatment with boron, thermo-chemical treatment like case hardening, carbonitriding, nitriding and nitro-carburising. It can also simulate Surface hardening processes like laser beam hardening, Induction hardening, electron beam hardening, plasma beam hardening, friction hardening and flame hardening. The software computes distortions of parts, residual stresses, plastic strains and the yield strength depending on the mixture of phases of the material in use both during and at the end of the heat treatment process, plus the hardness at the end of the process. But the input for the software has to be generated by the user and need to determine the furnace boundary conditions.

2.8 Summary

Heat treatment is an important manufacturing process. The furnace is key element in the heat treat process. The heat treat process variations can often be attributed to temperature variations in the process. So a tight control of temperature during the process is key to achieve minimum part variations during heat treatment. Also the modeling study is very limited. The current research is focused mostly on Finite Element Analysis based approach. And all the tools predict the microstructure and material properties for a given workpiece. The key input for these tools is the thermal profile of the heat treat process and there is no comprehensive solution currently available.

CHAPTER – 3

CHT furnace model

3.1 Overview of current Computerized Heat Treatment (CHT) furnace model

Common to all process heating systems is the transfer of energy to the material to be heat treated. Direct heating methods generate heat within the material itself (microwave, induction, controlled exothermic reaction), whereas indirect methods transfer energy from a heat source to the material by conduction, convection, radiation, or a combination of these functions. In most processes, an enclosure is needed to isolate the heating process and the environment from each other. Functions of the enclosure include, but are not restricted to, the containment of radiation (microwave, infrared), the confinement of combustion gases and volatiles, the containment of the material itself, the control of the atmosphere surrounding the material, and combinations thereof. Common industrial heat treat process heating systems fall in one of the following categories:

- Combustion-based process heating systems
- Electric process heating systems

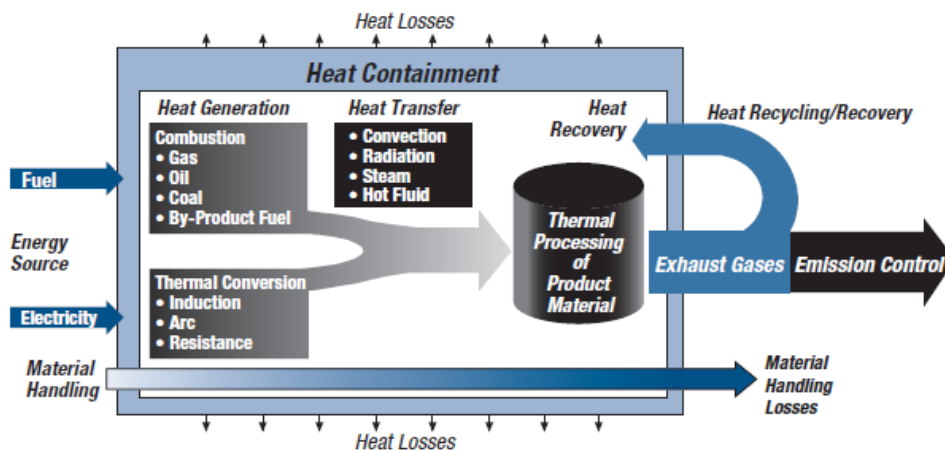


Figure 3.1 - Key components of a process heating system [15]

Temperature control is one of the most important aspects in heat treatment process. Heat treatment temperature mainly refers to soaking temperature and time. The soak temperature and time significantly affect the material properties of parts. The furnace productivity and efficiency are maximized by aggressive part load design and optimum thermal schedules.

Currently in the industry part load design is determined based on experience and empirical rules. With the advent of several heat transfer simulation tools it is now possible to simulate heat transfer of the workpieces in a furnace. Although there are a lot of commercial FEA tools available for simulation they all require a boundary condition for the simulation. Determining the boundary condition is difficult as it involves a complex furnace model.

The CHT software was developed for simulating the thermal profiles of the parts inside a furnace based on a hybrid FDM and empirical solution. The core of the software is the furnace model that was developed based on several empirical equations determined through experiments and knowledge and expertise derived from the furnace manufacturers. To accurately calculate the part temperature it is important to calculate the furnace temperature and heat balance in the furnace. Figure 3.2 shows the flow chart for the calculation of furnace temperature using the CHT furnace model.

The CHT furnace model can be divided into furnace energy balance model, heat transfer model and furnace control model.

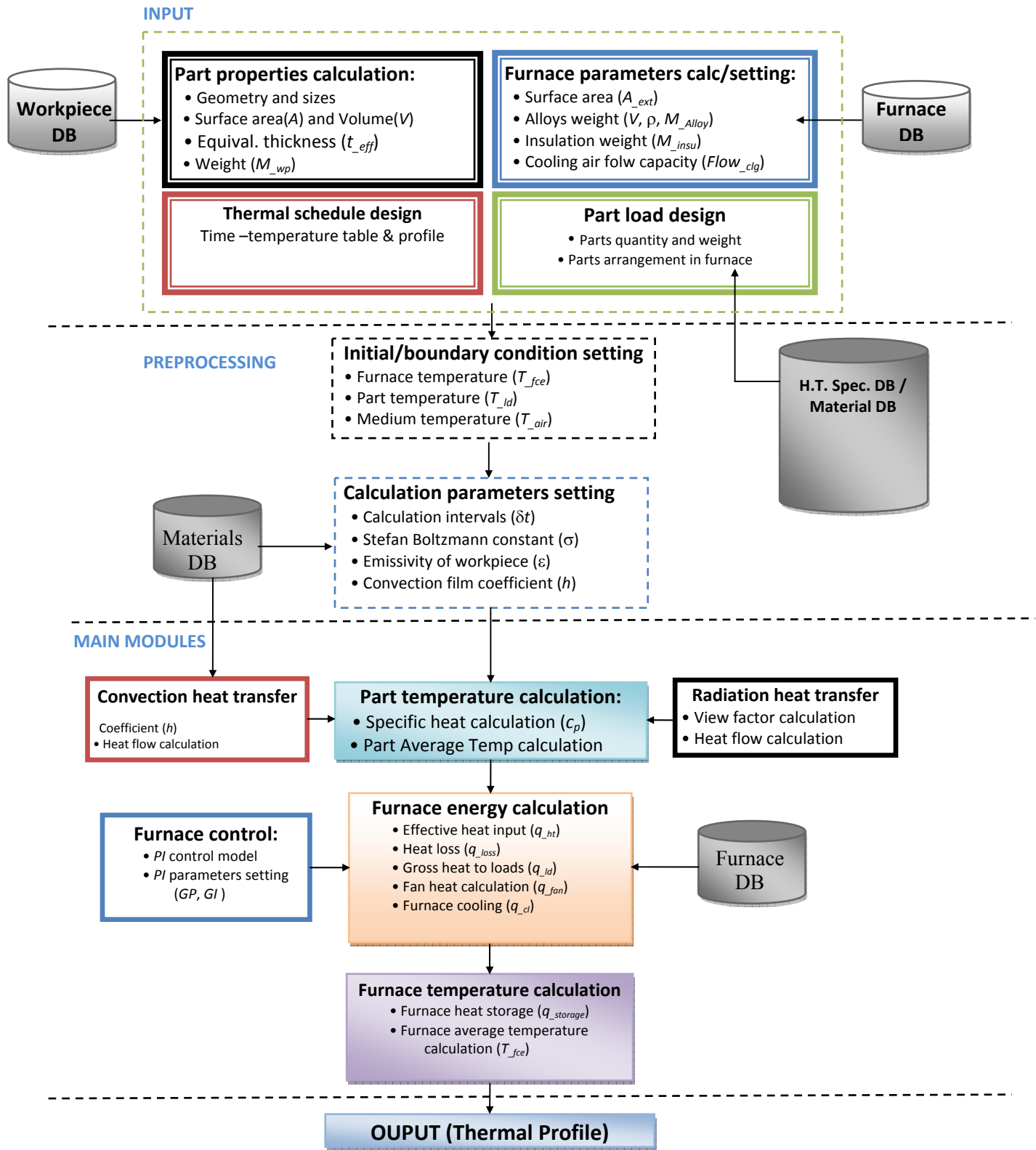


Figure 3.2 - Flowchart for temperature calculation of loaded furnace

3.2 Furnace energy balance model

Heat storage is calculated according to the energy balance,

(Heat storage) ~ Function of [(Available heat), (Heat to load),(Wall losses), (Radiation losses)]

(Available Heat) ~ Function of (Gross input)

Table 3.1 - Energy terms and their definitions[11]

Energy Items	Definitions
Gross Input	The total amount of heat used by the furnace.
Available Heat	Heat that is available to the furnace and its workload, including workpiece, furnace structural components, accessories, and heat losses due to furnace itself.
Heat to Load	Heat that ultimately reaches the product in the furnace.
Wall Losses	Heat conducted out through the furnace walls, roof and floor due to the temperature difference between inside and outside.
Radiation Losses	Heat lost from the furnace as radiant energy escaping through openings in walls, doors, etc.
Heat Storage	Heat absorbed by the insulation and structural components of the furnace to raise them to operating temperature.

$$q_{storage} = q_{ht} - q_{ld} - q_{loss} - q_{air} + q_{fan} \quad (3.1)$$

where q_{ht} is effective heat input; q_{loss} is heat loss; q_{ld} is the heat to the workpieces; q_{air} is heat absorbed by atmosphere; and q_{fan} is the heat input effect created due to the increase in convection by fan. (Fig. 3.3)

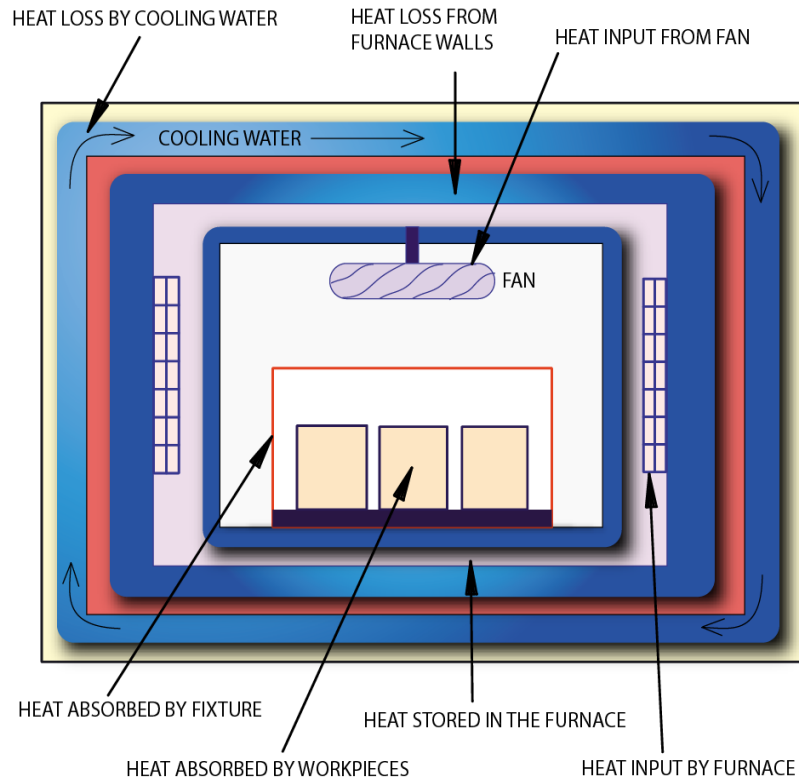


Figure 3.3 – Schematic of a heat balance in a batch furnace.

3.2.1 Energy terms calculation (Indirect gas-fired batch furnace)

Effective heat input (q_{ht}) :

$$q_{ht} = Htg \cdot AHC \cdot q_{conn} \quad (3.2)$$

where Htg is an adjust coefficient for heat input. The calculation will be given in the next section.

AHC is the corrected coefficient to the gross heat input

$$AHC = AH1 + AH2 + AH3 \quad (3.3)$$

where, the values $AH, AH2$ & $AH3$ are based on the experimental data:

Heat to load (q_{ld}):

The heat to load, is mainly subjected to the hybrid convection and radiation heat transfer.

It can be calculated using the following equation:

$$q_{ld} = k_{ld} \cdot \left(\frac{dT_{ld}}{dt} \right) = h \cdot (T_{fce} - T_{ld}) + \sigma \cdot \varepsilon \cdot (T_{fce}^4 - T_{ld}^4) \quad (3.4)$$

Heat loss (q_{loss}):

Heat loss depends on the design factor for the heat loss of furnace and the surface area of furnace. Following is an empirical equation:

$$Q_{loss} = DF \cdot (Q_{loss_wall} + Q_{loss_rad}) \quad (3.5)$$

where, DF is the design factor, and A_{ext} is the surface area of furnace.

Furnace wall losses:

$$Q_{loss_wall} = A_{fce} \times f(T_{fce}) \quad (3.6)$$

where A_{fce} is furnace wall area (inside); $f(T_{fce})$ is a function for heat loss, in Btu/ft²-hr.

Typical heat loss data are tabulated in Table 3.2

Radiation losses:

$$Q_{loss_rad} = A_{open} \cdot \sigma \cdot (T_{gas}^4 - T_{amb}^4) \quad (3.7)$$

where, Q_{loss_rad} is the radiation losses, A_{open} is the opening area, T_{gas} is the temperature of furnace gas, T_{amb} is the temperature of ambient outside furnace, σ is Stefan-Boltzmann constant.

Table 3.2 - Heat loss for different furnace walls construction (Btu/hr-ft²)[11]

Wall Construction	Hot Face Temperature, °F							
	1000	1200	1400	1600	1800	2000	2200	2400
9" Hard Firebrick	550	705	862	1030	1200	1375	1570	1768
9" Hard Firebrick + 4.5" 2300° Insulating F.B.	130	168	228	251	296	341	390	447
9" Hard Firebrick + 4.5" 2000° Insulating F.B. +2" Block Insulation	111	128	155	185	209	244	282	325
4.5" 2000° Insulating F.B.	185	237	300	365	440	521	-	-
9" 2000° Insulating F.B.	95	124	159	189	225	266		
9" 2800° Insulating F.B.	142	178	218	264	312	362	416	474
9" 2800° Insulating F.B. + 4.5" 2000° Insulating F.B.	115	140	167	197	232	272	307	347
9" 2800° Insulating F.B. + 4.5" 2000° Insulating F.B. + 2" Block Insulation	71	91	112	134	154	184	204	230
9" 2800° Insulating F.B. + 3" Block Insulation	114	142	172	201	232	264	298	333
8" Ceramic Fiber – Stacked Strips, 8 #/cu ft Density	27	45	64	86	114	146	178	216
10" Ceramic Fiber – Stacked Strips, 8 #/cu ft Density	16	35	54	76	94	120	142	172
12" Ceramic Fiber – Stacked Strips, 8 #/cu ft Density	13	27	43	60	79	98	118	143
9" Hard Firebrick + 3" Ceramic Fiber Veneer, 8 #/cu ft Density	177	240	309	383	463	642	721	800
9" 2800° Insulating F.B. + 3" Ceramic Fiber Veneer, 8 #/cu ft Density	102	125	151	183	227	274	325	408

Fan heat input effect (q_{fan}):

It is calculated based on an empirical equation:

$$q_{fan} = HP_{fan} \cdot \left(\frac{520}{460 + T_{fce}} \right) \quad (3.8)$$

where, HP_{fan} is the horsepower of re-circulating fan.

Heat absorbed by air (q_{air})

$$q_{air} = Clg \cdot Flow_{air} \cdot \rho \cdot cp \cdot (T_{fce} - T_{air}) \quad (3.9)$$

where Clg is the PID control variable,

$Flow_{air}$ is the airflow heated by the fuel gas and it equals to

$$Flow_{air} = \frac{Q_{Gross}}{hv} \cdot R \cdot (1 + xs_{air}) \quad (3.10)$$

where hv is the gross heating value of commercial fuel gases, as listed in Table 3.3; R is the stoichiometric air/gas ratio, listed in Table 3.3; Q_{gross} is the gross heat input; xs_{air} is the combustion access air; ρ is air density; cp is the air specific heat; T_{fce} is the furnace temperature; and T_{air} is the air temperature before mixed enter furnace.

Table 3.3 - Combustion properties of typical commercial fuel gases[11]

Gas type	Heating value (Btu/ft ³)	Heating value (Btu/lb)	Air/Gas Ratio (ft ³ air/ft ³ gas)	Air/Gas Ratio (lb air/lb gas)
Acetylene	1498	21,569	11.91	13.26
Hydrogen	325	61,084	2.38	33.79
Butane (natural gas)	3225	21,640	30.47	15.63
Butylene (Butene)	3077	20,780	28.59	14.77
Carbon Monoxide	323	4368	3.38	2.46
Carburetted Water Gas	550	11,440	4.60	7.36
Ethane	1783	22,198	16.68	15.98
Methane	1011	23,811	9.53	17.23
Natural (Birmingham, AL)	1002	21,844	9.41	15.68
Natural (Pittsburgh, PA)	1129	24,161	10.58	17.31
Natural (Los Angeles, CA)	1073	20,065	10.05	14.26
Natural (Kansas City, MO)	974	20,259	9.31	14.59
Natural (Groningen, Netherlands)	941	19,599	8.41	13.45
Propane (natural gas)	2572	21,500	23.82	15.37
Propylene (Propene)	2322	20,990	21.44	14.77

3.2.2 Heat balance in continuous furnace

The calculation deals with static condition. Therefore the heat balance is dynamic. It is assumed furnace temperature doesn't vary to load changes. So the heat storage in the furnace need not be calculated. (Fig 3.4) The heat terms only refer to the heat input, heat absorption by the load and moving accessories and heat loss. The furnace structure and

accessories are classified into two types: moving and fixed/shaking. The moving accessories take away heat while the fixed or shaking accessories do not take away heat.

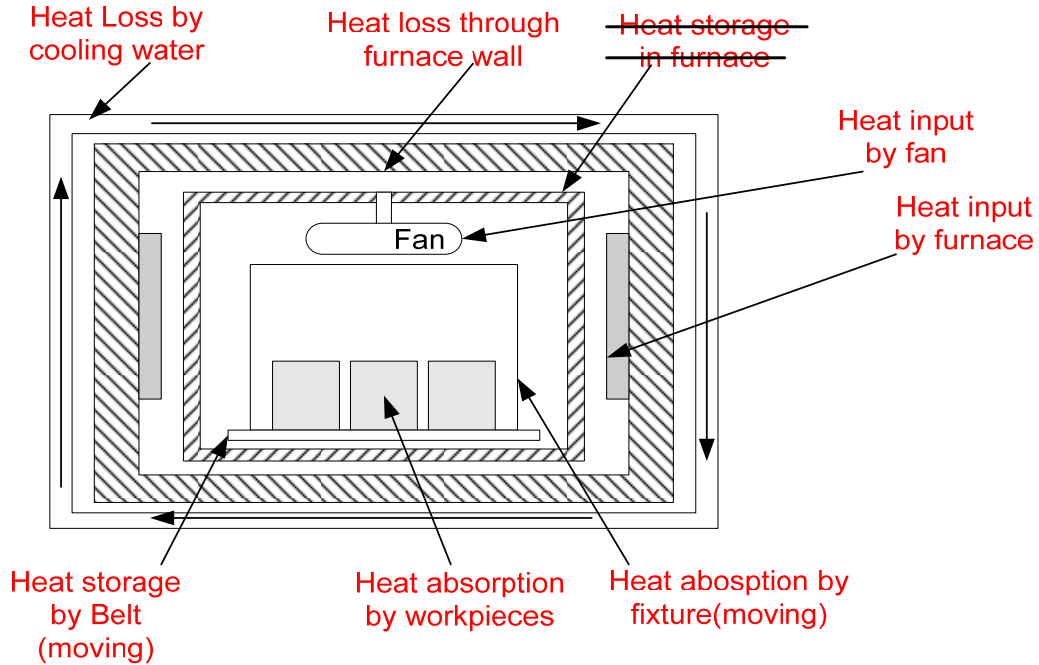


Figure 3.4 – Schematic of a heat balance in a continuous furnace.

Heat balance in each zone:

The dynamic heat balance is

$$Q_{input_p} + Q_{fan_p} = Q_{load_p} + Q_{fix_p} + Q_{belt_p} + Q_{wall_loss_p} + Q_{zone_p} + Q_{shell_cooling_p} \tag{3.11}$$

where,

Q_{input_p} ---the heat input by furnace

Q_{fan_p} --- the heat input by fan

Q_{load_p} ---the heat absorption by load

Q_{fix_p} ---the heat absorption by fixture

Q_{belt_p} ---the heat absorption by belt

$Q_{wall_loss_p}$ ---the heat loss from furnace wall

Q_{zone_p} ---the heat transfer between zones and heat loss from the end zones

$Q_{shell_cooling_p}$ ---the heat absorption by shell cooling water

From the above equation the heat input by furnace can be calculated indirectly as follows,

$$Q_{input_p} = Q_{load_p} + Q_{fix_p} + Q_{belt_p} + Q_{wall_loss_p} + Q_{zone_p} + Q_{shell_cooling_p} - Q_{fan_p} \quad (3.12)$$

It is compared with the power of the furnace to see if it exceeds the power, which means the heat balance cannot be maintained. So the furnace temperature control system such as PID is not considered.

The heat balance is calculated when a cycle is finished. Then the heat absorption in each zone is calculated based on the relationship between calculation domain and zone length. These heat terms are the functions of furnace temperature. The furnace temperature is adjusted to maintain the heat balance. The heat input should also be calculated directly by the connected heat input and the available heat coefficient.

Energy terms calculation

In the following equations, p refers to furnace zone number, i,j,k refers to workpiece number, m refers to time constant. The following equations discuss the heat balance in each zone during a time step delta t.

Heat absorbed by the load:

$$Q_{load_p} = C_{load_p} \sum_i \sum_j \sum_k (\rho g c)_{wp} (T_{i,j,k}^{m+1} - T_{i,j,k}^m) \quad (3.13)$$

where C_{load_p} is the ratio of load held in each zone over the calculation domain; the total of i, j, k is for the calculation domain and not for the whole furnace zone.

Heat absorbed by fixture:

Fixture is defined here as an element that directly holds or supports workpieces and moves forward with workpieces. Fixture doesn't include belt or conveyor. They always maintain the same temperature as the fastest heated workpieces.

$$Q_{fix_p} = (w c)_{fix} (T_{fix}^{m+1} - T_{fix}^m) \quad (3.14)$$

Here it is assumed the fixture temperature is uniform in each zone and has the same temperature of the fastest heated workpiece.

Heat absorbed by moving belt or conveyor:

$$Q_{belt_p} = L_p (w c)_{belt} (T_{belt}^{m+1} - T_{belt}^m) \quad (3.15)$$

Where w is the weight of belt unit length.

It is assumed the belt temperature is uniform in each zone and has the same temperature of the fastest heated workpiece.

Heat loss from furnace wall:

$$Q_{loss_p} = 2(L_p W_p + L_p H_p + H_p W_p) \frac{T_{fce_p} - T_{room}}{t_1/k_1 + t_2/k_2 + 1/\alpha} \quad (3.16)$$

where T_g and T_a are the temperature of furnace gas inside and outside of furnace respectively; t_1 and t_2 are the thickness of first and second insulations; k_1 and k_2 are the heat conductivity of two insulations; α is the thermal diffusivity from furnace outside to atmosphere.

Heat absorption by furnace shell cooling water:

$$Q_{shell_cooling_p} = (\rho g c)_{water} v \Delta t (T_{out} - T_{in}) \quad (3.17)$$

where v is the flow rate.

Heat transfer between adjacent zones and heat loss from ends:

$$Q_{zone_p} = \text{wall height} * K \quad (3.18)$$

K- constant. The heat transfer between heating zones can be neglected. While the heat transfer between hot zone and cold zone, between end zones and atmosphere cannot be neglected.

Heat release by circulation fan:

$$Q_{fan_p} = HP_{fan} \cdot \left(\frac{520}{460 + T_{fce}} \right) \Delta t \quad (3.19)$$

where HP_{fan} is the power of the fan.

Heat input by the furnace:

$$Q_{fce_p} = K_{AH} \cdot q_{conn} \Delta t \quad (3.20)$$

Net heat input:

$$Q_{net_p} = K_{PID_p} K_{AH_p} q_{conn_p} \Delta t \quad (3.21)$$

where K_{PID_p} is the constant for PID control; K_{AH} is the constant for combustion. For electric furnace K_{AH_p} is 1. q_{conn_p} is the heat connected input by dialog . K_{PID_p} is calculated as follows

$$K_{PID_p} = \frac{(T_{sp_p}^m - T_{fce_p}^m)}{P \cdot T_{span}} + D \frac{T_{fce_p}^m - T_{fce_p}^{m-1}}{\Delta t} + I \sum (T_{sp_p}^m - T_{fce_p}^m) \Delta t \quad (3.22)$$

3.3 Heat transfer model

The temperature history of the loaded furnace in the heat treating cycle is a hybrid convection/radiation heat transfer process. According to the heat transfer theory and energy balance equation, the heat exchange of loaded furnace can be mathematically presented in the following model:

$$q_{_storage} = \sum_{i=1}^N (\rho_i \cdot cp_i \cdot V \cdot \frac{\partial T_i}{\partial \tau}) \quad (3.24)$$

where N is the quantity of accessories in the furnace. For convenience, we assume that all the accessories have the same Let time step be k and time calculation interval be $\delta\tau$. The equation can be rearranged in the time step $(k+1)$ for the average furnace temperature.

$$T_{_fce}^{k+1} = T_{_fce}^k + \frac{q_{_storage}^k \cdot \delta\tau}{\sum_{i=1}^N (\rho_i \cdot cp_i \cdot V_i)} \quad (3.25)$$

where $q_{_storage}$ is the average storage of heat flux in loaded furnace; $\delta\tau$ is the time interval; ρ_i , cp_i , and V_i are the density, specific heat, and the volume of accessory i in the furnace. These accessories include all the components involved in the heat treating process except for the workpieces. Eq. 3.25 can be used to calculate the furnace average temperature at time step $(k+1)$. The equation is further grouped and rewritten as:

$$T_{_fce}^{k+1} = T_{_fce}^k + \frac{Q_{_storage}^k \cdot \delta\tau}{HC_{_fce}} \quad (3.26)$$

where, $Q_{_storage}$ is the heat storage in heat-treating furnace; $HC_{_fce}$ is the heat capacity of furnace components; k is the time step; and $\delta\tau$ is the time interval.

3.3.1 Factors that affect the furnace temperature calculation

The main factors affecting the furnace temperature are loads and heat storage. Loads include parts and all the furnace accessories, and heat storage is related to the furnace heat input, furnace control method, and furnace heat loss as shown in Fig. 3.5

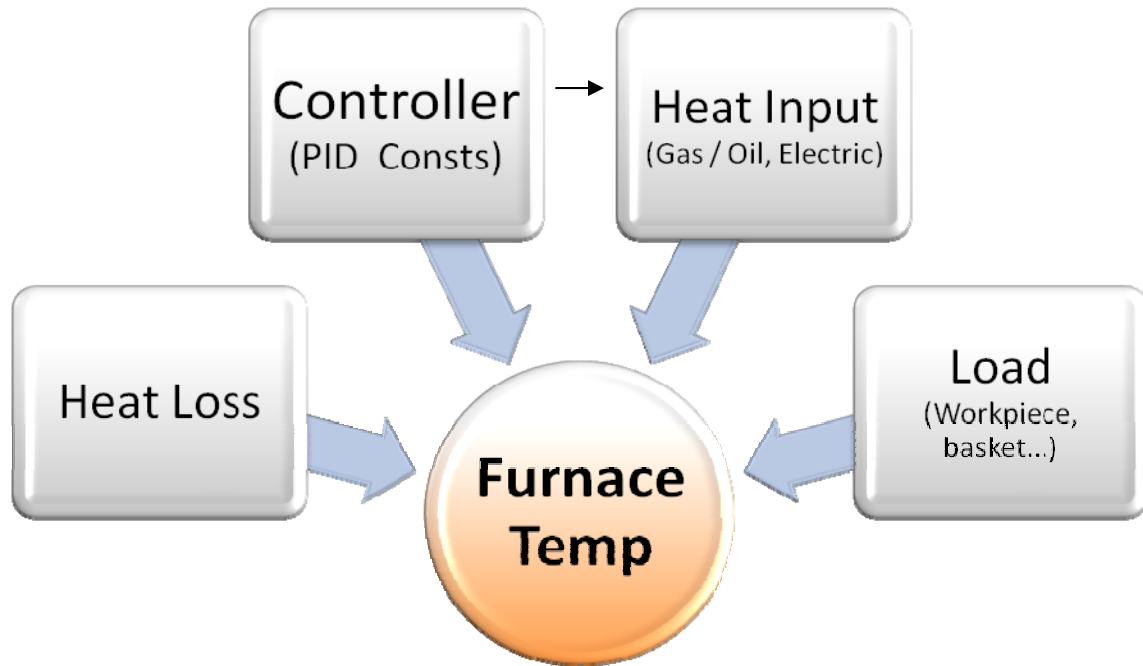


Figure 3.5 - Factors that affect the furnace temperature

3.3.2 Different loads considered for temperature calculation

In a loaded furnace, many components are involved in the heat treating cycle besides workpieces and all are referred as ‘load’. These include furnace alloy, insulation wall, and heating elements as shown in Figure 3.5. Generally the loads other than workpieces are divided into three types: ① furnace alloy including grate, firing-ring, U-tube, fixture, roller, fan and diffuser, etc; ② heating elements; ③insulation.

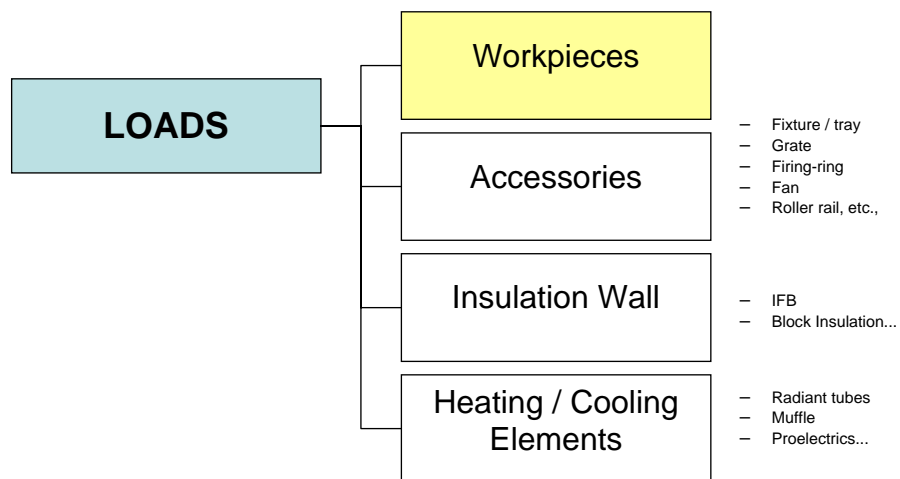


Figure 3.6 - Loads in a heat treating furnace

Effective heat capacity calculation of furnace components

$$HC_{fce} = HC_{alloy} + HC_{heater} + HC_{insulation} \quad (3.23)$$

where, HC_{alloy} is the furnace alloy heat capacity,

HC_{heater} is heater heat capacity,

HC_{insu} is furnace insulation heat capacity

3.3.3 Factors that affect the part temperature calculation

There are four main factors affecting part temperature in heat treatment, they are part properties, part loading, part materials, and furnace condition and control, as shown in Figure 3.7. The part temperature history in the heat treating furnace is a 3-D conduction heat transfer process with hybrid convection/radiation boundary conditions. It depends on the furnace temperature, working conditions, and part properties. Part load patterns and the thermal schedule design are the main tasks in the heat treatment process planning to guarantee the heat treatment quality. In order to simplify the temperature calculation, three basic assumptions are made here first:

- Lumped-mass problem, i.e., temperature in part is uniform;
- Air temperature in the furnace space is uniform; and
- Convection heat transfer on the part surface is uniform.

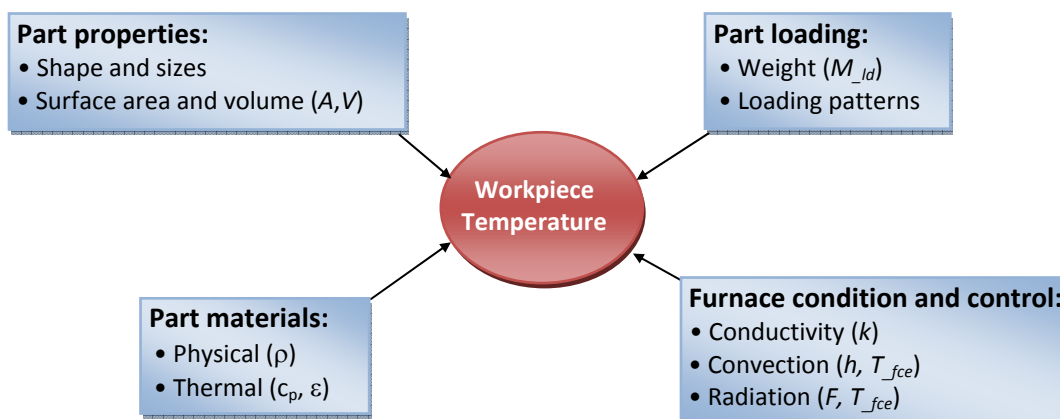


Figure 3.7 - The factors affecting the workpiece temperature

In a heat treating process, parts are subjected to both convection and radiation heat transfer. Apply the energy balance equation to the part, then,

$$E_{\text{storage}} = E_{\text{convection}} + E_{\text{radiation}} \quad (3.27)$$

where, E_{storage} is the heat storage in the workpiece; $E_{\text{convection}}$ and $E_{\text{radiation}}$ are the heat obtained from convection and radiation heat transfer, respectively.

Let the volume and surface area of the part are V and A . The energy terms in Eq. 3.27 can be calculated using following equation:

(1) Convection at ambient temperature T_{fce} :

$$E_{\text{convection}} = h \cdot A \cdot (T_{fce} - T) \quad (3.28)$$

where h is the convection heat transfer coefficient, T is the temperature of workpiece, T_{fce} is furnace temperature.

(2) Radiation at heat source temperature T_{heater} :

$$E_{\text{radiation}} = \varepsilon \cdot \sigma \cdot F \cdot A \cdot (T_{fce}^4 - T^4) \quad (3.29)$$

where ε is emissivity, σ is Stefan Boltzmann constant, F is view factor between furnace wall and workpiece, T is the temperature of workpiece.

(3) Heat storage interior workpiece:

$$E_{\text{storage}} = \rho \cdot c_p \cdot V \cdot \frac{dT}{d\tau} \quad (3.30)$$

where ρ is the density of workpiece, c_p is the specific heat, and τ is the time.

Combine Eqs. 3.28, 3.29 and 3.30 into Eq. 3.31, then

$$\rho \cdot c_p \cdot V \cdot \frac{dT}{d\tau} = h \cdot A \cdot (T_{fce} - T) + \varepsilon \cdot \sigma \cdot F \cdot A \cdot (T_{fce}^4 - T^4) \quad (3.31)$$

Since the part is taken as the lumped-mass body, we can imagine an equivalent workpiece or “visual workpiece” to represent the real workpiece, as shown in Fig. 3.13.

In this way the calculation can be further simplified.

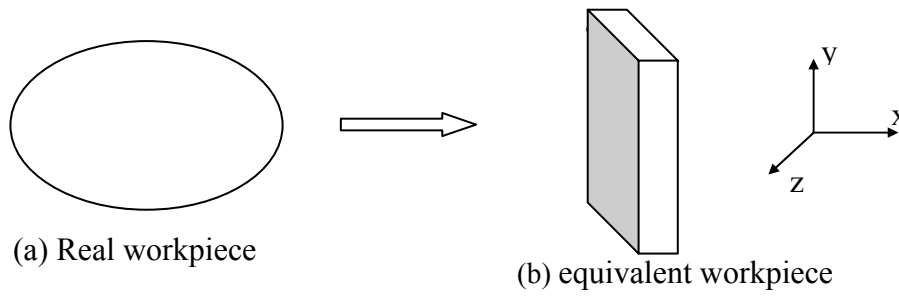


Figure 3.8 – *The equivalent workpiece*

Let $V = A \cdot t_{equ}$, where t_{equ} is the equivalent thickness of the part. Apply finite difference method to the left-side of Eq. 3.31, then

$$\frac{\partial T}{\partial \tau} = \frac{T^{k+1} - T^k}{\delta \tau} + O(\delta \tau) \quad (3.32)$$

where k is the time step. By combining Eqs. 3.31 and 3.32, at time step k , the equation becomes,

$$T^{k+1} = T^k + \frac{\delta \tau}{\rho \cdot c \cdot t_{equ}} \left[h \cdot (T_{fce}^k - T^k) + \varepsilon \cdot \sigma \cdot F \cdot \left((T_{fce}^k)^4 - (T^k)^4 \right) \right] \quad (3.33)$$

Eq. 3.33 can be used to calculate the part temperature with uniform temperature distributions at any time in a heat treating cycle.

Above equations can be used to calculate the part temperature at arbitrary position in the furnace. Because there are different work environment at different positions in furnace space, the temperatures are different for different parts too. In practice, the temperature histories of all the parts have to be considered so as to get the good products.

The effect of workpiece quantity and equivalent thickness

If lots of parts are treated in a heat treat cycle, we have to assure that all the parts are well heated during the process. It is not necessary to calculate the temperature-time profile for every part in furnace. Instead, the temperature-time profiles of some typical parts are considered in the furnace (such as the parts close to furnace wall and in the

middle of furnace). The part load effect on the part temperature is mainly contributed from the radiation heat transfer and will be discussed in a later section.

The reason to calculate equivalent thickness is that sometime we need not only the surface temperature on the workpiece, but also the core temperature. This is a simple method used to calculate the interior temperature of a part. There are several methods that can be used to calculate the equivalent thickness of a workpiece. The calculation methods will depend on the load conditions and calculation methods:

- The minimum dimension of heaviest cross section in workpiece
- The value of workpiece volume divided by surface area: $t_{eff} = V/A$
- The value of 3 times of volume divided by surface area: $t_{eff} = (3 \cdot V)/A$
- The value of volume divided by exposition area to heater: $t_{eff} = V/A_{exposition}$

In our development of CHT, the first method is used as default value which can be changed through a user interface.

The effect of convection heat transfer

In practice, the convection heat transfer around part surface is not uniform. This can be described using convection film coefficient h . Following is one of the calculation methods for the coefficient h :

$$h = (k \cdot Nu) / L^* \quad (3.34)$$

where Nu is Nusselt number, a dimensionless heat transfer coefficient, and can be calculated using an experimental equation[11]:

$$Nu = c \cdot Re^m \quad (3.35)$$

where Re is Reynolds number, a dimensionless group charactering a viscous flow; the characteristic dimensions c and m are calculated from experimental values. Note that this equation is only used to gases medium.

$$Re = (V \cdot L^*) / \nu = (\rho \cdot V \cdot L^*) / \mu \quad (3.36)$$

where L^* is a characteristic length of the part; k is the thermal conductivity; V is air velocity; ν is the kinematic viscosity; ρ is density; and μ is dynamic viscosity.

The effect of radiation heat transfer

Because the parts are located in the different positions in the furnace, the heat they receive from the radiation transfer are different. This effect can be represented by the view factors. The value of view factor is affected mainly by the distance between furnace wall and the part, as well as the shadowing among workpieces. A CAD-based method of calculating the view factors is developed, the view factors can be specified based on the CAD-based calculation method.

3.4 Furnace temperature control model

The furnaces are controlled by temperature controllers. The temperature controllers get their inputs from a thermocouple located inside the furnace and send necessary control action to the burner to maintain the process setpoint.

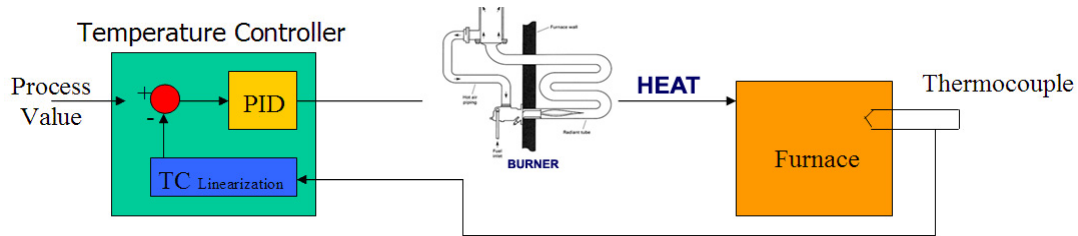


Figure 3.9 - Schematic of the Temperature controller in a radiant tube type furnace.

3.4.1 Commonly used schemes in heat treatment furnaces

The control action for the temperature controller can be either on/off or proportional. Process tolerances and the final device being controlled normally determine the type of control action.

On/off control is simple to understand. For example in a heat treat furnace during the heating process, if the measured process temperature is below the control setpoint, burners are continuously fired by the controller. If the measured value exceeds the control setpoint, the controller shuts the burners. Switching the heat on and off takes place at setpoint. This type of control causes the process value to oscillate around the control setpoint.

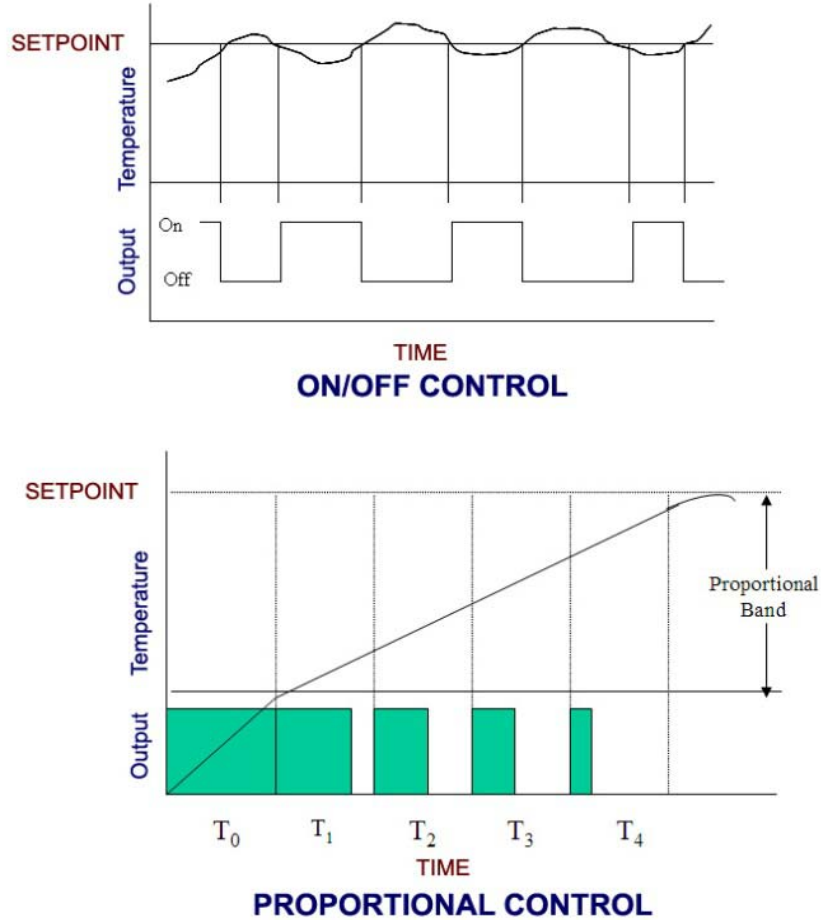


Figure 3.10 - On/Off & Proportional type controllers commonly used in furnaces.

Proportional control (PID) is a more sophisticated control approach which results in tighter control around a setpoint and less process oscillation.

Proportional control consists of 3 basic control functions:

1. Proportional band
2. Reset, or Integral
3. Rate, or Derivative

Proportional band is the process range over which proportioning control action takes place. In a heating situation, if the process temperature is below the proportional band,

burners are continuously fired by the controller. If the process value is above the proportional band, the burners are shut. Within the proportional area, as the process temperature increases the amount of heat being called for decreases proportionately. (as shown in Fig 3.15 where T1, T2, T3... are the proportionally decreasing time values)

To determine the proper proportional band setting, the time required to approach setpoint must be balanced with the processes' ability to withstand overshoot. If proportional band is too narrow, the heat input will not be cut back soon enough and the process will overshoot. A wide proportional band begins cutting back the heat input sooner. A narrow proportional band (means heat is on longer) will approach setpoint quicker than a wide proportional band.

Reset (Integral) shifts the proportional band in relation to the desired setpoint. Reset action is used to compensate for sustained process offset from the control setpoint.

Rate (Derivative) is used to compensate for initial overshoot and sudden process disturbances. Rate will temporarily compress the proportional band around setpoint to bring the process under control.

3.4.2 Controller tuning

It is necessary to tune a controller to a particular process. This will enable the controller to maintain tight control of the process. This will remain so even if process variables (ambient temperature, load size, hearth/gasket condition, etc.) change over time.

Properly tuning a controller to a process is an absolute necessity to ensure tight control. Manually tuning a controller is a time consuming and tedious exercise. There are several features available in today's controllers which facilitate tuning. Autotune capability now allows a controller to tune itself to a process. Autotune will introduce a minor process disturbance and this enables the controller to determine how the process should react to the change and the amount of time required to recover. Based on these parameters the controller determines the necessary constants.

Another method of tuning the modern controllers is by using the Adaptive tuning. Adaptive tuning is implemented by the controller and results in minor proportional band, reset, and rate changes. Adaptive tune does not introduce process disturbances.

Fuzzy logic is the newest function incorporated into controllers. It is supposed to enable a controller to learn a process, and subsequently react quicker to changes. Currently the CHT model can accept the PID based controller values. The controllers with adaptive and fuzzy logic based schemes need to be translated to PID based values.

3.4.3 CHT furnace - PID control model

The typical temperature control method in the furnace is *PID* controller. When the measured temperature is different from the set point temperature, the heating or cooling input is controlled to minimize the error. It is a typical feedback control system as shown in Figure 3.11.

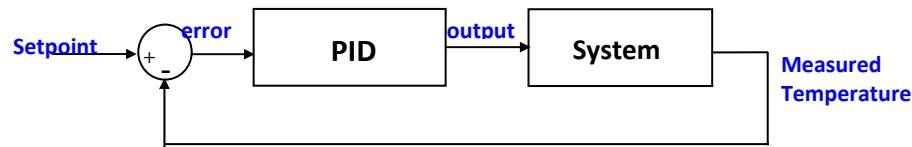


Figure 3.11 - Control feedback loop of PID control

Generally PID method uses following equation to control the loop:

$$u = P \cdot \left[(T_s - T_o) + D \cdot \frac{d}{dt}(T_s - T_o) + I \cdot \int (T_s - T_o) dt \right] \quad (3.37)$$

where T_s is the set point temperature, T_o is the furnace temperature, the error value $e = (T_s - T_o)$; P , D , and I are known as proportional gain, damping, and integral gain, respectively.

In a *PID* control process, one of the most important things is to set the P , D , and I . Tuning these constants so that the weighted sum of the proportional, integral, and derivative terms produces a controller output that steadily drives the process variable in the direction required to eliminate the error. There are several methods that can be used to determine the P , D , and I value. One of them is Ziegler and Nichols approach, which is a practical method of estimating the values of K , T , and d experimentally. Where K is the

process gain used to represent the magnitude of the controller's effect on the process variable, T is the process time constant used to represent the severity of the process lag, and d is the deadtime used to represent another kind of delay present in many processes. With the controller in manual mode (no feedback), a step change is included in the controller output and the process reaction is analyzed. The process gain P can be approximated by dividing the net change of the process variable by the size of the step change generated by the controller. The dead time is estimated from the interval between the controller step change and the beginning of a line drawn tangent to the reaction curve at its steepest point. They are also used the inverse slope of that line to estimate the time constant T .

$$\left. \begin{aligned} P &= \frac{1.2 \cdot T}{K \cdot d} \\ I &= \frac{0.6 \cdot T}{K \cdot d^2} \\ D &= \frac{0.6 \cdot T}{K} \end{aligned} \right\} \quad (3.38)$$

Sometimes, when the sensor measuring the furnace temperature is susceptible to other electrical interference, derivative action can cause the heater power to fluctuate wildly. In this case $D = 0$, and a PI controller is often used instead of PID controller. The typical application of PD control in furnace is to control heat/cool gases input. The adjustment coefficient of heat input, Htg , is calculated using following equation:

$$Htg = \frac{PG}{Span} \cdot (T_{-sp} - T_{-fce}) + \frac{PG \cdot IG}{Span} \cdot \int_0^{\tau} (T_{-sp} - T_{-fce}) \quad (3.39)$$

where the proportional gain $PG=10$ and the integral gain $IG=0.05$.

3.5 Summary

The CHT furnace model is a comprehensive model with a capability to model several different types of furnaces and control schemes. Currently there are several proprietary models used internally by the industry that is not publicly available. The CHT model is the most comprehensive model currently available to the industry and is in use at several CHT member companies since 2002. The model used in the CHT software system and has been validated with several case studies.

CHAPTER - 4

Furnace model analysis

The experiments conducted using the CHT software at various customer locations are listed in Appendix-A and grouped by Furnace type and the results are analyzed. The CHT-b/f & CHT-c/f calculated results are compared to the measured thermocouple results. The comparison between the results are performed by focusing on the following areas / issues,

- Heat up rate accuracy
- Time taken to reach furnace setpoint (comparison)
- Accuracy of soak time and temperature
- Abnormal peaks – gradients, flame screens,...

Each area with high error percentages was analyzed to determine the cause of the problem. Some minor problems were attributed to software bugs which were fixed later. The major problems were studied in detail and expert opinion from the shop floor was requested to further understand the problem. A detailed list of problems in the current model due to furnace issues like gradients, furnace aging, and the model constraints are documented. The results presented in this chapter as based on the observations and conclusions based on the experimental results documented on Appendix – A.

Table 4.1. *List of case studies in different furnaces and locations*

Furnace Type	Company	Location	Number of experiments
Continuous Furnaces	American Heat Treating	Monroe, CT	4
	Bodycote	Waterbury, CT	6
		Worcester, MA	1
	Caterpillar	Peoria, IL	13
			(24)
Vacuum Furnace	Bodycote	Worcester, MA	4
	Bodycote	South Windsor, CT	2
	Bodycote	Wisconsin	2
	Sousa Corporation	CT	1
	American Heat Treating	Monroe, CT	5
			(14)
Batch Furnace	Bodycote	Worcester, MA	12
	American Heat Treating	Monroe, CT	1
	Surface Combustion	Maumee, OH	1
	Queen city steel	Cincinnati, OH	1
			(15)
Total			53

4.1 Furnace model study

To breakdown the analysis task, the model was studied from three practical perspectives,

1. Structural model
2. Control schemes model
3. Process related parameters

4.1.1 Structural model

The furnace was studied from a structure stand point and several factors were classified and important to the accuracy of the model. The several problems and their effects are listed below.

Universal furnace

The current model is universal for all furnaces. Due to this issue its unable to calculate the heat losses that are more specific to certain kinds of furnace. The effect of having a universal furnace is in the improvement in the accuracy certain heat loses and heat heat storage in the furnace (Q_{fce}) if we have more specific furnace categories. (eg: Vacuum, Box, Pit, etc.,)

Burner locations

Thermal gradient in the furnace due to location of the burners and their BTU's. There is a thermal gradient inside the furnace and the BTU is not distributed uniformly inside. Current model assumes uniform furnace temp. And Accuracy issues especially in Continuous furnaces.

Atmosphere flow

The effect of atmosphere flow and calculating a constant to adjust the heating parameters due to the heat losses. These result in accuracy issues. Case studies done for validation in the atmosphere furnaces show the inconsistency especially during heat up.

Incomplete accessory data

Make a generic list of accessories for each kind of furnace. Improves the model accuracy by considering all the furnace elements.

4.1.2 Control model

Similar to the structural model all the elements that contribute to the furnace control were studied separately and their effects are listed below.

Furnace controller

In the current model there is no option to specify the exact control schemes used in the furnace. This results in approximation of the control scheme that is deployed in the shop floor.

Multiple controllers

There is no option to specify multiple controller parameters for different zones. Also the controllers are tuned differently for different zones based on the process parameters especially in the continuous furnaces. These result in inaccurate thermal profile calculation.

Control thermocouple

There is often a thermal gradient inside a furnace and one of the reasons is due to the location of the control thermocouple. Currently the model assumes a uniform temperature distribution. The control thermocouple location information helps to calculate the gradient present inside the furnace.

4.1.3 Process parameters

Several processes require the furnace to be controlled differently. The main differences are in the atmosphere control and the temperature control. The experiments were conducted for the current list of processes,

1. Annealing
2. Tempering
3. Carburizing
4. Brazing

4.2 Problem identification in the current CHT furnace model

A detailed study of the experimental analysis based on Furnace classification, Control schemes and Process related parameters revealed the following limitations or issues in the current CHT model. Several of these also have an effect on the model accuracy.

1. Universal furnace model

The current model is based on an universal model for all furnaces. Hence it cannot accurately calculate the heat losses that are more specific to certain kinds of furnaces. (eg: Vacuum, Box, Pit, etc.,)

2. Burner locations

Current model assumes uniform furnace temperature, often there is a thermal gradient in the furnace due to location of the burners and their capacities.

3. Atmosphere flow

Case studies done for validation in the atmosphere furnaces show the inconsistency especially during heat up. The effect of atmosphere flow and the heat losses and heat transfer affects the accuracy of the model.

4. Furnace accessories

Furnace accessories like baskets, fixtures, etc, also consume heat inside furnace along with the load. The current model uses a generic fixture approximation.

5. Door operations

The current furnace model does not take into effect the heat loss arising due to the door operations during charging and discharging the parts from the furnace. From the experimental analysis this was not an issue in Batch furnaces but it had an impact on the continuous furnaces.

6. Furnace controller

Inability to translate the control schemes used in the furnace to the PID based control in the furnace model.

7. Multiple furnace controllers

The furnaces often use multiple controllers for different zones. The controllers are tuned differently for different zones based on the process parameters, especially in the continuous furnaces. Currently CHT model uses a universal controller.

8. Control thermocouple location

It was found a thermal gradient inside the furnace may be present due to the location of the control thermocouple.

9. Process data

Several processes require operating the furnaces differently. (For example, in the carburizing furnace, the enriching gas is added to the furnace after the load reaches the temperature. The ability to specify in the CHT model the amount of gas added in the cycle improves the calculation of heat loss, which is currently not possible)

10. Proprietary furnace control schemes

The furnace and controller manufacturers use several proprietary furnace control techniques. Its difficult to model these control schemes. (for example – its difficult to determine the PID constants (for CHT model) from a controller tuned with an adaptive tuning algorithm)

11. Furnace deterioration (wear/tear)

The furnace refractory and burners deteriorate over time, increasing heat losses and reducing heat available respectively.

12. Faulty or incorrectly tuned burners

The burners need to be tuned properly for complete combustion. An incorrectly tuned burner or a faulty burner does not produce the specified heat.

4.3 Summary & conclusions

After analyzing all the list of limitations and problems in the current CHT furnace model the following were determined to have significant effect on the furnace model accuracy.

1. Heat loss due to door operations
2. Thermal gradients inside the furnace
3. Furnace deterioration over time

The heat loss in the furnace due to door operation is a problem more significant in continuous furnaces than batch furnaces. With several experimental data and modeling we can develop new model to incorporate in the CHT model to account for this loss. The thermal gradients present inside the furnace is a complex phenomenon, it is caused due to several factors like burner and control thermocouple location, the furnace construction, etc., and it is also unique to every furnace, so more detailed study is required to understand and model this phenomenon. Furnace wear phenomenon can be modeled by conducting calibration experiments with virtual load and the parameters reverse calculated. These are the development proposed for the improvement of the CHT furnace model.

CHAPTER - 5

Improved furnace model

5.1 Introduction

The Furnace Model Analysis study gave an insight on the current CHT Furnace model's shortcomings and opportunities to improve the overall accuracy. From one of the experimental results on a Continuous Pusher Furnace (as seen in Fig. 5-1a) we can see a significant thermal gradient present inside the furnace in the holding chamber and also there was a wave due to the heat loss from the door openings and the controller action. This problem is specific to this type of furnace and more due to the design and arrangement of the burners.

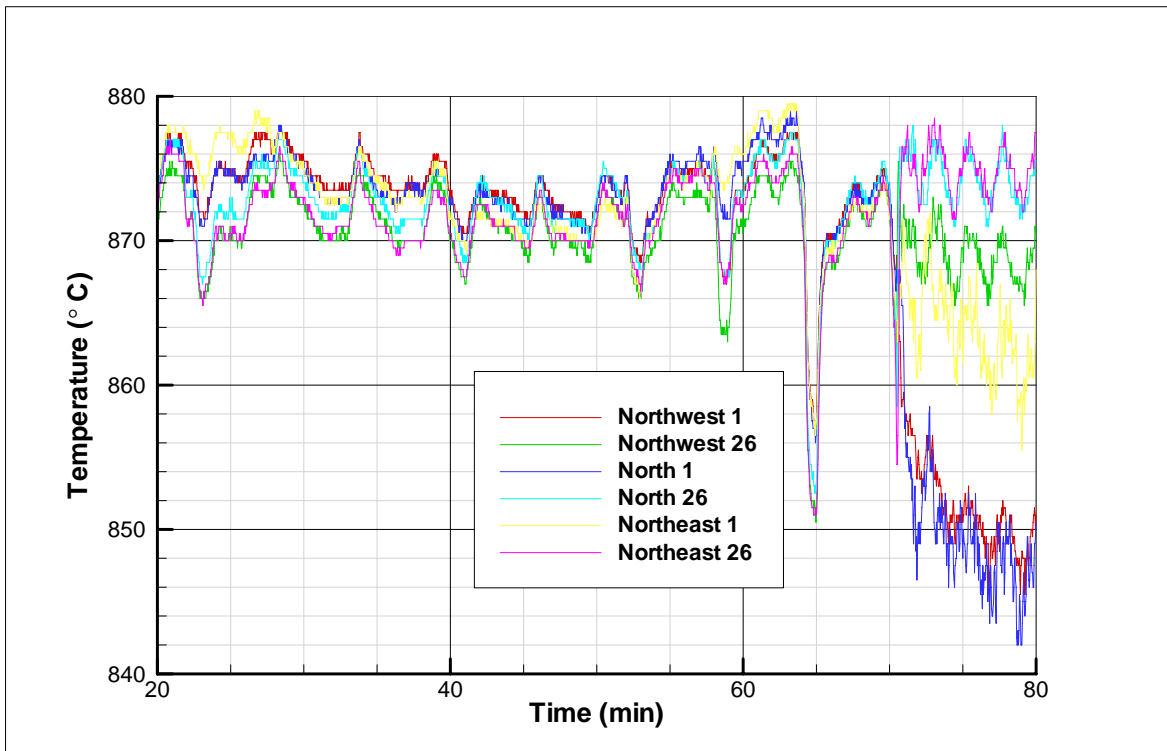


Figure 5.1a - *The thermal gradients inside a Continuous Pusher Furnace, experimental data from continuous datapak with 6 thermocouples.*

Based on the furnace model analysis presented in the earlier chapter and from discussion with customers and experts, the key focus was narrowed down to 3 specific problems,

- (i) Heat loss due to furnace charge / discharge door operations (specific to continuous furnaces)
- (ii) Thermal gradients present inside the furnace
- (iii) Furnace deterioration and related inaccuracies in the model.

The new model is represented as follows by addition of 3 new terms to the original equation,

$$T_{fce}^{k+1} = T_{fce}^k + \Delta T_{fce_door}^k + \Delta T_{fce_gradient}^k(x, y, z) + \Delta T_{fce_virtual}^k \quad (5.1)$$

where,

T_{fce}^k = Furnace temperature (at time step, k)

$\Delta T_{fce_door}^k$ = Furnace temperature variation due to door operations

$\Delta T_{fce_gradient}^k(x, y, z)$ = Temperature gradient inside furnace in 3D space

$\Delta T_{fce_virtual}^k$ = Furnace calibration using virtual load

Detailed explanation of the 3 terms, how they are calculated and used in the model are described in the following chapters. Experimental case studies are also conducted to verify the results.

5.2 The door open model ($\Delta T_{fce_door}^k$)

The CHT model does not calculate the heat loss and the heat exchange between zones that occur as a result of the door operation. Currently the furnace temperature is not calculated in the continuous furnace model based on the PID control. The calculated furnace temperature does not reflect the variation observed in the experiments. This chapter discusses addition of a heat term to compensate for the heat loss arising out of door operations.

5.2.1 Introduction

A series of experiments were conducted at a beta test facility to evaluate the accuracy of the continuous furnace model under different conditions. The experiments were conducted on a brand new furnace undergoing production trials. This helped us eliminate some of the guess work out of calculation especially the heat loss factor due to the physical wear and tear of the furnace. After conducting the experiments a significant variation between furnace set-point temperature and the measured workpiece temperature (around 25°C) was noticed. There also existed a uniform pattern to the thermal profiles in all the experiments. This pattern matched with that of the door open sequence. This thermal pattern is shown in the Fig.5-1b.

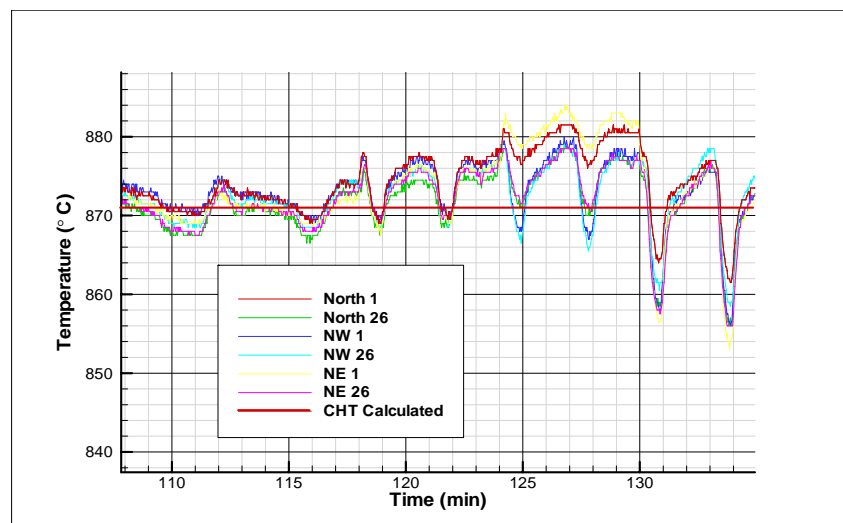


Figure 5.1b - The thermal profile of the CHT calculated and measured workpiece temperature at 6 different locations in a Continuous Furnace.

The current furnace model (CHT model) was developed based on the batch furnace model and the main assumptions in the model are,

- (i) The furnace temperature does not change with varying load conditions. It always remains same. (So the heat balance is not calculated and PID control is not considered either)
- (ii) The workpiece movement is considered linear. (either step movement or continuous)
- (iii) The workpiece is fixed and the furnace is moving. So the thermal schedule is a function of the movement speed. The furnace temperature is the same as thermal schedule.
- (iv) The heat transfer at the calculated domain boundary to other loads is zero.

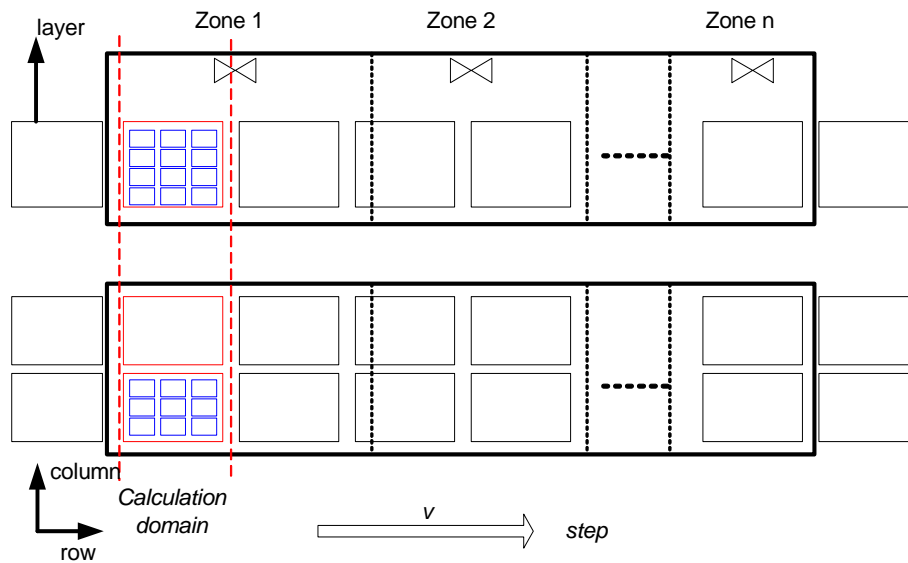


Figure 5.2 - Pusher type Continuous Furnace Model

With the workpiece as a reference, the furnace temperature involved in the calculation changes with the workpiece row number and time, as shown in Fig.5-2 the temperature is calculated for different zones. The furnace temperature distribution is a function of furnace zone and corresponding transition zone. It is depicted as follows:

$$T_{_fce}(d) = \begin{cases} T_{_zonej} + \frac{T_{_zone(j+1)} - T_{_zonej}}{L_j + L_{j+1}} (d - (\sum_{i=0}^j L_i - L_j)) & \sum_{i=0}^j L_i - L_j \leq d \leq \sum_{i=0}^j L_i + L_{j+1} \\ T_{_zonej} & \sum_{i=0}^{j-1} L_i + L_j < d < \sum_{i=0}^j L_i - L_j \end{cases} \quad (5.2)$$

where,

i and j are the zone numbers,

d is the distance from the beginning of the furnace, in the range of 0 to the whole length of the furnace; L is the length of furnace zone.

Since the temperature variations observed during the experiments were significant from a heat treatment processes stand point, it was decided to integrate new terms to the current Continuous Furnace model to improve the furnace temperature accuracy to reflect the real world conditions.

There are two modes of heat loss arising due to the door operation. A radiation heat loss and heat loss due to the exchange of the furnace gas between zones and to the atmosphere in the final zone. There are several doors in the furnace between zones.

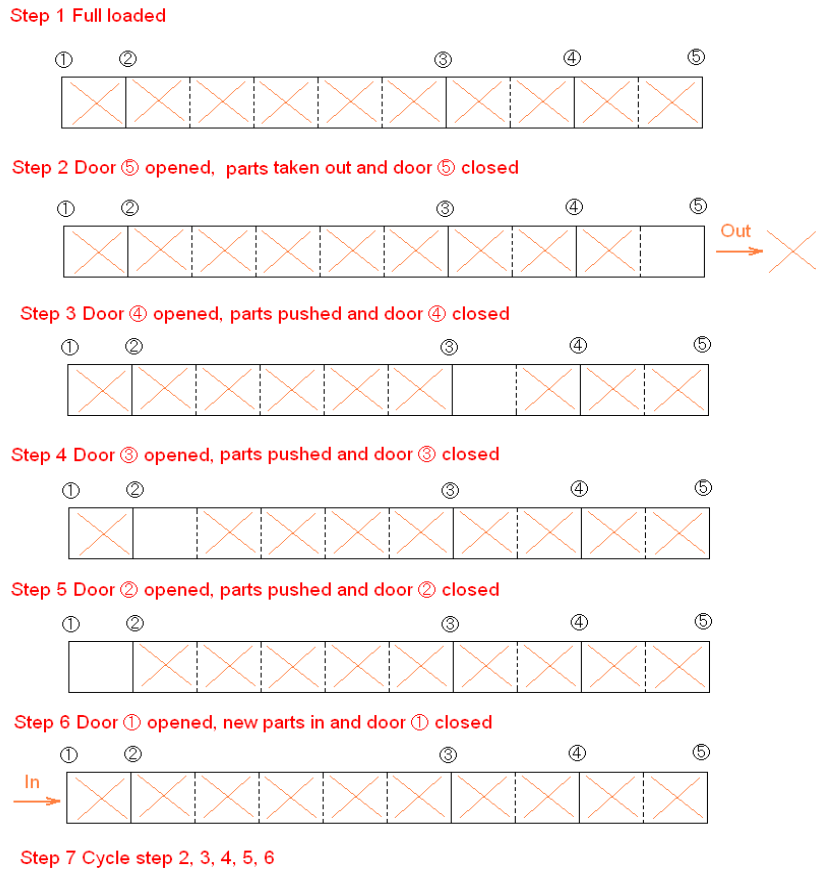


Figure 5.3 - Door open/ Push sequence in a Continuous Furnace Model

As illustrated in Fig. 5-3 the door open sequence can be simulated starting from a fully loaded furnace. The door 5 is opened through a slot door for quenching, during this operation there is a radiation heat loss and also heat loss due to the loss of furnace atmosphere. Once the door 5 is closed the door 4 opens and parts are pushed in the final zone. During this operation there is a heat exchange through radiation depending upon the zone temperatures and normally there is not a significant amount of atmosphere exchange. (Assumed based data on the pressure variation during the door operation is presented later). The same sequence of operations follow during the operation of doors 3 and 2. When the door 1 opens a new cold part is loaded in the furnace. We do not model the first few zones, as there is a significant cold mass entering the furnace. There is no temperature swings in the first few zones and the burners are firing at the maximum rate to achieve the set-point temperature.

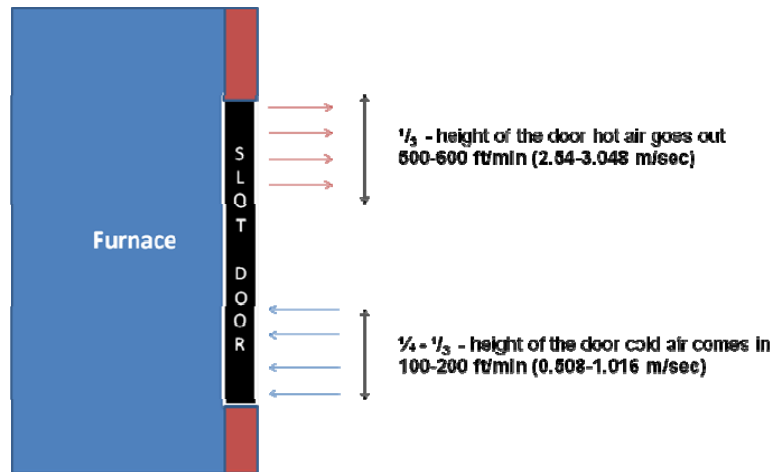


Figure 5.4 - Empirical data used by a furnace manufacturer based on experiments and experience to predict the loss of atmosphere during the door operation in a continuous furnace

The atmosphere exchange and heat loss in the final zone is complex as shown in Fig.5-4. When the slot door opens, due to the pressure differential the furnace hot atmosphere escapes the furnace and at the same time there is cold air entering the furnace due to the vacuum created inside the furnace. This happens due to a drop in the furnace atmosphere volume because of the heat loss. It's difficult to calculate the exact volume of atmosphere lost and air added. Based on experimental data presented from a furnace manufacturer the velocity of hot air leaving the furnace is around 500-600 ft/min and usually this takes place in the top 1/3 space of the slot door. And the cold air velocity entering the furnace is around 100-200 ft/min.

5.2.2 Experiments on pressure differences between zones & during door operations

Further experiments were conducted to understand the gas exchange between the different zones in the furnace and to the atmosphere during the door operations. A series of experiments were conducted to study the pressure in the different zones in the furnace and the changes in pressure during the door operation.

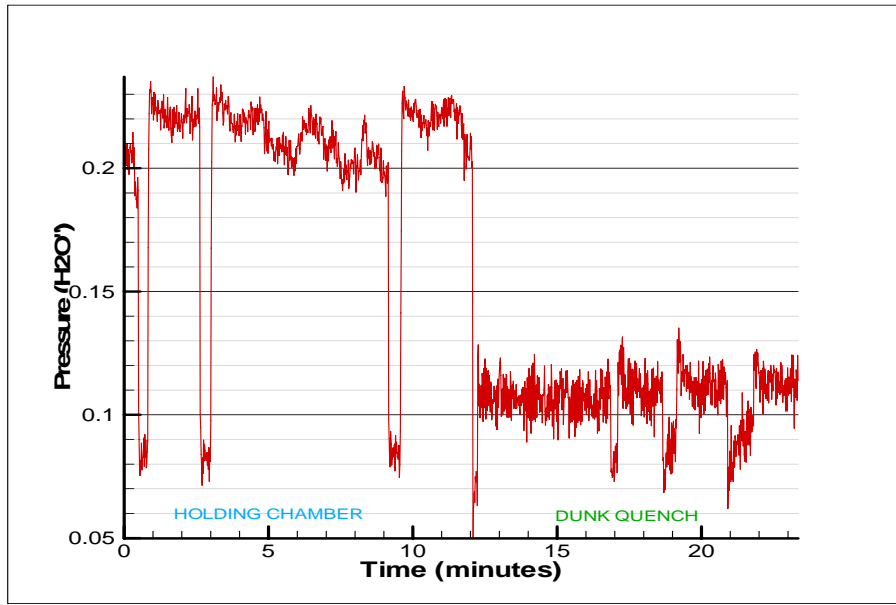


Figure 5.5 - *The pressure in two different final zones in a Continuous Pusher Furnace*

Figure 5-5 shows the plot of pressure in Holding Chamber and Dunk Quench Chamber in inches of water (27.7 inches of Water = 1 PSI at 62° F). The pressure inside the furnace is slightly above the atmospheric pressure. Also the pressure in the holding chamber is maintained above the dunk quench chamber to prevent the gas from entering the holding chamber. This is done to prevent decarburization in the holding chamber.

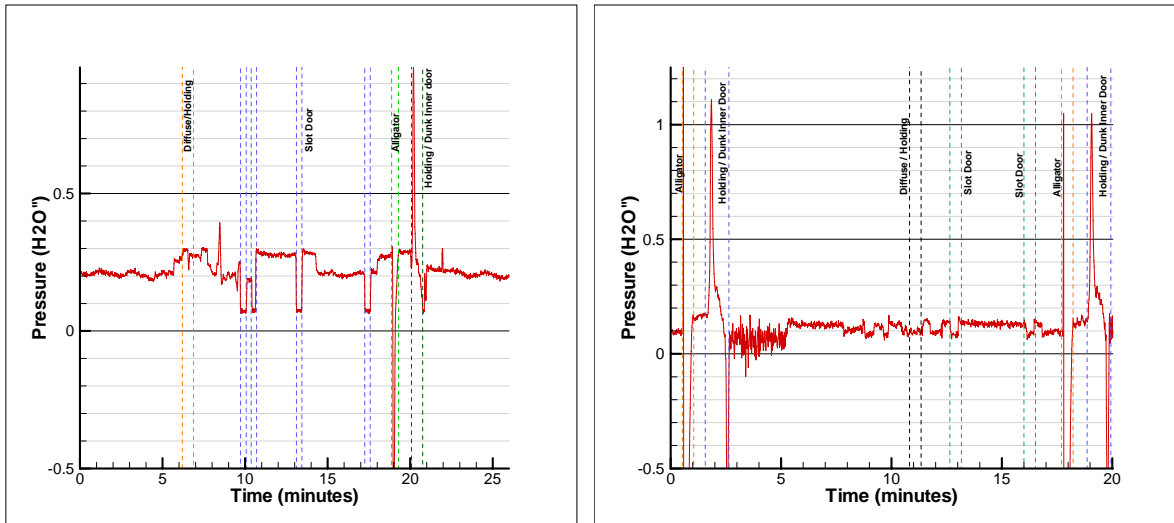


Figure 5.6 - The pressure variations as a function of different door operations events. *Holding Chamber (left) & Quench Chamber (right)*

As observed in Fig. 5-6 the pressure variations in the different zones are plotted as a function of the different door operation events. One of the observations is that the door openings in a zone had an effect on the pressure on several different zones. It had a clear influence on the pressures in the adjacent zones and this implies that the intermediate zone doors are not pressure tight and hence there is exchange of gases that takes place during the door openings.

The negative pressure formed after the door operation is created due to the reduction in volume of gas. When the door opens a significant amount of air enters the furnace and creates combustion of the endothermic gas present in the zone. When the door closes, pressure spikes due to the expansion of the gas due to higher temperature resulting from the combustion. And the combustion stops once all the oxygen is consumed from the air and this result in a significant reduction in the temperature and volume causing the pressure to go in the negative.

Based on the experimental data on temperature and pressure a new term was added to the current Continuous furnace model to account for the heat loss.

5.2.3 Modified model to include door open term

$$q_{storage} = q_{ht} - q_{loss} - q_{ld} - q_{cl} + q_{fan} - q_{dopn} \quad (5.3)$$

where, q_{dopn} is the heat loss caused by radiation and mass loss during doors operation. , q_{dopn} is also a function of time calculated from the door open schedule.

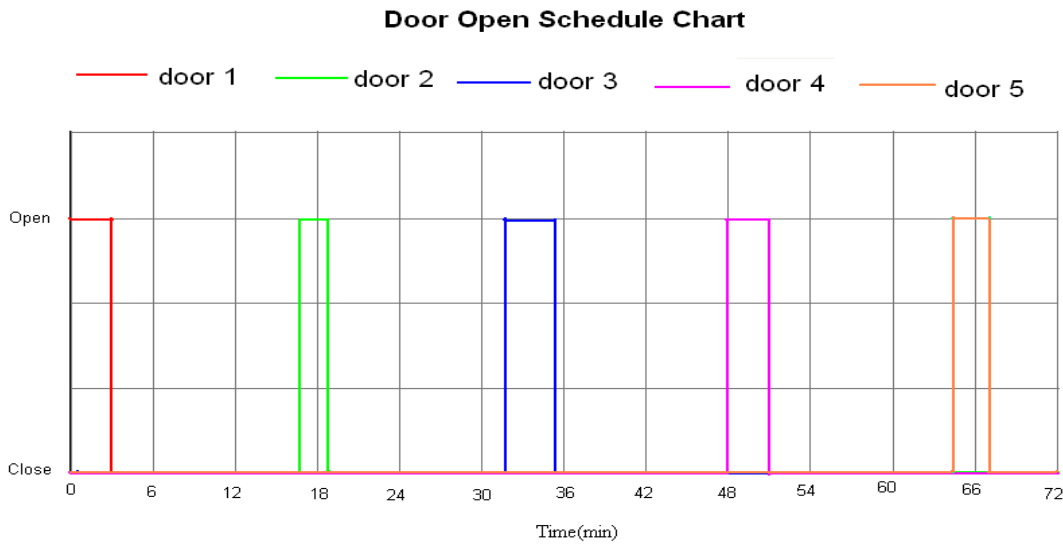


Figure 5.7 - The door open schedule based on the furnace layout represented in the time domain

An assumption was made for creating the door open schedule. The door is either open or closed so the intermediate positions are not considered in the schedule as shown in Fig.5-7.

The q_{dopn} is calculated based on the following equations,

$$q_{dopn} = \begin{cases} q_{dopn_rad} + q_{dopn_air_exchange}, & \text{while the last door} \\ q_{dopn_rad}, & \text{while not the last door} \end{cases} \quad (5.4)$$

$$q_{dopn_rad} = \eta \cdot \varepsilon \cdot \sigma \cdot A_{open}(\tau) \cdot (T_{fce}^4 - T_{door_outside}^4) \quad (5.5)$$

$$A_{open}(\tau) = \begin{cases} A_{door,m}, & \text{while door open} \\ 0, & \text{while door close} \end{cases} \quad (5.6)$$

As shown in equation (5.4) another assumption was made based on the experiments that there is not significant loss of heat in the intermediate zones due to the air exchange.

$q_{dopn_air_exchange}$ is calculated only for the last zone.

$$\begin{aligned} q_{dopn_air_exchange} &= c \cdot \sqrt{\frac{\pi^2 d^5}{16 \lambda l R T_{fce}}} \cdot (p_{fce}^2 - p_{door_outside}^2) \cdot (T_{fce} - T_{door_outside}) \\ &= c \cdot k_d \cdot (T_{fce} - T_{door_outside}) \end{aligned} \quad (5.7)$$

where,

d is the equivalent diameter of the door,

λ is the coefficient of heat conductivity,

l is the thickness of the door, R is the gas constant,

p_{fce} is the pressure in the door,

$p_{door_outside}$ the pressure outside the door, and

k_d is the empirical coefficient of heat convection (for the current furnace its 3.5 m/s based on the pressure experiments).

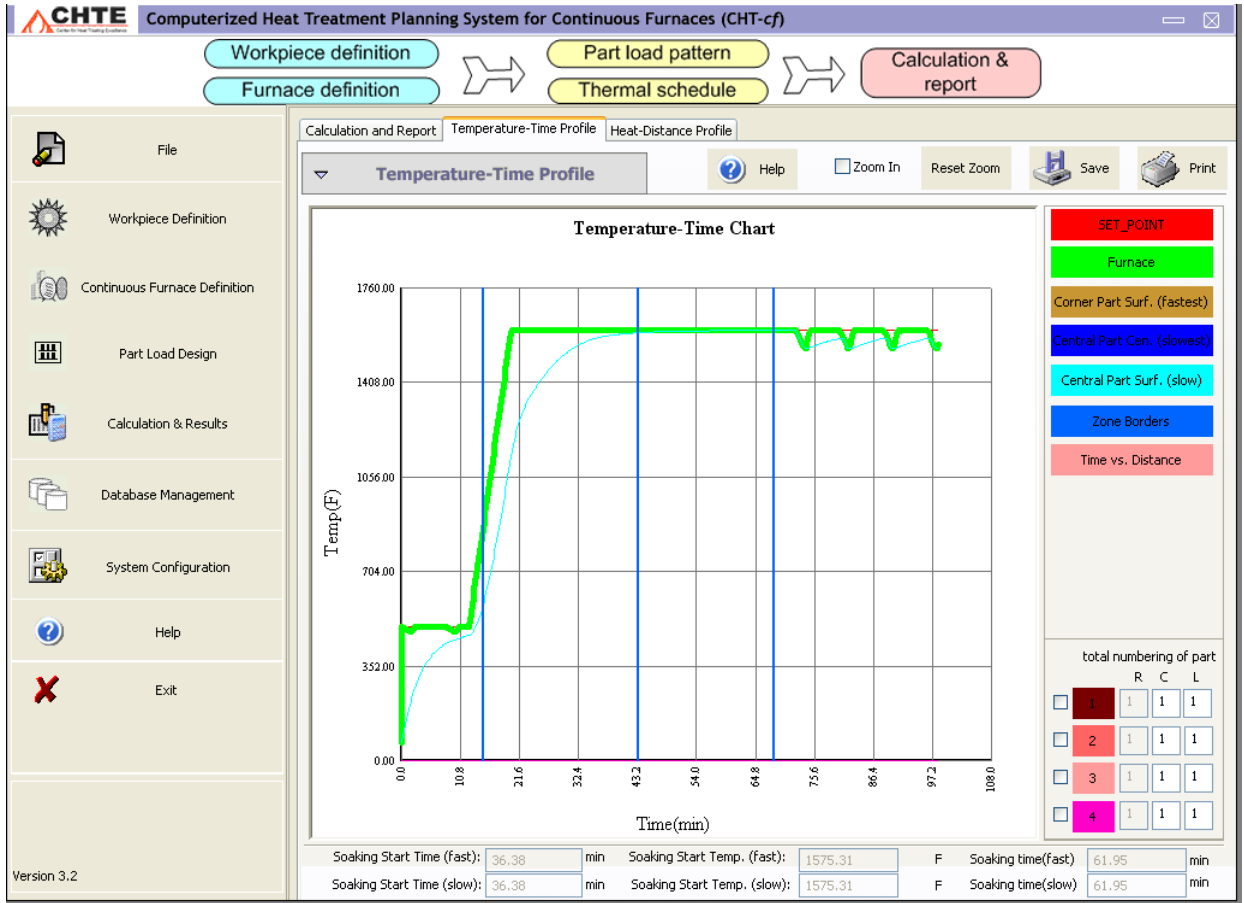


Figure 5.8 - The screen shot of the furnace thermal profile computed by CHT-c/f software using the improved furnace model

As observed in Fig. 5-8 the new thermal profile computed using the improved furnace model reflects the furnace temperature drops due to the door operation in the first and the final zones. This plot also shows the effect on the part temperature due to the variation in the furnace temperature. Another experiment was conducted to verify the improved furnace model.

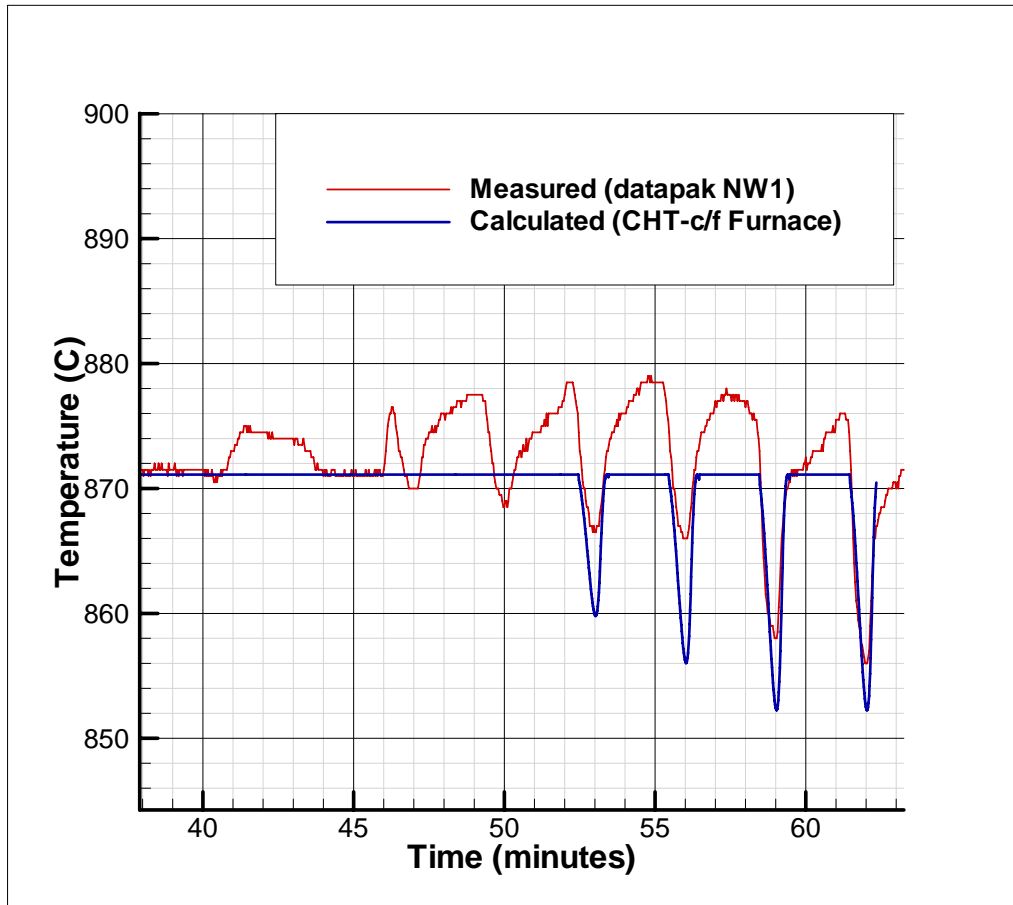


Figure 5.9 - *The comparison of the furnace thermal profile computed using improved furnace model and measurement results.*

As seen from the above Fig. 5-9 as well as from Fig. 5-8 the computed results now take into account the heat loss due to the furnace door operations. Fig. 5-9 also illustrates that the calculated furnace thermal profile is in good agreement with the measured results. This helps in accurate calculation of the part temperature profile especially in the last zones where the temperature of the part is critical in carburizing operations.

5.2.4 Conclusions

The new improved model was verified with experiments to take into consideration the heat loss involved with the door operations. The same modeling method can be used to determine the heat loss involved with other type of continuous furnaces, but in this study the model was verified only with the Pusher type continuous furnaces. Some of the problems with this new door model are: to accurately determine the heat loss due to door opening, and to differentiate the peaks arising due to the PID controller. The key to accurately determine the door opening peaks is to understand and filter the false peaks arising out of the controller activity.

5.3 The furnace gradient model ($\Delta T_{fce_gradient}^k(x, y, z)$)

5.3.1 Introduction

The furnace temperature gradient is a phenomenon that exists inside a furnace due to non uniform heating. This non uniformity in temperature directly affects the part temperature profile. And it has direct impact on the heat treating processes. For example a carburizing process operating at a carbon potential of 1% and running at 927 °C yields a 1.35mm case depth. If the carburizing temperature is reduced to 850 °C the carburized case depth achieved is only 0.8mm (for the same material and same carburizing duration a 40% reduction)

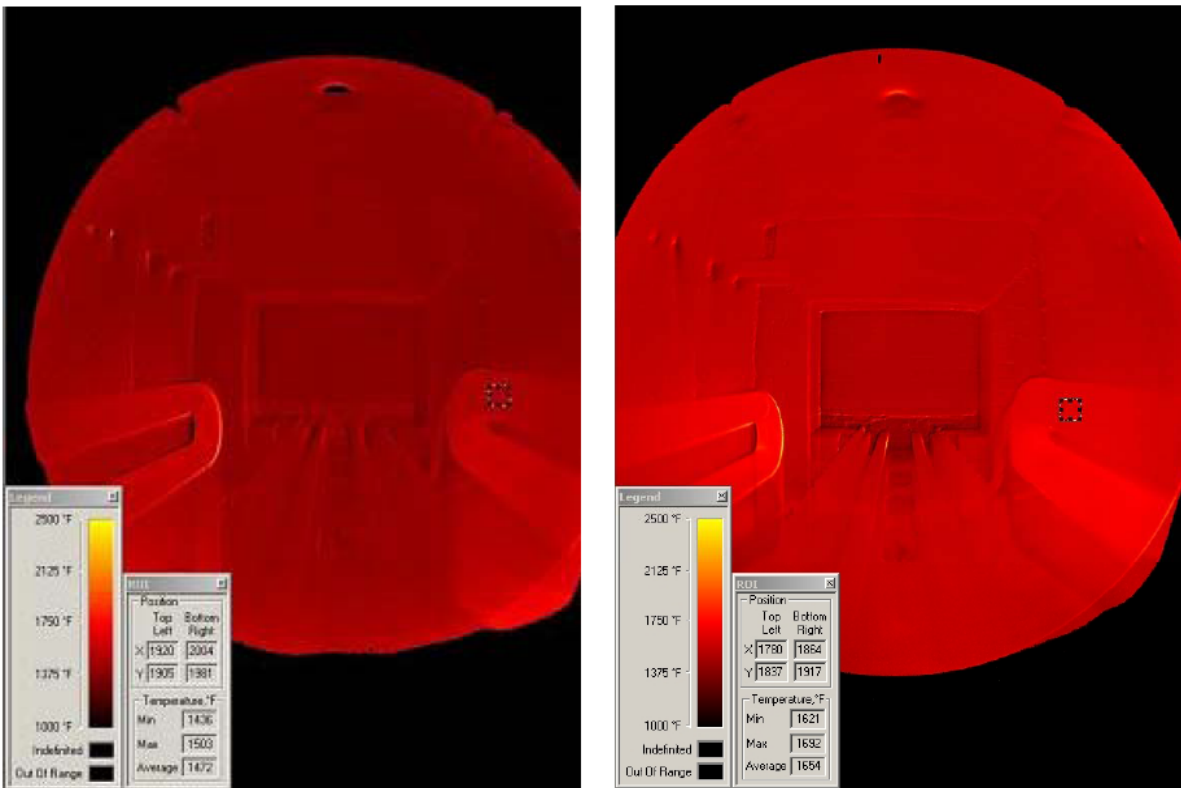


Figure 5.10 - The thermal gradients inside a batch type heat treating furnace[6]

The Fig 5-10 shows a thermal image captured inside a batch type heat treating furnace. There is a 22 °C variation (Max. 1692 & Min 1621 Fig. 5-10-right) with no load in the furnace.

5.3.2 Study of thermal gradients in continuous furnace (at 2 locations in 4 zones)

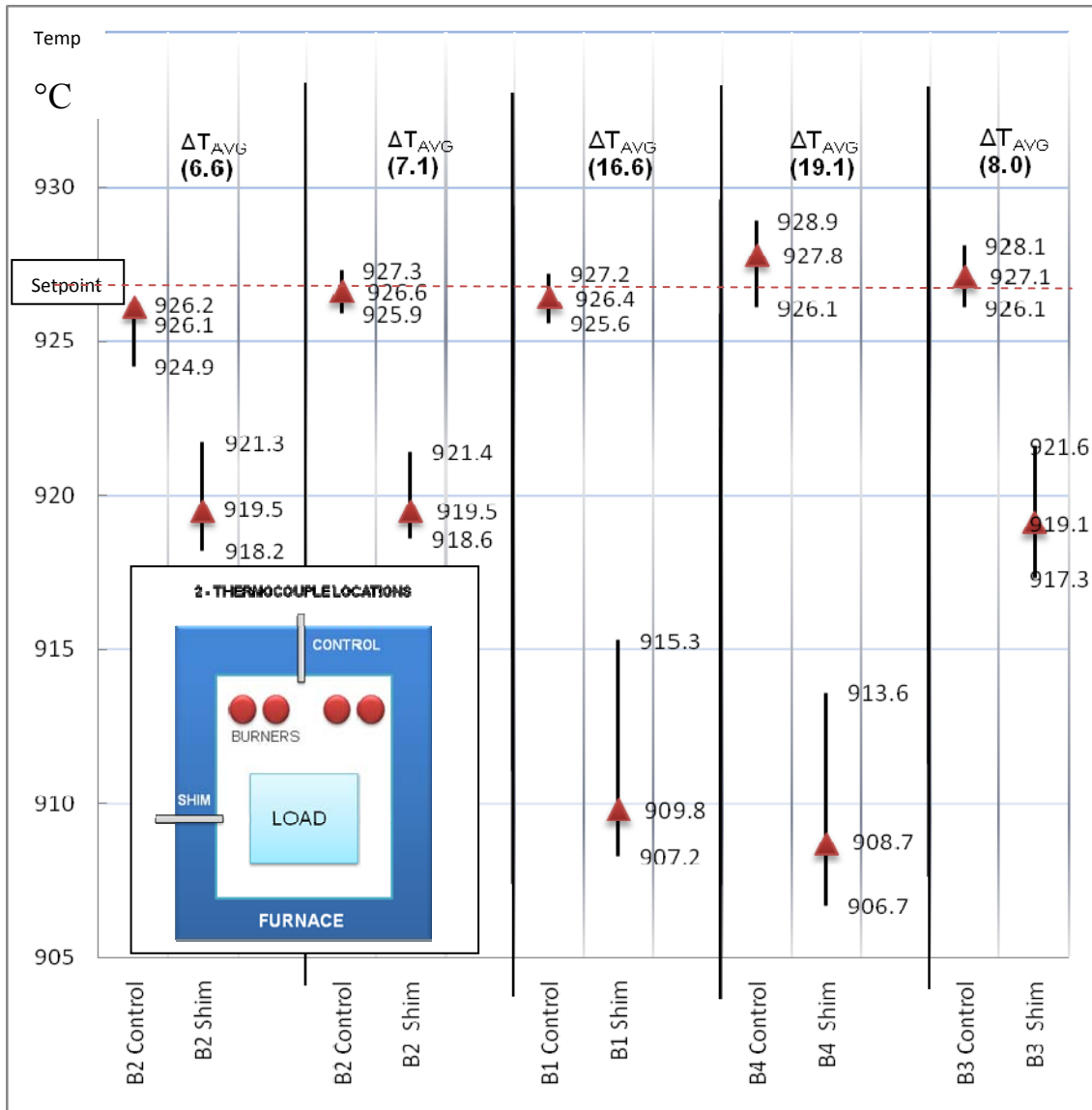


Figure 5.11 - Furnace temperature gradients and gradient variations in a fully loaded furnace over a period of 40 minutes in a Continuous Pusher type Carburizing Furnace with a push cycle time of 16 minutes.

Another experiment was performed to study the effect of load and the thermal gradient and variation in the gradient over a period of time in a continuous furnace. A carburizing type

pusher furnace was selected for the experiment and two thermocouple locations were selected. The first thermocouple was inserted close to the control thermocouple location, which is located near the top wall of the furnace above the burners and the second thermocouple was inserted through the shim port on the side wall of the furnace and was inserted around 6" from the inside wall of furnace. The temperature data were recorded simultaneously using two different data recorders. To check the repeatability of the experiments since two different experimental setups (different type of data recorders) were used, the experiments were repeated in Boost Zone 2 (B2) by swapping the control and shim setup after the first experiment was completed. As shown in Fig. 5-13 they had a good repeatability and the error was within 0.5°C, this gave us confidence to go ahead with the rest of the experiments in the other zones with two different experimental setups.

As observed in Fig. 5-11 furnace zones boost 1 and boost 4 (B1 & B4) had the highest average temperature gradient (ΔT_{AVG}) 14.6°C and 18.4°C respectively. And coincidentally the temperature variation was also the highest at the shim location in the zones B1 and B4 which was recorded over a period of 40 minutes. At the time of the experiments the furnace had a push time of 16 minutes, so 40 minutes gave an opportunity for the thermocouples to gather data over two push cycles. There were several observations made from the collected data. The T_{AVG} was always less than the median value (the data was collected at 10 second intervals and averaged). Also at the locations B1 and B4 where the temperature gradients were highest the T_{AVG} was closer to the min value. So from the experiments it can be concluded that the load has an effect on the furnace thermal gradient (ΔT_{AVG}).

5.3.3 Study of thermal gradients in pusher furnace

As discussed in the earlier door open model, when we conducted experiments to evaluate the accuracy of the continuous furnace model we came across thermal gradient problem that prevails in several industrial heat treat furnaces. In this particular furnace in which we were conducting experiments, the thermal gradients were significant (around 30°C) especially in the last zone due to the complex design of the furnace and lengthy radiant tube burners. Fig. 5-12b

illustrates the experimental temperature data collected using a datapak device with 6 thermocouples placed at different locations. Fig 5-12a shows the experimental setup and the location of the thermocouples.

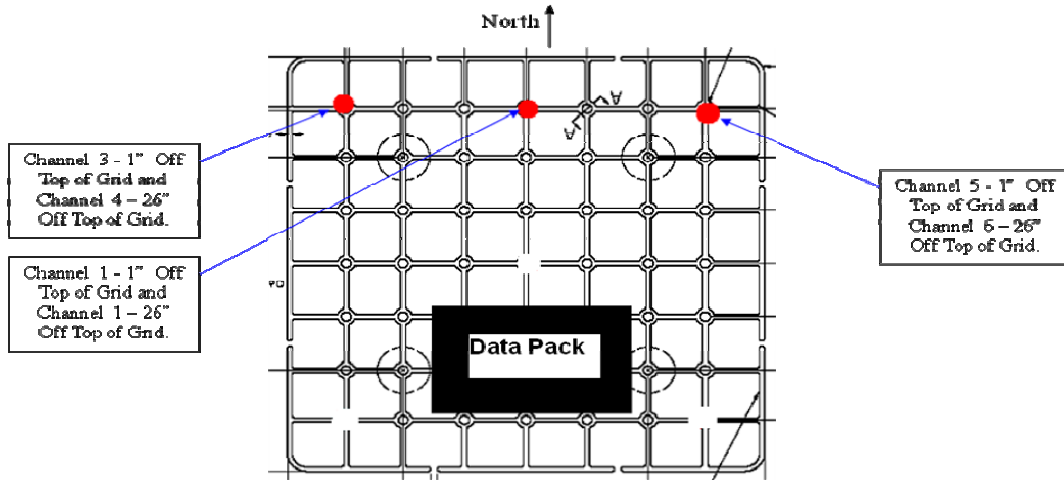


Figure 5.12a - Experimental setup showing the datapak and thermocouple locations inside the Pusher Furnace.

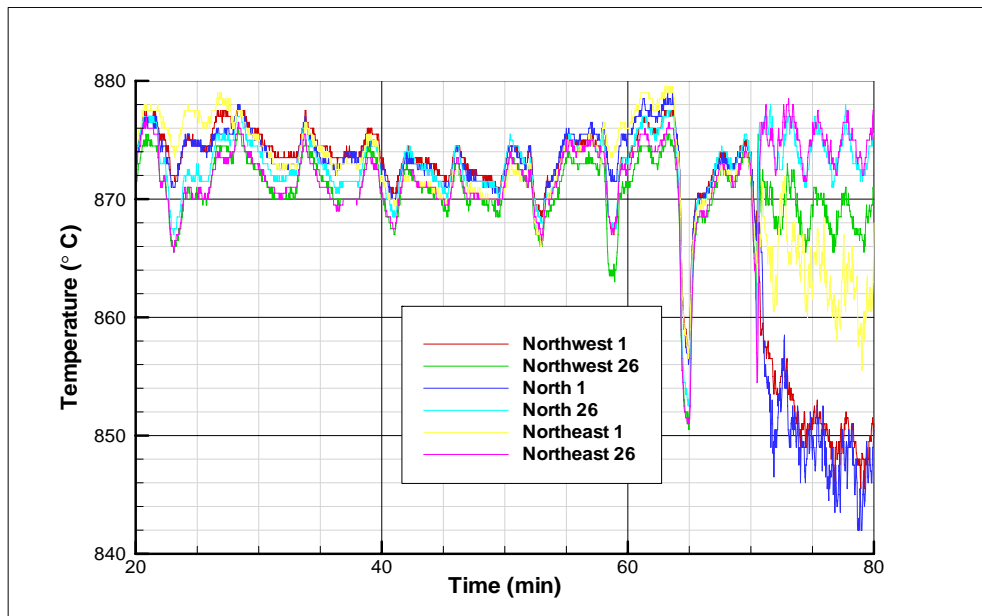


Figure 5.12b - The thermal gradients inside a Continuous Pusher Furnace, experimental data from continuous datapak with 6 thermocouples.

The thermocouples were placed in two groups, first set of 3 thermocouples were placed 1” from the top of the fixture grid and the second set of 3 thermocouples were placed 26” from the fixture grid. The thermocouple locations were marked North, Northeast and Northwest. North being the furnace push direction as shown in Fig. 5-12a. From the experiments it was clear the thermocouples that were located 1” from the fixture grid had a lower temperature compared with the rest of the thermocouples and this was significant in the last zone of the furnace. In certain locations where the furnace temperature drop was more than 30°C, it had a huge impact on the accuracy of the calculated furnace and part temperatures in the CHT furnace model.

5.3.4 Study of thermal gradients in rotary type continuous furnace (at 2 planes & 12 locations in 3 zones)

Since most of the experiments were conducted in continuous pusher type furnace several more experiments were conducted in different types of continuous furnaces to study the prevalence and the extent of the thermal gradients inside the furnaces.

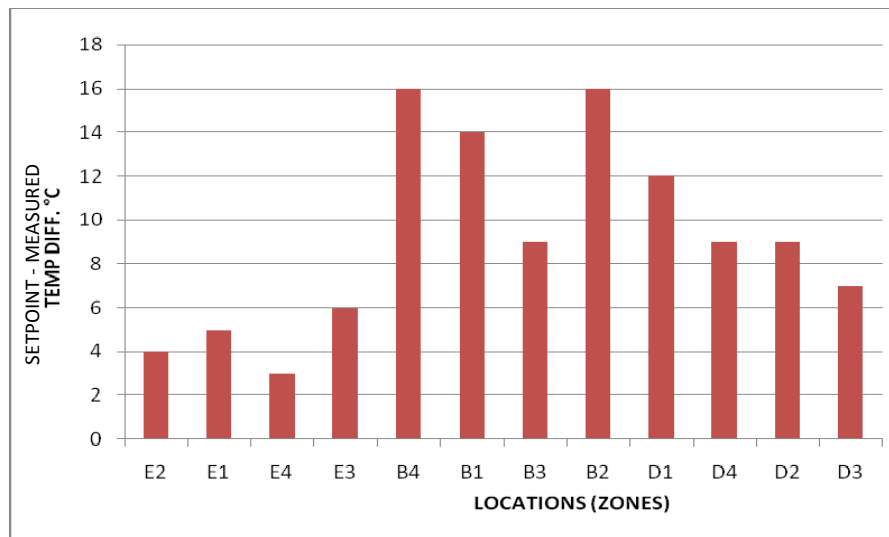


Figure 5.13 - *Temperature gradient between the set point temperature and the work area (center of furnace) at 3 different zones and locations in a Rotary type Continuous Furnace*

Figure 5-13 shows the thermal gradients present inside a rotary type continuous furnace. The different bars in the chart indicate 3 different zones (B – Boost zone, D – Diffuse zone and E – Equalize zone) and 4 different locations (1, 2, 3 and 4) in each zone. At the time of the experiments the Boost zone was at 927 °C, Diffuse zone was at 880°C and the Equalize zone was at 850 °C. All the four locations where the temperatures were measured were in the same place (near the work pieces). As seen in the graphs the Boost zone had the highest temperature difference between the setpoint thermocouple and the measured results. Again a 16 °C inaccuracy in the CHT furnace model due to the gradient that is present in the furnace is significant.

5.3.5 Gradient patterns

It is important to understand why thermal gradients exist inside the furnace. It is a complex issue to study all the possible gradients that exist inside the furnace. So only the gradients that are significant to the process and quality of the product are focused. In a carburizing furnace 10°C variation in the temperature in the boost zone affects the carbon potential by 3% and in the diffuse zone a 10 °C variation in the temperature affects the carbon potential by 10% C so any temperature variation in the 10 °C magnitude has consequences for the product quality.

Several experiments were conducted in different furnaces to determine the thermal gradients and the gradients that were more than 10°C from the set point temperature were analyzed. Out of the several possible causes the most predominant occurrence in the thermal gradient was when the burners were not symmetrically placed (for example if there were not equal number of burners on top and bottom of the furnace). It was observed in the experiments that if a zone has a long radiant tube burner a thermal gradient was present. The different burner schemes or layouts that are commonly used in the furnaces are shown in Fig. 5-14. As shown there are three different schemes that are commonly used,

1. Equal number of burners on top and bottom
2. Unequal number of burners (more burners on one side)
3. Burners on only one side (only on top)

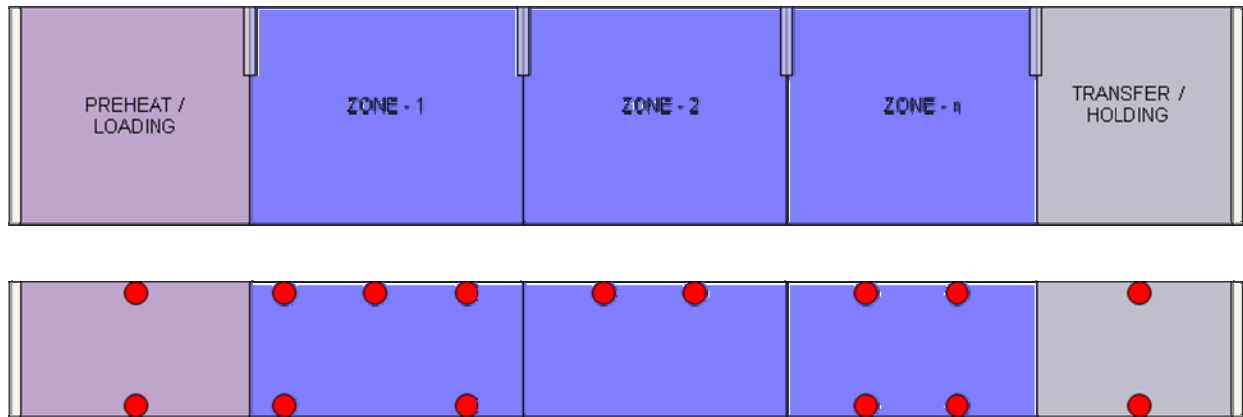


Figure 5.14 - *Different burner patterns / schemes commonly used in the Pusher Type Continuous Furnaces*

Several experiments were conducted with furnace with all three burner configurations. The case (iii), when there was burner present only on top side had the highest gradients observed. Fig. 5-15 shows the thermal gradients present in a furnace inside different zones. The zones 1-4 had equal number of burners on top and bottom. And zone 5 had burners only on the top.

5.3.6 Effect of burner layout on gradient patterns

As illustrated in Fig 5-14 there is a different layout of burners used in different zones of the continuous furnaces depending on the furnace design parameters. Usually the initial zones have the most number of burners with maximum energy to bring the parts to temperature as soon as possible. And different furnace manufacturers design and locate the burners differently inside the furnace. An experiment with a continuous pusher type furnace was conducted and the time scale was translated to distance and the effect of burner layout is analyzed. The burner layout pattern had a direct effect on the gradient patterns. The zone 5 had burners only on the top wall and no burners in the bottom and also due to the furnace design it had long burners.

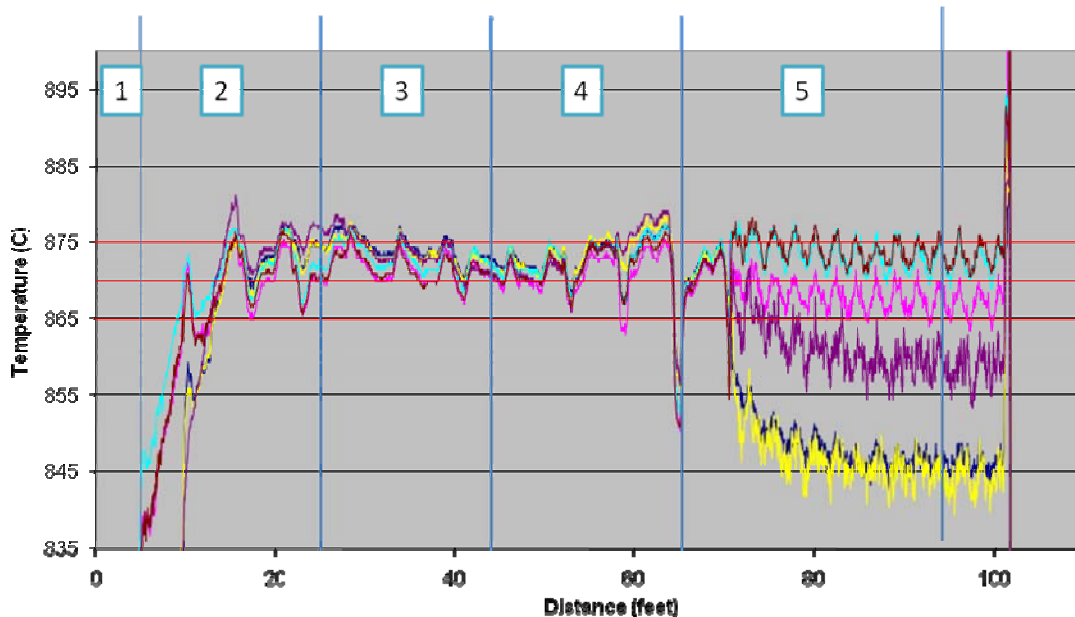


Figure 5.15 - Thermal gradients measured at different locations in a Pusher type Continuous Furnace with different zones marked.

From the graphs above in Fig 5-15 we can clearly see a gradient of almost 30°C is present. Also Holding Chamber (5 in Fig-5-15) had a long radiant tube so this created another variation in the temperature along the length of the radiant tube burner.

5.3.7 Different common burner layout types and gradient pattern (at furnace cross sections)

In order to understand the burner layout effects on the thermal gradient, a series of experiments were conducted in a relatively old continuous pusher type furnace that had all the 3 types of burner layouts in the different zones. A thermocouple was inserted at a location directly

underneath the burner through the hole on the top of the furnace and the temperature was measured for 2 parts pushed in the furnace and the average temperature was recorded. And the thermocouple was lowered into the furnace 1/3, 2/3 the total distance and all the way down from the top wall and measurements were repeated.

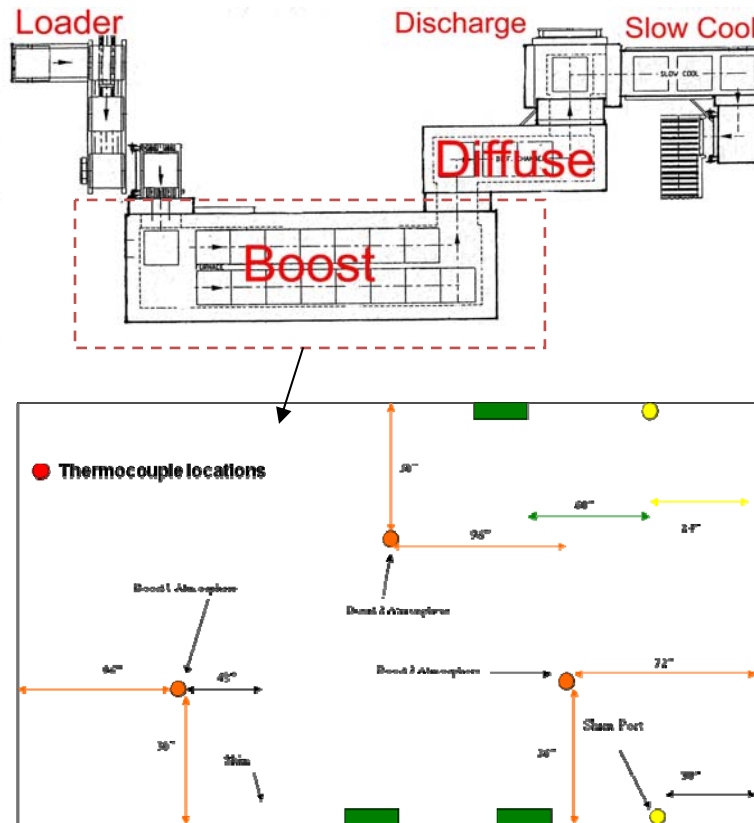


Figure 5.16 – The top view of boost zone with thermocouple locations and the corresponding shim port locations for the data gathered.

And the thermocouple was inserted into the side wall through the shim port of the furnace wall and the temperature was recorded near the furnace wall. And another data was recorded by inserting the thermocouple through the gas port located just above shim port on the side of the furnace wall. Fig. 5-16 shows the location of ports locations.

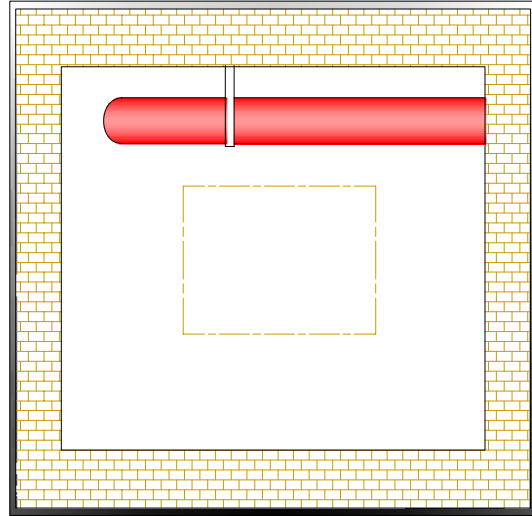
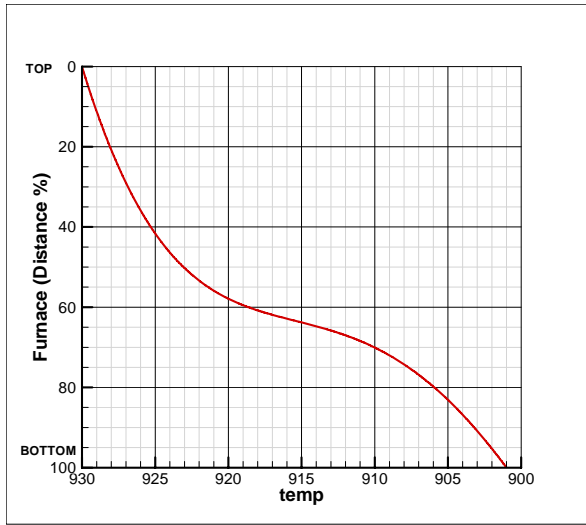


Figure 5.17a – The measured temperature gradient pattern inside furnace
– Holding Chamber (Burner layout – I)

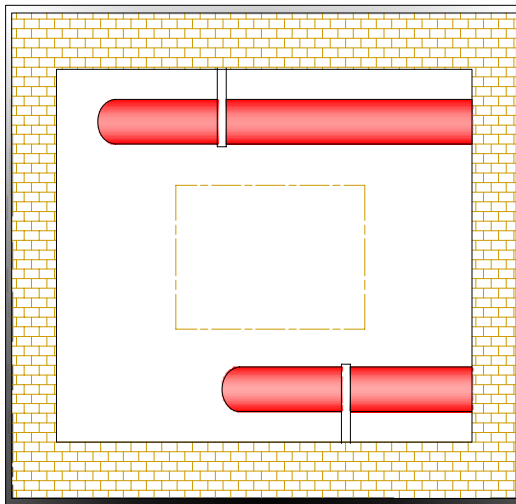
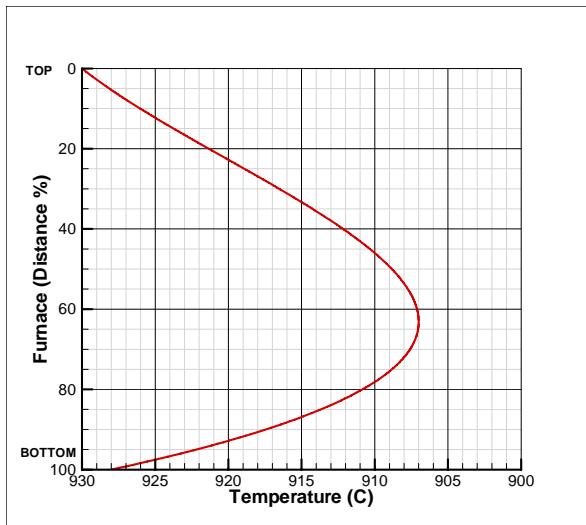


Figure 5.17b – The measured temperature gradient pattern inside furnace (Burner layout – II)

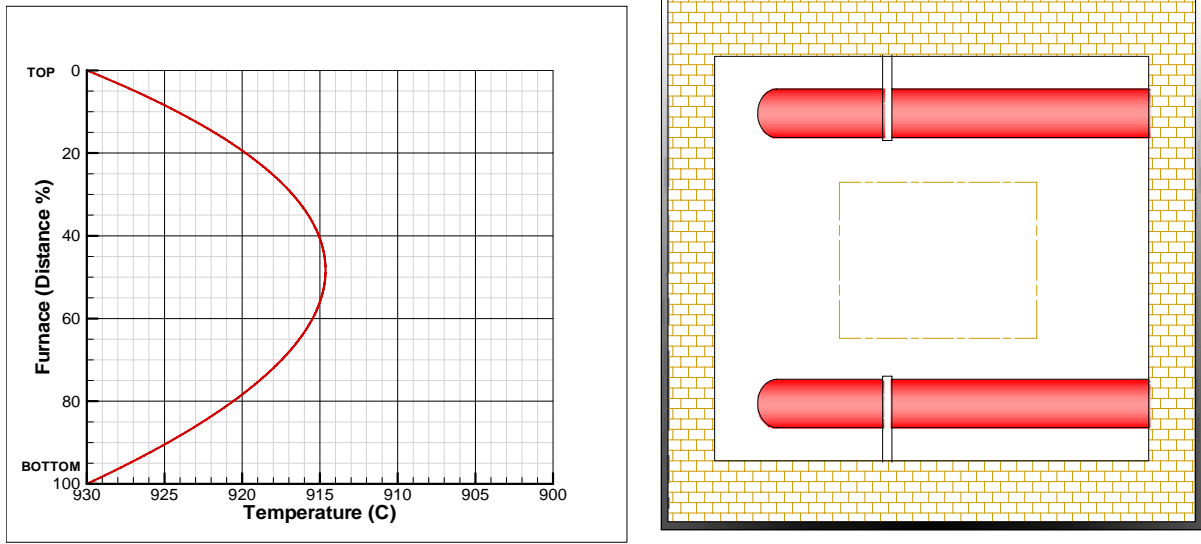


Figure 5.17c – The measured temperature gradient pattern inside furnace (Burner layout –III)

The Fig. 5.17 a, b & c represent the various gradient patterns that exist inside the furnace measured at 3 cross sections across the furnace. The next task was to use this cross-sectional data

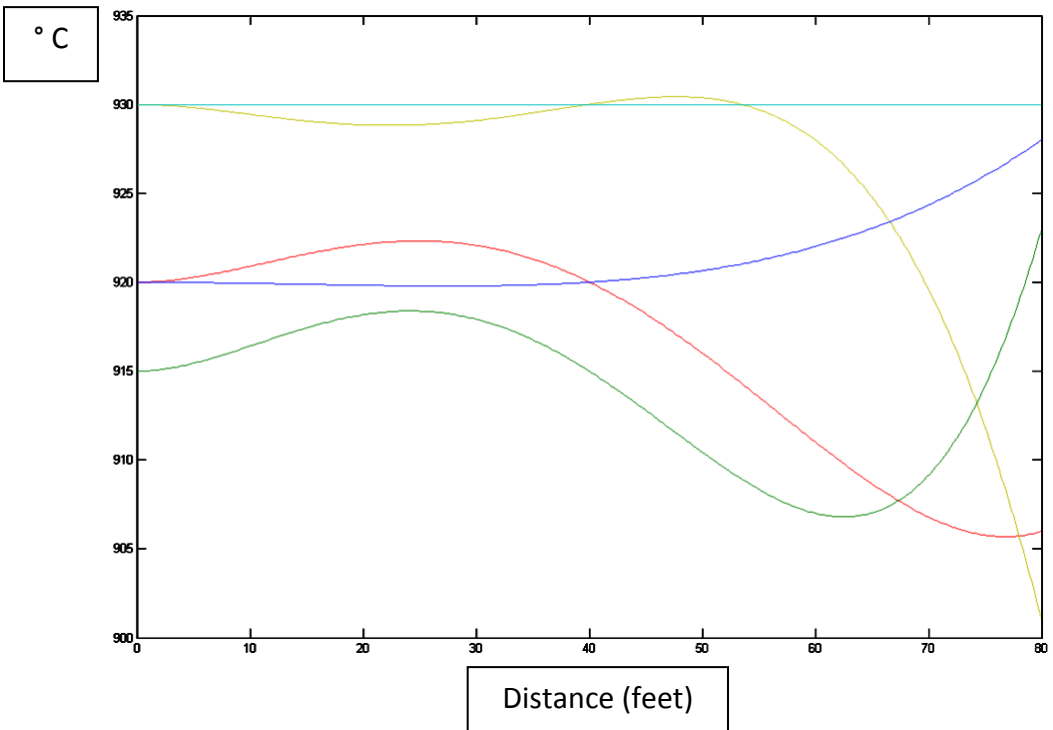


Figure 5.18 – The gradient generated across the entire furnace using the static experiments.

to generate the gradient pattern across the entire furnace length. The interpolated data generated from the cross sectional experimental gradients is shown in Fig. 5.18.

5.3.8 Furnace gradient model development

A new improved furnace model is developed in order to calculate the furnace temperature accurately by accounting the thermal gradients. A new term is added to the existing model to calculate the furnace temperature. The $\Delta T_{fce_gradient}^k$ is calculated based on the experimental data. Also a load constant A is included in the equation to account for the load size. The constant A is dependent on the size of the load that was used to determine $\Delta T_{fce_gradient}^k$.

$$T_{fce}^{k+1} = T_{fce}^k + \frac{Q_{storage}^k \cdot \delta\tau}{HC_{fce}} + A \cdot \Delta T_{fce_gradient}^k \quad (5.8)$$

where,

k is time space in the original equation and can be translated to space domain.

A=Load size constant

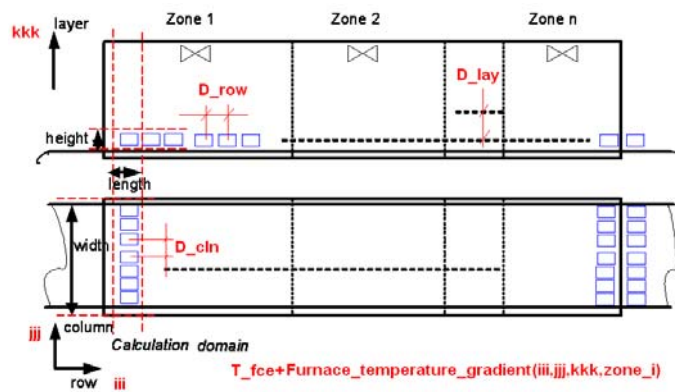


Figure 5.19 - Calculation domain of the $\Delta T_{fce_gradient}^k$ represented in the space domain and the location of i, j, k and zone in a Continuous Pusher Furnace.

Experiment design to calculate $\Delta T_{fce_gradient}^k$

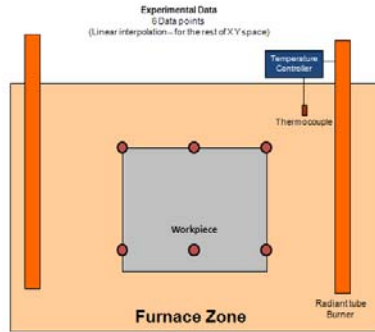


Figure 5.20 - Experimental setup to determine $\Delta T_{fce_gradient}^k$

An experiment is designed with 6 thermocouples either embedded in the workpiece or in a thermal probe and depending on the mass of the load the load constant A is calculated. The setup is run through a continuous furnace with the aid of a datapaq setup (as shown in Fig.5-11). This experiment provides us with data at 6 different points, but this data is not sufficient to create a gradient map for the entire furnace. The data from the experiments contain $\Delta T_{fce_gradient}^k$ (x,y,z,zone_i). This data is present in a certain work envelope inside the furnace and it is required to determine the rest of the gradients. We use trilinear interpolation in 3D space as illustrated in Fig. 5.21 to populate the gradients in the entire workspace inside the furnace.

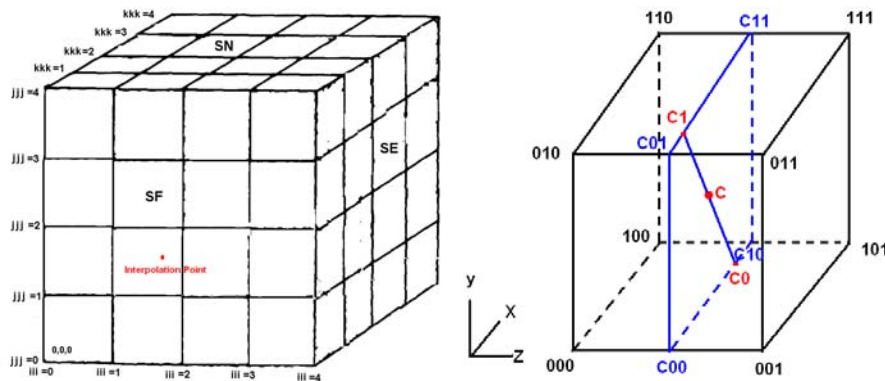


Figure 5.21 - Trilinear interpolation scheme to populate the thermal gradients from the experimental data.

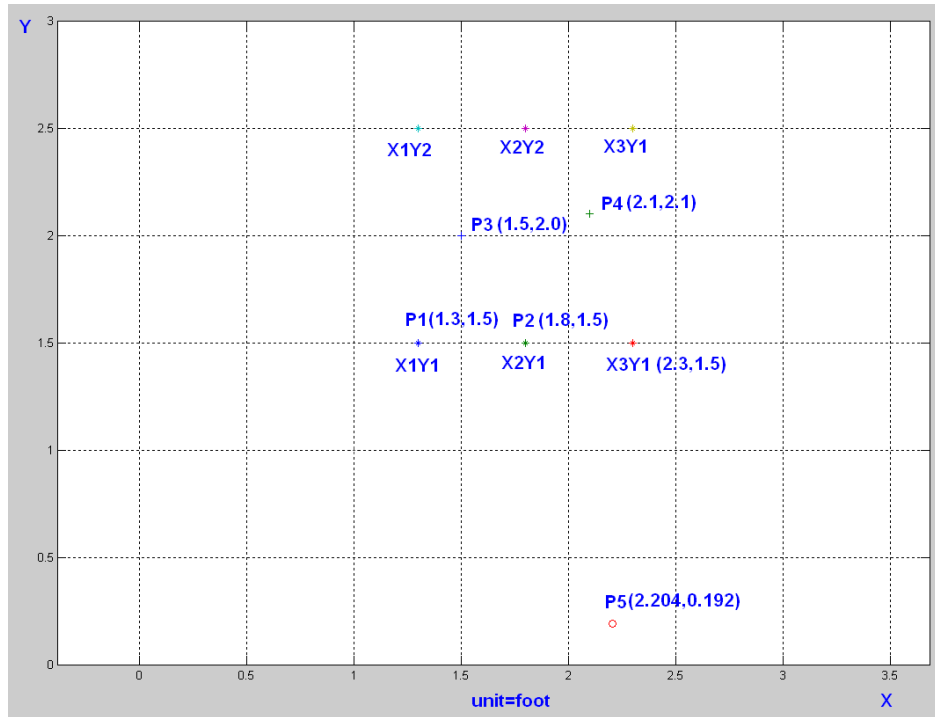
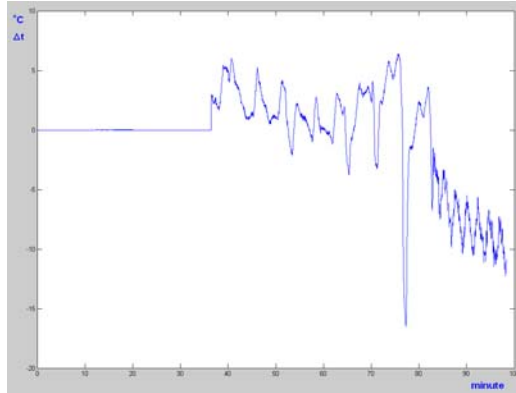
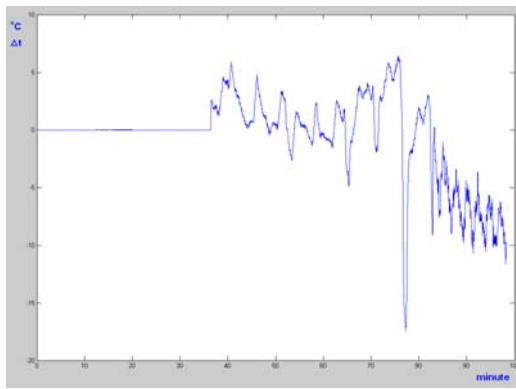


Figure 5.22 - Plot of workspace inside the furnace showing locations of the 6 $\Delta T_{fce_gradient}^k$ points measured using the experiments and 3 interpolated points (P3, P4 & P5)

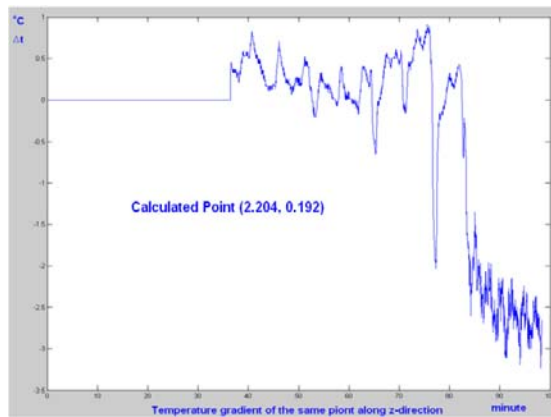
The experimental data from 6 points are used in the CHT furnace model to compute the thermal gradients. To verify the results from the model a new set of experiments are performed to calculate the furnace temperature based on the gradient model. Fig.5.22 shows the several points picked for the verification. X1Y2, X2Y2, X3Y2, X1Y1, X2Y1 and X3Y1 are the measured points where the data were collected. P1 and P2 were picked exactly at X1Y1 and X2Y1 to verify the calculated results match with the measured results. P3 and P4 were picked inside the measured workspace and P5 was picked outside the workspace.



5.23(a) - Interpolated $\Delta T_{fce_gradient}^k$ at point P3



5.23(b) - Interpolated $\Delta T_{fce_gradient}^k$ at point P4



5.23(c) - Interpolated $\Delta T_{fce_gradient}^k$ at point P5

Figure 5.23 - Plots of calculated $\Delta T_{fce_gradient}^k$ at points P3, P4 & P5 (refer Fig.5.22 for locations)

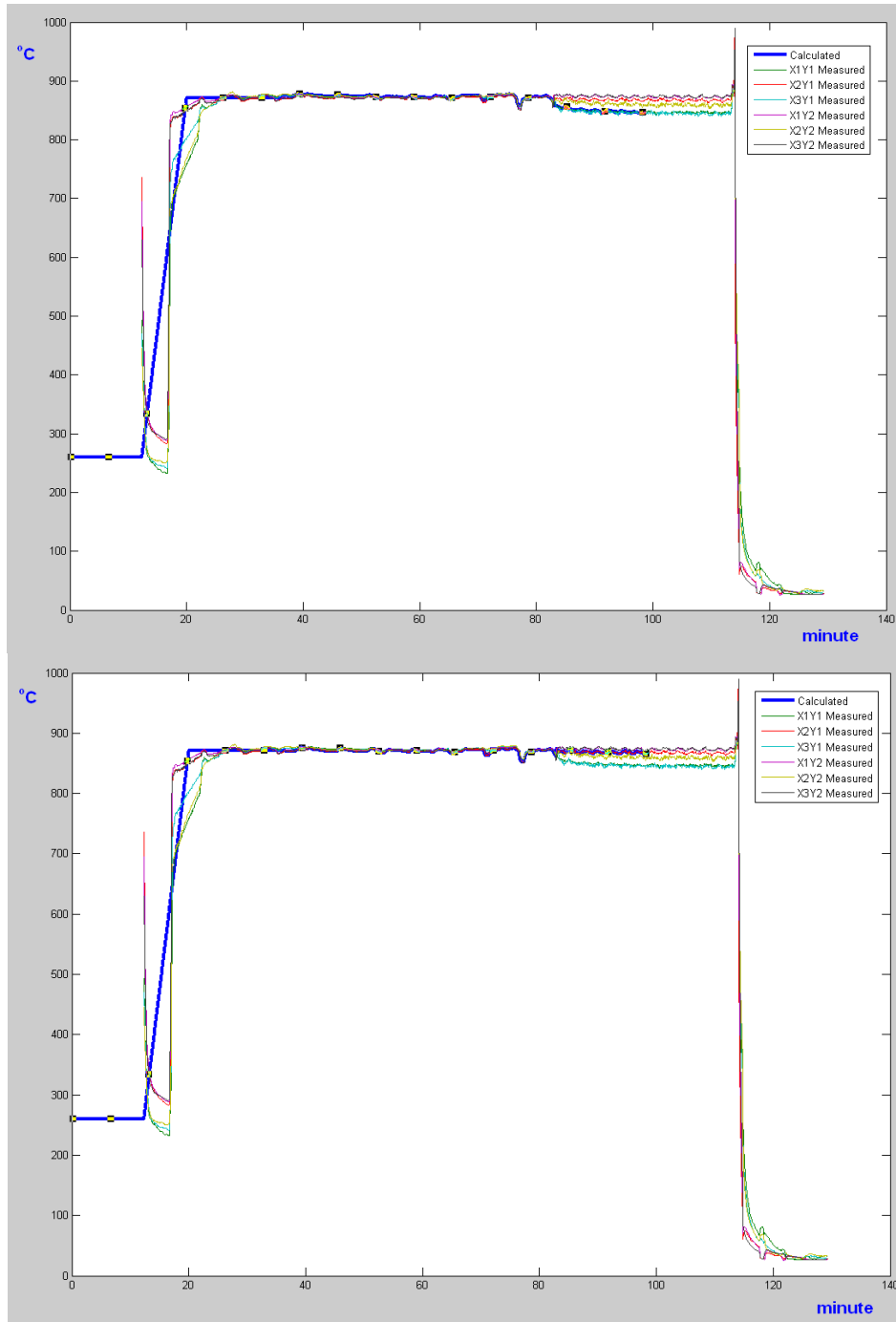


Figure 5.24 - Comparison of the measured and improved CHT model calculated results in a Pusher type Continuous Furnace. (Top figure - calculated near top of the load, Bottom figure- calculated near bottom of load)

Fig. 5.23 shows the plots of $\Delta T_{fce_gradient}^k$ interpolated from the measured result and they agreed with the rest of the data. Fig. 5.24 shows the comparison of the measured and the calculated results based on the improved CHT furnace model with thermal gradients. The comparison was done at two points - one on top of the load shown on the top figure and another at the bottom on the load shown in the bottom figure in Fig. 5.24. The computed results were in good agreement with the measured results and the improved model also reflected a change in the calculation of the part temperature due to the furnace temperature gradient. This ultimately enables us to accurately predict the part temperature of the workpiece present in different locations in the furnace by taking into account the furnace gradient anomaly.

5.3.9 Conclusion

The gradient model for furnace gradient determination was developed and verified by using continuous experiment data (datapaq), conducting several experiments at different cross sections of the furnace zones and constructing the gradient thermal profile across the furnace length. The method demonstrated good accuracy in predicting the gradient pattern existing in the furnace. But a thorough experiment is required to construct the gradient pattern accurately. Under the cross sectional experiments the generated profile was not verified with the experimental data but it is a quicker alternative to develop the furnace gradients.

5.4 Virtual load design and calibration ($\Delta T_{fce_virtual}^k$)

During the course of experiments at different CHT customer locations, one of the feedbacks was the furnace that we have do not have the exact furnace in the CHT software database. And they were of opinion if we had a specific model tailored to the furnace at the customers location our accuracy would be better. The main problem currently is the universal furnace model and it's difficult to design a specific furnace model for every furnace in the shop. So the idea was to build a comprehensive furnace model, one for Batch furnaces and another for continuous furnaces. And to overcome the different issues we currently face a virtual load is used to determine and adjust various key parameters to accurately reflect the current state of the furnace in the shop floor. The virtual load is not real workpiece, it's made of the same material as real load, but in simple geometry, such as cylinder, block, and plate etc., to conduct the experiment for the calculation of several key parameters required for the furnace model.

Some of the key problems encountered with the CHT model were the inaccuracy in the furnace and the part temperature especially during the initial heatup. After a detailed analysis of the experimental results the key reason of these inaccuracies was attributed to a deteriorated furnace condition. The furnaces like other machine tools wear over time and their heat inputs and heat loss change, especially the insulation gets spalled and corroded and furnace structures fail due to creep. Fig. 5.25 shows the pictures of the furnace walls deteriorated over time. These introduce inaccuracies in the input information for the furnace model, and reflect in the final furnace temperature. Although several factors could be attributed to this problem, it was decided to focus on the top parameters that likely will reduce the errors. The key factors selected for improvement were,

1. Furnace emissivity
2. Heat loss (Q_{LOSS}) & Heat input (Q_{HT})



Figure 5.25 - *Spalled and corroded furnace refractory walls [12]*

5.4.1 Furnace emissivity

Currently the furnace emissivity is determined from the CHT database. The data in database is populated based on the data available from the furnace and refractory manufacturers. And the emissivity data is sensitive to the surface condition of the refractory, and the data is compiled based on an assumption of brand new furnace. As shown in the Fig. 5-25 the furnace wall emissivity changes over time and this affects the furnace model.

Heat input (Q_{HT}) & Heat loss (Q_{LOSS})

In the current model the Heat Input (Q_{HT}) & Heat Loss (Q_{LOSS}) are calculated based on empirical equations determined from experiments. These values are calculated based on the ideal new furnace conditions. The heat input from the radiant tube burners is also dependant on several parameters, often a leaky radiant tube or an improperly tuned burners result in a reduced heat input as high as 30% [13]. The heat loss also becomes significant if the furnace refractory bricks are spalled and it exposes the external furnace wall or the consecutive refractory layers.

5.4.2 Designing virtual load

The virtual load is not real workpiece, it's made of the same material as real load, but in simple geometry, such as cylinder, block, and plate etc., and the dimension should meet the following criteria. The *Biot* number of the virtual load should be less than 0.1. The Biot number means the ratio of outside heat transfer coefficient to the conductive heat transfer coefficient inside the workpiece[11]. It is used to assess the temperature uniformity of the workpiece .The criteria is defined as,

$$Biot = \frac{ht_{eff}}{\lambda} \begin{cases} < 0.1 & \text{lumped} \\ \text{Otherwise} & \text{massive} \end{cases} \quad (5.9)$$

where,

h is the heat transfer coefficient of the workpiece surface and environment, it's the combination effects of convection and radiation, $h = h_{convection} + h_{radiation}$, λ is the thermal conductivity,

t_{eff} is the equivalent thickness of the workpiece.

For different shapes the equivalent thickness calculation is different, as follows:

$$t_{eff} = \frac{V}{A} \quad \text{Plate} \quad (5.10)$$

$$t_{eff} = \frac{2V}{A} \quad \text{Cylinder/ bar with rectangular section} \quad (5.11)$$

$$t_{eff} = \frac{3V}{A} \quad \text{Sphere/cubic} \quad (5.12)$$

where V is the workpiece volume.

By selecting virtual load with *Biot* number less than 0.1, the heat transfer between the furnace walls and virtual load can be easily solved as 1D problem, discussed in next section.

5.4.3 Determination of the furnace model constants using virtual load

The furnace temperature is calculated from the following equations

$$T_{fce}^{k+1} = T_{fce}^k + \frac{Q_{storage}^k \cdot \delta\tau}{HC_{fce}} \quad (5.13)$$

where,

$$Q_{storage}^{k+1} = Q_{ht}^k - Q_{loss}^k - Q_{load}^k - Q_{cooling}^k + Q_{fan}^k \quad (5.14)$$

Correcting the heat loss (Q_{loss}^k)

A new method using the virtual load is used to calculate the heat loss. The heat loss is related to the layers thickness, density and specific heat, the exterior surface temperature.

$$Q_{loss_VLoad}^k = \frac{T_1 - T_0}{\frac{s_1}{\lambda_1} + \frac{s_2}{\lambda_2} + \dots + \frac{s_n}{\lambda_n} + \frac{1}{\alpha}} \quad (5.15)$$

where s_i , λ_i are the thickness and conductivity of the furnace wall insulation layers, respectively. T_1 is the temperature of the virtual load and T_0 is the outside temperature of the furnace wall. α is the thermal diffusivity from furnace outside to atmosphere.

Correcting furnace emissivity

For the virtual load ($Biot < 0.1$), the emissivity of radiation between furnace walls and the virtual load can be solved by the Lumped Heat Capacity [14]

$$Q_{radiation} = m \cdot c_p \cdot \frac{dT}{dt} = \sigma \cdot \varepsilon \cdot A \cdot (T_{fce}^4 - T_{ld}^4) \quad (5.16)$$

where

m is the mass of the virtual load,

c_p is the specific heat of load material,

σ is the Stefan-Boltzmann constant,

ε is emissivity,

A is the exposure surface area of the workpiece,

T_{fce} and T_{ld} are the temperatures of furnace and load respectively.

Therefore heat the virtual load in the furnace shutting down the fan and atmosphere, and measure the load and the furnace wall temperature by embedded thermal couples, the emissivity of the material can be reverse calculated by

$$\varepsilon_{measured} = \frac{m \cdot c_p \cdot \frac{dT}{dt}}{\sigma \cdot A \cdot (T_{fce}^4 - T_{ld}^4)} \quad (5.17)$$

This procedure is also helpful to build a life time emissivity model E (lifetime) for a specified material by knowledge discovery the customer data sets.

5.5 Conclusion

Several challenging issues that affect the accuracy of the furnace model are analyzed and incorporated in the improved furnace model. The three key areas where the model was improved were in calculation of accurate heat loss due to door operations, modeling the thermal gradients present inside the furnace and the virtual load design and calibration for determining the different furnace parameters associated with furnace deterioration over time.

CHAPTER – 6

Knowledge data discovery based furnace model

In the United States, approximately 5,000 facilities operate roughly 55,000 furnaces[15]. Furnaces are widely used in heat treating metal products to achieve the desired material properties by accurately controlling the furnace temperature close to the set points. In order to study and optimize the heat treating process by numerical modeling, the key is the furnace model. The furnace model is used to simulate the furnace operations, evaluate the energy input and heat distribution in the furnace, and finally predict the furnace temperature, which is required for calculating the load's temperature profiles.

Current furnace model

During the heating process of heat treatment, the workpieces are heated in the furnace. The mixed fuel gases are fired in the burner, and the cold workpieces, furnace walls, furnace accessories etc. will absorb heat from the hot burner. Furnaces which are equipped with a water cooling system also absorb part of the heat. Heat loss also occurs through the opening area, like holes on the wall of the furnace. Thus, heat is distributed to different parts inside the furnace through the above mentioned processes, see Fig. 6-1.

The total heat in the furnace will be in balance, therefore

$$Q_{ht} = Q_{fue} + Q_{ld} + Q_{loss} + Q_{cl} \quad (1)$$

where,

Q_{ht} is the heat input generated by the mixed fuel gases that are burning in the furnace

Q_{fce} is the heat stored in the furnace wall and accessories

Q_{ld} is the heat distributed to the load of workpieces via radiation and convection

Q_{loss} is the heat loss through opening areas, and

Q_{cl} is the heat absorbed by water cooling system.

These Q variables are called heat items, and are described in the earlier chapters.

It's assumed that all the accessories have the same temperature and the temperature distribution in accessories is uniform, therefore the heat exchange of a loaded furnace can be mathematically presented in following model:

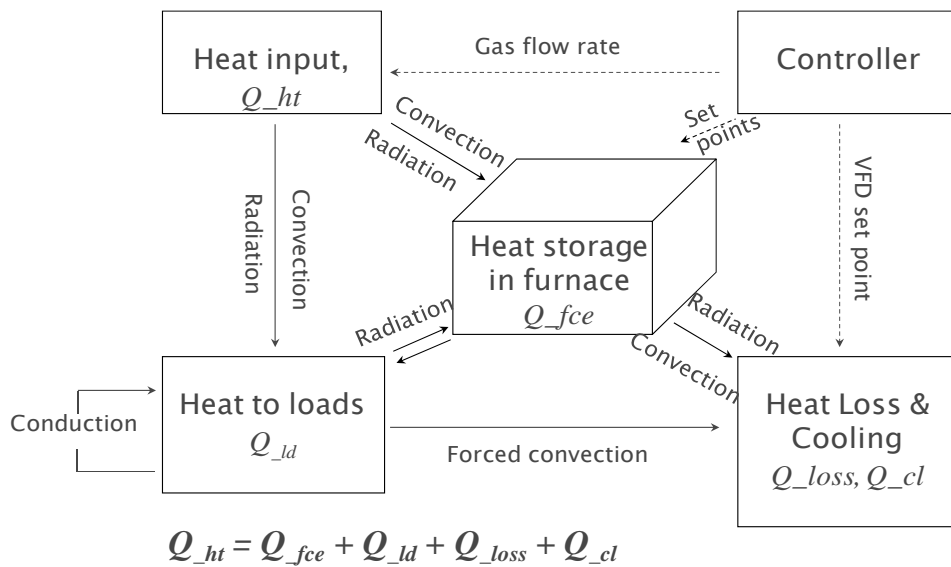


Figure 6.1- Heat distribution and balance in the furnace

$$Q_{fce}^{inc} = \sum_{i=1}^N (\rho_i \cdot cp_i \cdot V \cdot \frac{\partial T_i}{\partial \tau}) \quad (2)$$

where N is the quantity of accessories in the furnace. And the average furnace temperature increment in a small time step can be calculated by

$$T_{fce}^{inc} = \frac{Q_{fce}^{inc} \cdot \delta\tau}{\sum_{i=1}^N (\rho_i \cdot cp_i \cdot V_i)} \quad (3)$$

where,

T_{fce} is average furnace temperature

Q_{fce} is the average storage of heat flux in a loaded furnace, superscript *inc* means increment

$\delta\tau$ is the time interval

ρ_i , cp_i , and V_i are the density, specific heat, and the volume of accessory i in the furnace.

These accessories include all the components involved in the heat treating process except the workpieces.

Problem Identification

Based on the furnace model and CHT Technology, the CHTE center at WPI have developed thermal analysis models and simulation tools for loaded batch (CHT-*bf*) and continuous (CHT-*cf*) furnaces for the heating up processes. The CHT technology has been tested and validated via more than twenty cases studies using production data. The prediction accuracy is generally good, but varies case by case. The main issue of current CHT technology has been identified as,

- Universal furnace model is used for all furnaces even though the individual furnaces are designed differently;

- Even for the same type of furnaces, the performance may vary under different production environments and at different life time of the furnace;
- Since the furnace model used is an approximation, the user can not modify the model accurately to achieve the desired results; and
- There is no method to evaluate the different models to help diagnose the issue, and find a solution.

Consider the heat distribution in a small time step i , from Eq. 1,

$$q_{fce}^i = q_{ht}^i - q_{ld}^i - q_{loss}^i - q_{cl}^i \quad (4)$$

where $Q = \{q^1, q^2, \dots, q^m\}$. The heat items are empirical equations gained from experience and essential to the furnace temperature prediction. However furnaces are of different types, operation strategies, working conditions etc.

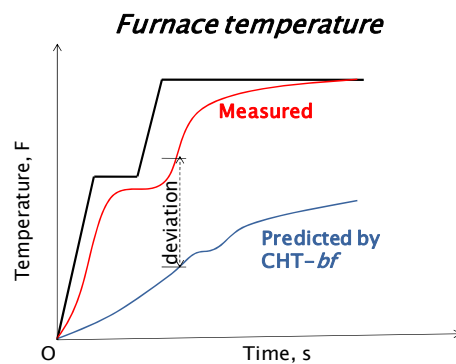


Figure 6.2 - Error of predicted furnace temperature (Illustration)

Therefore the predicted furnace temperature deviates from the actual measurements in some cases, as shown in Fig. 6-2. This means the calculated heat distribution inside the furnace is not accurate.

Developing a breakthrough technology through adaptive modeling to improve the simulation accuracy is necessary to commercialize the CHT technology, and thus promote the market growth for the CHT technology and broaden the utilization of the CHT software tools.

Strategy of Technical Solution

For CHT technologies, CHT-*bf* and *cf*, an accurate set of furnace rules and knowledge are essential to simulate and optimize the heat treatment processes. This knowledge is hard to discover from the limited number of furnace studies, and production data that are available. Since this data will change from furnace to furnace, load to load, a more flexible furnace model which is adaptable to these changes is desired.

In this project in order to improve the accuracy of the heat distribution, an upgraded furnace model based on KDD technology is developed, which can flexibly re-adjust the heat distribution using the test data. A series of undetermined coefficients are employed in Eq.4, these coefficients are dependent on the furnace type, and load pattern.

The technical solution strategy is plotted in Fig.6-3.

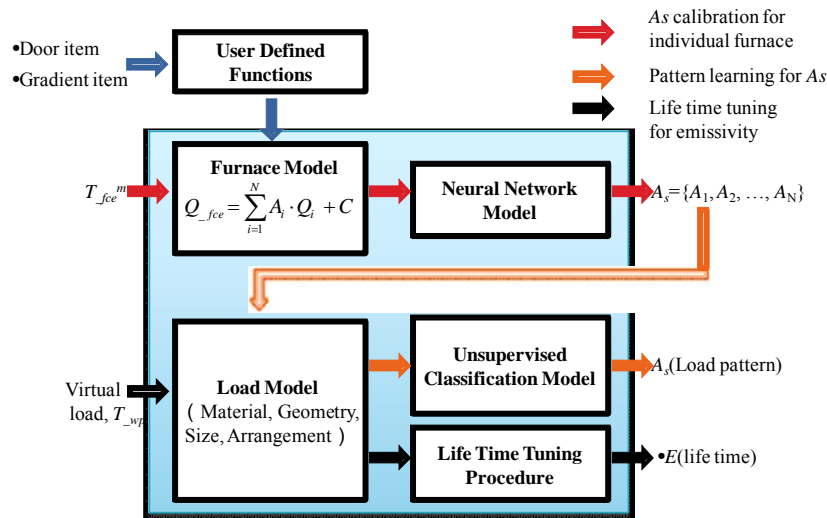


Figure 6.3 - Strategy logic of KDD furnace model solution

To find a set of coefficient values, the new furnace model will be studied using a neural network which will produce minimum error between the predicted results and measured furnace temperature (red arrow). Since different load patterns may have different coefficient values, a maximum entropy model will be used to classify the load patterns into groups, and all the load patterns in a particular group will have similar coefficient values. Consequently, the rules between the undetermined coefficient and load patterns will be discovered, and used to improve the prediction accuracy (orange arrow).

The black arrow represents the proposed calibration procedure. The heating, especially the radiation ability of furnace varies during the life time of the furnace. This can be studied by reverse calculating the emissivity of the virtual load heated in the furnace. Calibration can also be applied to the convection model to study the heat transfer coefficient. Furthermore, the new developed hypothesis model will allow the user to customize Q item, which can be calculated by

the calibration, and adjusted by the red and orange arrows itself or together with the original items.

6.1 Furnace calibration model

Theoretically, if all the heat items in Eq. (4) are correctly defined in the empirical equation, which estimates the heat stored in the furnace accessories, the furnace model will produce accurate furnace temperature. But an error in the prediction of the furnace temperature (Fig. 6-2) cannot be avoided, since these empirical equations are obtained from the studies of limited types of furnaces, and do not consider the effects of real production conditions. An error in the furnace temperature prediction means the estimation of heat stored in separate furnace parts is not accurate, and thus the heat items must be adjusted.

It's hard to verify and modify heat items one by one, because these items are related to each other.

However, all the heat items must be in balance in Eq. (4). It's possible to assume that the heat items can be adjusted such that the total heat is redistributed in the furnace. Therefore keeping all the heat items same, but their proportions of the total energy are adjusted for different conditions.

The solution is to introduce the undetermined coefficients in equation (4), which then becomes

$$q_{fce}^i = A_1 \cdot q_{ht}^i - A_2 \cdot q_{ld}^i - A_3 \cdot q_{loss}^i - A_4 \cdot q_{cl}^i + C \quad (5)$$

where,

A_1, A_2, A_3, A_4 , are the proportions of different q items,

C is a constant used to evaluate the heat storage of the undiscovered heat item.

6.1.1 Neural Network Calibration Procedure

Since these A 's can be considered as weight functions, Eq. (5) is also used to evaluate the contribution of the heat items to the furnace temperature, and adjust the heat redistribution (value of q items) based on calibration for individual furnace.

Eq. (5) can be studied by carefully designed neural network as shown in Fig. 6-4, to determine the optimized A_s vector $\{A\}$ by minimizing the error between the predicted furnace temperature T_{fce}^{nm} and measured furnace temperature T_{fce}^m . Finally A_s are introduced to CHT- bf , and will predict the new furnace temperature T_{fce} , which is close to T_{fce}^m

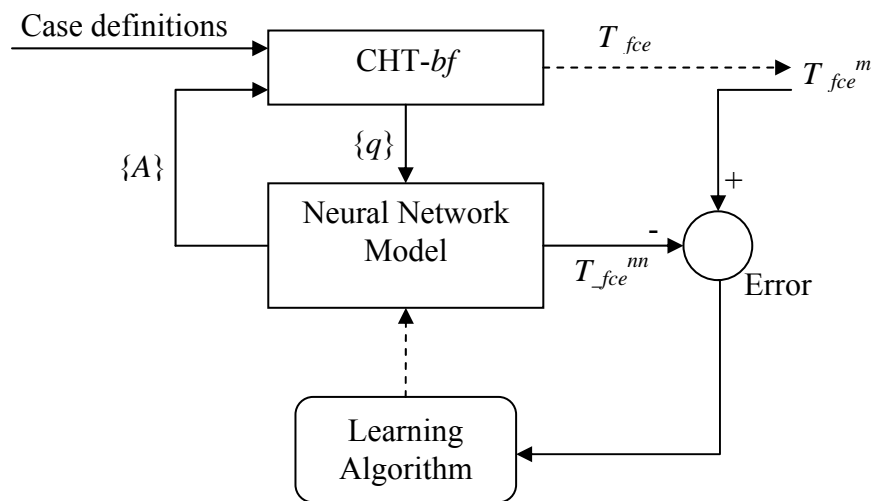


Figure 6.4 - Neural Network based calibration furnace model

The whole procedure is defined as follows:

- ▶ Step 1-Measurements

Measurement of furnace temperature during production, have $T_{fce}^m(t)$

- ▶ Step 2-Calculate heat items in equation (4) using the measured furnace temperature

- $q^i_{ht} = f_{ht}(T_{fce}^m(t), \dots)$
- $q^i_{ld} = f_{ld}(T_{fce}^m(t), \dots)$
- $q^i_{loss} = f_{loss}(T_{fce}^m(t), \dots)$
- $q^i_{cl} = f_{cl}(T_{fce}^m(t), \dots)$

► Identify A's by Neural Network calculation

- Initial NN network

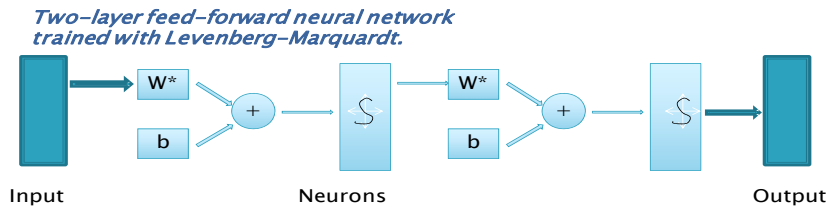


Figure 6.5- Two layer feed forward neural network

- Import $\{ q^i_{ht} \}, \{ q^i_{ld} \}, \{ q^i_{loss} \}, \{ q^i_{cl} \}$ to NN network as input
- Import $T_{fce}^m(t)$ to NN network as target
- Initial weights, and bias(θ, b)
- Calculate NN output, have $T_{fce}^{mm}(t)$
- Calculate least mean square error (LMS)

$$mse = \frac{1}{N} \sum_{t=1}^N e(t)^2 = \frac{1}{N} \sum_{t=1}^N (T_{fce}^m(t) - T_{fce}^{mm}(t))^2 \quad (6)$$

- Adjust weights, and bias using Levenberg-Marquardt algorithm

$$\theta_{t+1} = \theta_t - [J_1^T J_1 + \mu I]^{-1} J_1^T e \quad (7A)$$

$$b_{t+1} = b_t - [J_2^T J_2 + \mu I]^{-1} J_2^T e \quad (7B)$$

where J_1, J_2 is the Jacobian matrix that contains first derivatives of the network errors with respect to the weights and biases, i.e. the matrix of all first-order partial derivatives of a vector-valued function, and e is a vector of network errors (mse).

- Repeat 5, 6, 7 until
- mse is less than the goal
- Reach the max epochs
- Calculate A_s , and output

$$A_s = \{A_1, A_2, A_3, A_4\} = f(\text{weights, bias}) = f(\theta, b) \quad (8)$$

- ▶ Update CHT furnace model with A 's
- ▶ Predict new results

Evaluation model

If all important heat items are included in the furnace model, the energy should be only redistributed between the defined items. Therefore, the constant C in Eq. (5) should be a very small number, which can be ignored, and

$$E(H) = \left(\frac{1}{A_1} \cdot \frac{q_{fce}^i}{q_{ht}^i} + \frac{A_2}{A_1} \cdot \frac{q_{ld}^i}{q_{ht}^i} + \frac{A_3}{A_1} \cdot \frac{q_{loss}^i}{q_{ht}^i} + \frac{A_4}{A_1} \cdot \frac{q_{cl}^i}{q_{ht}^i} \right) \cong 1 \quad (9)$$

and $A_1 \leq \frac{q_{input}^i}{q_{ht}^i}$, q_{input}^i is the connect input .

If neural network generates a large C value, either it's wrong, require a new NN calculation, or it may indicate new energy items required to be identified, and can be add to the furnace model by user defined functions

6.1.2 Case study

A case study was conducted to test the neural network furnace model. The workpiece is made of stainless steel 403, box shape, 6.7 inch long, 2 inch wide, and 5.25 inch in height, the load of workpieces in one fixture is 2 row, 32 columns and 1 layer, total 8 fixtures arrange in, 2 row, 1 column and 4 layers, loaded in the Bodycote-350 electric furnace.

The controller in this furnace had a proprietary algorithm and it was difficult to model the furnace accurately. This was one of the reasons this case was selected to verify the KDD model. Since several experiments were conducted on this same furnace, the data from those experiments helped for the learning process.

As seen in the predicted furnace temperature profile (Fig 6.6) below, the furnace is not heating up as desired, therefore the loads' temperature are not correctly heated up either, especially in the ramp 2. The model was trained using more experimental data and the furnace temperature corrected closer to the actual results.



Figure 6.6 - CHT-bf Temperature prediction with KDD model

To attain this goal, the problem is solved by studying the A's with neural network furnace model, using set points as target, and q items obtained from CHT-bf as inputs, and finally the optimized A's are calculated at different time steps and they were used for correction. The A's value are used in the new prediction, the results are plotted in Fig.6-8. (The thermocouple locations shown in Fig. 6.7) As seen from the figure there is a clear improvement in the furnace temperature prediction when compared with the original CHT-bf model. The furnace temperature profile is predicted more accurately although the controller algorithms are not known.

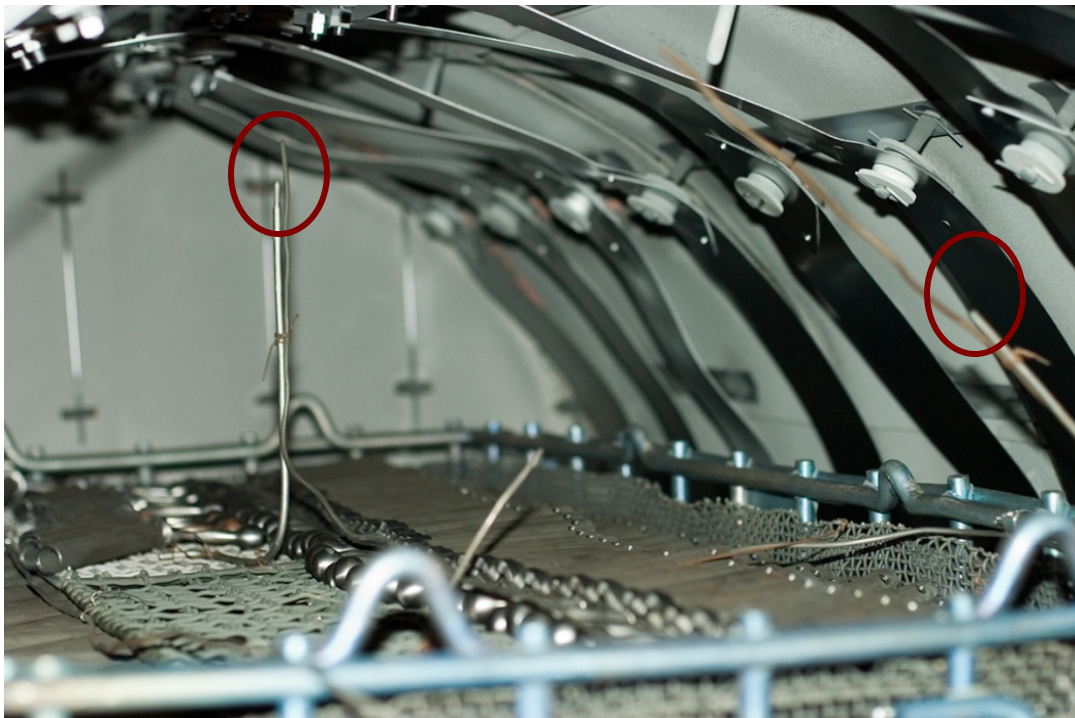


Figure 6.7 - Arrangement of workpieces in the basket and thermocouple placements

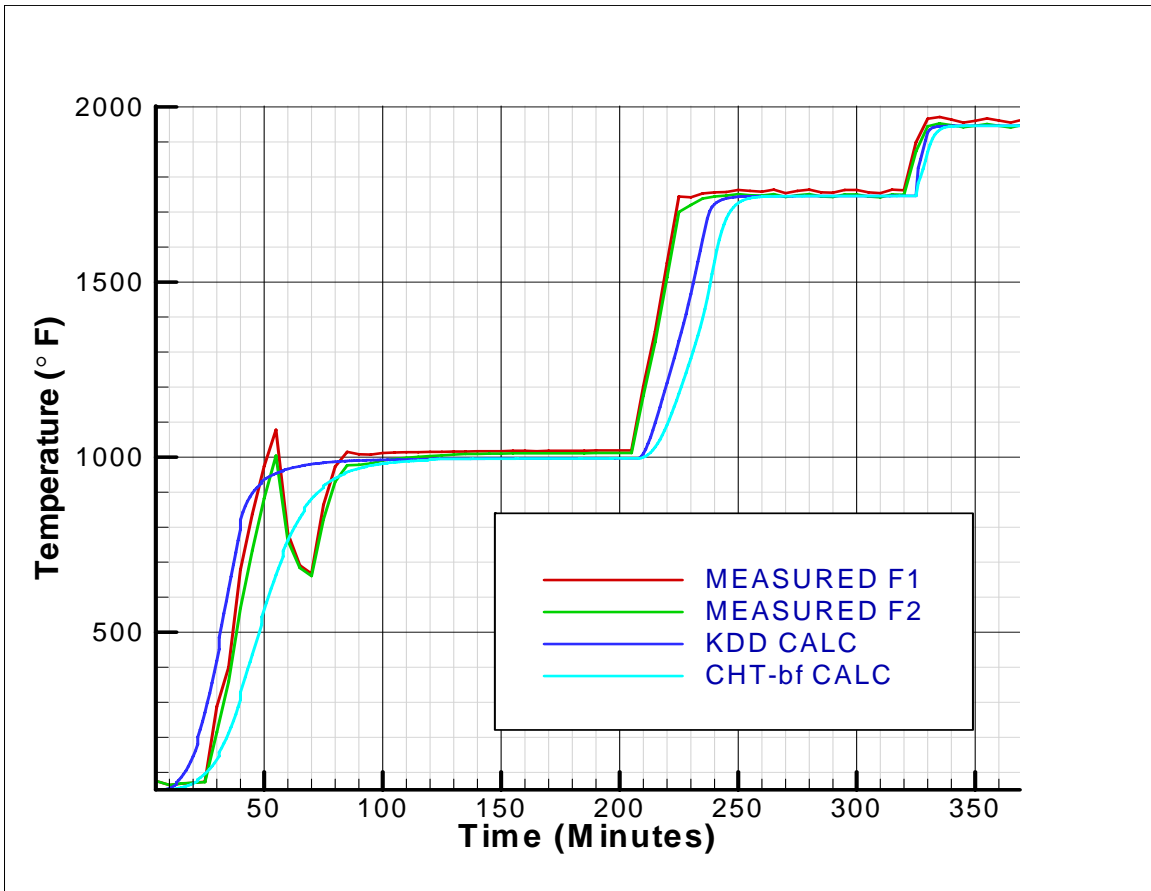


Figure 6.8 - Comparison of CHT-bf & KDD Temperature prediction with measured results

From this case study, the neural network furnace model is proven to improve the furnace temperature prediction. The furnace model can be tuned by the neural network model based on the experimental thermal profiles available for the furnace.

6.2 User defined item

Furnaces are of various types, structures, accessories, equipments etc. Therefore to study a wide variety of furnaces by the CHT technology, it's necessary to allow the user to customize the furnace model. In this project, the user defined function is left open to the customer to specify heat item in the furnace model.

6.2.1 Model description

To allow user defined heat item, Eq. 5 becomes adjustable by introducing new items

$$q_{fce}^i = A_1 \cdot q_{ht}^i - A_2 \cdot q_{ld}^i - A_3 \cdot q_{loss}^i - A_4 \cdot q_{cl}^i + \sum_{k=5}^N A_k \cdot q_{user}^k + C \quad (12)$$

where q_{user} is user defined heat item,

$$q_{user} = f_{user}(p_1, p_2, \dots, p_m, sys_1, sys_2, \dots, sys_n) \quad (13)$$

it's function consist of user parameters p_i , and system parameters, such as time, furnace temperature.

6.3 KDD auto-learning classification model

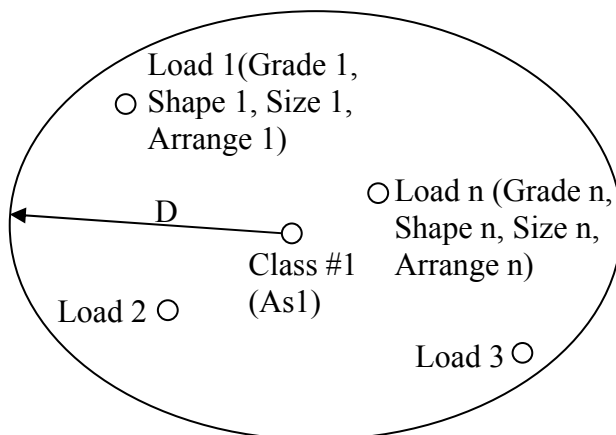
When the original CHT furnace model was built, it mainly considered only the furnace parameters itself, i.e. our maximum furnace knowledge was obtained without running real load. So this model can only used when dealing with different workpieces, load size, and load pattern (arrangement), even the neural network furnace model can be calibrated.

Furnace model should include the effects of load parameters, but it's not easy to reach such a general equation. One possible approach is that

- first calibrate the neural network furnace model to determine the coefficients A's for all kinds of loads,
- then classify these sets of coefficients into different groups by unsupervised classification method,
- finally predict the class label for new production load, and select the coefficients tied to the group and use these values in the neural network furnace model.

In practice, the procedure is ideal to discover the unknown classes from the huge heat treaters accumulated data sets.

6.3.1 Model description



D is the maximum distance range of the group,

$D \geq mse$, and

$$mse(load) = \frac{\sum_{k=1}^N (T_{fuz}^{m,k})^{m,k} - T_c}{N}$$

where $T_{fuz}^{m,k}, T_{fuz}^{nn,k}$ are measured and neural network predicted furnace temperature respectively.

Figure 6.9 - Classification Illustration of loads with same A_s

To accurately distinguish different groups, a class is defined as a group, with different loads in either material type, workpiece geometry, load size, or arrangement pattern, but all the loads can predict the correct furnace temperature by neural furnace model using the same coefficients A_s , see Fig. 6.9.

6.3.2 Unsupervised classification algorithm

The classification algorithm proposed here is a iterative self-organizing scheme, and designed as following steps

- (1) Define the project file for load(1) in CHT-*bf*, calculate heat items by CHT-*bf* for load(1)
- (2) Calculate $As(1)$ by NN_fur for load(1)
- (3) Assign $As(1)$ for the first group, class(1)
- (4) Define the project file for load(*i*) in CHT-*bf*, calculate heat items by CHT-*bf* for load(*i*)
- (5) Calculate furnace temperature using $As(1)$ in the neural network furnace model, and predict the mse

$$\frac{mse(load(i), As(j))}{N} = \frac{\left(\sum_{k=1}^N (T_{firs}^{m,k} - T_{firs})^{m,k^2} \right)}{N} \quad (17)$$

where $As(j)$ belong to class(*j*)

- (6) If mse is less than the maximum distance of class(1), label load(*i*) on class(1)
- (7) If not, search for all the labeled class, repeat (5),(6) until find load(*i*) belonging class,
- (8) If not, load(*i*) belong to the new class, and name the new class
- (9) Search the entire database, until all loads are labeled
- (10) Calculate the final D for each class.

After the first iteration, a new maximum radius is calculated for each class based on the actual load information, instead of the initial calculations. What occurs next depends on the actual load data distributions. Class can be (1) split or (2) merged. After each split or merge,

class means are recalculated and loads are reassigned to the new classes based again on a minimum distance criterion.

6.4 Tuning model and procedure

During production time, furnace walls heat up quicker than the whole load, therefore even after the burners are shutdown for a while, the walls which are still hot like radiator heat the workpieces up. A furnace continues to run for a long time, cyclically heating and cooling down. The wear and tear of furnace walls material will cause a loss of the heating ability, i.e. radiation of the furnace walls. To make up for this loss, the virtual load model proposed in the earlier chapter can be included along with this model to account for this loss.

6.5 Summary & conclusions

The KDD model has remarkable ability to derive meaning from complicated data and can be used to extract patterns and detect trends that are too complex to be modeled by numerical methods or other computer techniques. The KDD based furnace model is developed and validated with an experimental case study. Although a large dataset of experimental data is required for the model to learn, the knowledge is saved in the database and it gets richer and stronger over time.

CHAPTER – 7

Summary

The different models used in the CHT software, Energy balance model, Heat transfer model and Control model was studied and shown how they contribute to accuracy of the furnace and part temperature profiles. Around 53 experiments were conducted at 11 manufacturing locations to compare and analyze the CHT predictions with the measured results in the shop floor. Based on experimental analysis several problems were identified. Some of the problems were solved using knowledge from experimental data. The continuous furnace model was modified to account for the heat loss arising from the door operations. These specific problems like thermal gradients are prevalent only in furnaces with certain burner layouts. Taking the burner location and design into account two methods for predicting the thermal gradients inside the furnace are proposed. One of the methods is also experimentally validated. A new model was developed using the Knowledge Data Discovery technique. The model is expanded with addition of several constants and these constants are calculated using neural network. The neural network is trained based on the experimental data obtained. The model is also validated with a case study. The new KDD model improves the furnace model prediction accuracy especially in situations where it is difficult to use the CHT model to represent the current situation.

Limitations

Some of the limitations of the proposed work in this research are the availability of experimental data. The thermal gradient model is based on experimental data and is not possible to represent the gradients, unless a few experiments are conducted at several locations in the

furnace. In the continuous furnaces its difficult and expensive to conduct such experiments. A datapack device that has a thermally insulated data recorder to withstand high temperatures over the duration of the process (typically several hours) is required to measure the temperature inside the furnace. Also the specifications of the datapack device itself become constraints while conducting experiments. The time allowed for the datapack to stay inside the furnace at a specified temperature has to be considered while designing the experiments. The control model needs to be modified to represent more advanced control techniques used in the industry like adaptive controllers. The heat transfer model inside the load is complex and currently in this research it was not studied.

Future Work

The recommended future work for the project is the incorporation of a load optimization routine. Such a routine enables the furnace utilization and improves furnace efficiency. Also models specifically developed to different processes enable more accurate prediction of thermal profiles and also useful for process optimization. Another recommendation is creating furnace specific models for different kinds of furnaces instead of two general models. For example, a different model for pit furnace, box furnace, vacuum furnace, etc. Another idea is using FEA as a knowledge input to model the process variations once the thermal profile of the load is calculated. This module will be helpful in designing processes accurately.

REFERENCES

1. "Roadmap for Process Heating Technology Priority Research & Development Goals and Near-Term Non-Research Goals To Improve Industrial Process Heating", Industrial Heating Equipment Association, U.S. Department of Energy Office of Industrial Technologies, Capital Surini Group International, Inc., Energetics, Incorporated, March 16, 2001.
2. Improving Process Heating System Performance: A Sourcebook for Industry is a development of the Best Practices initiative under the U.S. Department of Energy (DOE) Industrial Technologies Program (ITP) and the Industrial Heating Equipment Association (IHEA)
3. Heat Treating, ASM Handbook -Volume 4, 1991
4. H. Ramamurthy, S. Ramadhyani, and R. Viskanta, "A Thermal System Model for a Radiant-Tube Continuous Reheating Furnace", Journal of Materials Engineering and Performance, Volume 4(5), 519-531, October 1995
5. K. S. Chapman, S. Ramadhyani, R. Viskanta, "Modeling And Analysis Of Heat Transfer In A Direct-Fired Continuous Reheating Furnace," Heat Transfer In Combustion Systems, 35-44 (1989).
6. "Thermal Imaging Control of Furnace and Combustors" David M. Rue, Serguei Zelepouga - Gas Technology Institute, Final Technical Report for U.S. Department of Energy, GTI Project-61118.
7. D. O. Marlow, "Modeling Direct-Fired Annealing Furnaces For Transient Operations," Appl. Math. Modeling, 20, 35-40 (1996).
8. K. S. Chapman, S. Ramadhyani, "Modeling And Parametric Studies Of Heat Transfer In A Direct-Fired Batch Reheating Furnace," Journal Of Heat Treating, 8(2), 137 -46 (1990).
9. K.S. Chapman, S. Ramadhyani, R. Viskanta, "Modeling And Analysis Of Heat Transfer In A Direct-Fired Continuous Reheating Furnace," Heat Transfer In Combustion Systems, 35-44 (1989).

10. Y. Rong, J. Kang, R. Purushothaman And W. Wang, "Development of An Analytical Tool for Part Load Design and Temperature Control in Continuous Furnaces", Report 03-1 At CHTE Consortium Meeting, May 28-29, 2003.
11. Y. Rong, Q. Lu, J. Kang And R. Vader, "Development Of An Analytical Tool For Workpiece Load Design And Temperature Control Within Loaded Furnace," Center For Heat Treating Excellence Consortium Meeting, Report # 01-1, Worcester, MA., May.18 (2001).
12. Industrial Heating Magazine, June 2007
13. Burner Manual, Eclipse Inc, Rockford, IL
14. Y. Rong, J. Kang, R. Vader And C. Bai, "Enhancement Of Computer-Aided Heat Treating Process Planning System (CAHTPS)", Report 02-1 At CHTE Consortium Meeting, May 29-30, 2002.
15. W. Halliday, "Computer Control Model For Continuous Reheat Furnaces," Metallurgia, 57(10), 412-3 (1990).
16. P.V. Barr, "The Development, Verification, and Application of a Steady-State Thermal Model for the Pusher-Type Reheat Furnace", Metallurgical and Materials transactions b, Volume 26b, August 1995—pp 851-869.
17. W. Halliday, "Computer Control Model For Continuous Reheat Furnaces," Metallurgia, 57(10), 412-3 (1990).
18. D. O. Marlow, "Modeling Direct-Fired Annealing Furnaces For Transient Operations," Appl. Math. Modeling, 20, 35-40 (1996).
19. M.S. Liu, C.K. Choi And C.W. Leung, "Startup Analysis Of Oil-Fired Furnace – The Smoothing Monte Carlo Model Approach," Heat And Mass Transfer, 37, 449-457 (2001).
20. F. R. Steward, P. Cannon, "The Calculation Of Radiative Heat Flux In A Cylindrical Furnace Using The Monte Carlo Method," International Journal Of Heat And Mass Transfer, 14, 245-62 (1971).
21. E. P. Keramida, H. H. Liakos, M. A. Founti, A. G. Boudouvis And N. C. Markatos, "The Discrete Transfer Radiation Model In A Natural Gas-Fired Furnace," International Journal For Numerical Methods In Fluids, 34, 449–62 (2000).

22. H. K. Nandi, M. C. Tomason and M. R. Delhunty, "Software Tool Optimizes Furnace Design and Operation," *Industrial Heating Progress*, Nov. 2002.
23. F. Liu, H. A. Becker, Y. A. Bindar, "Comparative Study Of Radiative Heat Transfer Modeling In Gas-Fired Furnaces Using The Simple Grey Gas And The Weighted-Sum-Of Grey-Gases Models," *Int. J. Of Heat And Mass Transfer*, 41, 3357-71 (1998).
24. Ge Song, Tor Bjørge, Jens Holen And F. Bjørn Magnussen, "Simulation Of Fluid Flow And Gaseous Radiation Heat Transfer In A Natural Gas-Fired Furnace," *Int. J. Of Numerical Methods For Heat & Fluid Flow*, 7(2/3), 169-80 (1997).
25. R. Viskanta, K.S. Chapman, S. Ramadhyani, "Mathematical Modeling Of Heat Transfer In High Temperature Industrial Furnaces," *Proceedings of the First International Conference on Advanced Computational Methods in Heat Transfer*, Jul 17-20 Portsmouth, 117 (1990).
26. M. Gao, C. N. Reid, M. Jahedi And Y. Li, "Estimating Equilibration Times And Heating/Cooling Rates In Heat Treatment Of Parts With Arbitrary Geometry," *Journal Of Materials Engineering And Performance*, 9(1), 62-71 (2000).
27. A. Bejan, *Heat Transfer*, John Wiley & Sons, Inc., New York (1993).
28. Y. Rong, Q. Lu, J. Kang And R. Vader, "Development Of An Analytical Tool For Workpiece Load Design And Temperature Control Within Loaded Furnace," *Center For Heat Treating Excellence Consortium Meeting*, Report # 01-2, Cincinnati, OH., Nov.15 (2001).
29. L. He, J. Kang, T. Huang and Y. Rong, "The Integrated Technique for the Heat Treatment of Aluminum Alloy Castings: a Review", *Heat Treatment of Metals*, Vol. 31, No. 3, 2004, pp. 69-72.
30. J. Kang, Y. Rong, W. Wang, "Numerical simulation of heat transfer in loaded heat treatment furnaces", *Journal of Physics*, Vol. 4, France, No. 120, 2004, pp. 545-553.
31. Q. Lu, R. Vader, J. Kang and Y. Rong, M. Hoetzl, "Development of A Computer-Aided Heat Treatment Planning System", *Heat Treatment of Metals*, March 2002, pp. 65-70

32. R. Purushothaman, J. Kang, L. Zhang, and Y. Rong, "Application of CHT-bf and CHT-cf in Heat Treatment Process Operation Design", ASM Materials Science and Technology Conference and Exhibition, Sep. 25-28, 2005, Pittsburgh, PA
33. J. Kang, T. Huang, Y. Rong, "Modeling and Simulation of Heat Transfer in Loaded Heat Treatment furnace", The Third Sino-Korean Conference on Advanced Manufacturing Technology, Xi'an, China, June 10~13, 2004
34. J. Kang, R. Purushothaman, Y. Rong, "Industrial Applications of CHT-bf and CHT-cf", the 23rd ASM Heat Treating Society Conference and Exposition, September 26-28, 2005 in Pittsburgh, PA.
35. J. Kang, R. Vaidya and Y. Rong, "A Computer Aided Heat Treating Planning System," ASM 22nd Heat Treating Conference & 2nd International Surface Engineering Congress, Indianapolis, IN, September 15-18, 2003
36. J. Kang, Y. Rong and W. Wang, "Numerical Simulation of Heat Transfer In Loaded Heat Treatment Furnaces", 2nd International Conference on Thermal Process Modeling and Computer Simulation, (ICTPMCS), March 31 - April 2, 2003, Nancy, France, pp. 545-553
37. J. Kang and Y. Rong, "Modeling And Simulation of Heat Transfer In Loaded Heat Treatment Furnaces", The 13th International Federation for Heat Treatment and Surface Engineering Congress, Columbus, OH October 7-10, 2002
38. J. Kang, T. Huang, R. Purushothaman, W. Wang, Y. Rong, "Modeling and simulation of heat transfer in loaded continuous heat treatment furnace", Transactions of Materials and Heat Treatment, Vol. 25, No. 5, 2004, pp. 764-768
39. J. Kang, T. Huang, R. Purushothaman, W. Wang, and Y. Rong, "Modeling and Simulation of Heat Transfer in Loaded Continuous Heat Treatment Furnace", 14th International Federation for Heat Treatment and Surface Engineering Congress, Shanghai, China, Oct. 26-28, 2004.
40. J. Kang and Y. Rong, "Modeling And Simulation of Heat Transfer In Loaded Heat Treatment Furnaces", The 13th International Federation for Heat Treatment and Surface Engineering Congress, Columbus, OH October 7-10, 2002

41. Y. Rong, Q. Lu, J. Kang And R. Vader, "Development Of An Analytical Tool For Workpiece Load Design And Temperature Control Within Loaded Furnace," Center For Heat Treating Excellence Consortium Meeting, Report # 00-1 (2000).
42. Y. Rong, Q. Lu, J. Kang And R. Vader, "Development Of An Analytical Tool For Workpiece Load Design And Temperature Control Within Loaded Furnace," Center For Heat Treating Excellence Consortium Meeting, Report # 00-2 (2000).
43. Y. Rong, Q. Lu, J. Kang And R. Vader, "Development Of An Analytical Tool For Workpiece Load Design And Temperature Control Within Loaded Furnace," Center For Heat Treating Excellence Consortium Meeting, Report # 01-2, Cincinnati, OH.,Nov.15 (2001).
44. Y. Rong, J. Kang, R. Vader And C. Bai, "Enhancement Of Computer-Aided Heat Treating Process Planning System (CAHTPS)", Report 02-2 At CHTE Consortium Meeting, Nov. 13-14, 2002.
45. Y. Rong, J. Kang, R. Purushothaman, W. Wang, and W Hu, "Development of An Analytical Tool for Part Load Design and Temperature Control in Continuous Furnaces", Report 03-1 At CHTE Consortium Meeting, Nov 14-15, 2003.
46. Y. Rong, J. Kang, L. Zhang, R. Purushothaman, and A. Singh, "Development of Computer Aided Heat Treatment Planning System for Quenching and Tempering (CHT-q/t)", Report 05-01 at CHTE consortium meeting, May 2005.
47. Vader, Ranjeet D, "Development of Computer Aided Heat Treatment Planning System (CAHTPS)" Masters. Thesis, Department of Manufacturing Engineering, Worcester Polytechnic Institute, 2002-06
48. Vaidya, Rohit Subhash, "Experimental Testing of a Computer Aided Heat Treatment Planning System" Masters. Thesis, Department of Mechanical Engineering, Worcester Polytechnic Institute, 2003-08
49. Singh, Amarjit Kumar, Development of Computer Aided Heat Treatment Planning System for Quenching & Tempering (CHT – q/t) and Industrial Application of CHT-bf & CHT-cf Masters. Thesis, Department of Mechanical Engineering, Worcester Polytechnic Institute, 2006-05

50. National Productivity Council of India - National Certificate Examination for Energy Managers and Energy Auditors, Guide Book 2 "Energy Efficiency in Thermal Utilities"
51. Industrial Technologies Program E-Bulletin - DOE Energy Technology Solutions, US DOE, EERE, June 2006
52. Ben Krose and Patrick van der Smagt, Introduction to Neural Networks, The University of Amsterdam, Eighth edition, November 1996.
53. Singer, A. (1990). Implementations of Artificial Neural Networks on the Connection Machine (Tech. Rep. Nos. RL90-2). Cambridge, MA: Thinking Machines Corporation.
54. Widrow, B., Winter, R. G., & Baxter, R. A. (1988). Layered neural nets for pattern recognition. IEEE Transactions on Acoustics, Speech, and Signal Processing, 36(7), 1109-1117.

Appendix - A

List of Case Studies

Table A.1. *List of case studies in different furnaces and locations*

Furnace Type	Company	Location	Number of experiments
Continuous Furnaces	American Heat Treating	Monroe, CT	4
	Bodycote	Waterbury, CT	6
		Worcester, MA	1
	Caterpillar	Peoria, IL	13
			(24)
Vacuum Furnace	Bodycote	Worcester, MA	4
	Bodycote	South Windsor, CT	2
	Bodycote	Wisconsin	2
	Sousa Corporation	CT	1
	American Heat Treating	Monroe, CT	5
			(14)
Batch Furnace	Bodycote	Worcester, MA	12
	American Heat Treating	Monroe, CT	1
	Surface Combustion	Maumee, OH	1
	Queen city steel	Cincinnati, OH	1
			(15)
Total			53

CONTINUOUS FURNACES

The case studies for continuous furnace were done at three companies – American Heat Treating, Bodycote and Caterpillar. This section presents all the case studies grouped by company. The table below lists all the case studies that were done for continuous furnaces.

S. No.	Company	Workpiece	Furnace type
A1-1	Bodycote Thermal Processing, Waterbury, Connecticut	Seahorse	Mesh belt Furnace
A1-2		Clamp	Mesh belt Furnace
A1-3		PEG	Mesh belt Furnace
A1-4		XHD005 Screw	Mesh belt Furnace
A1-5		14004 Standard Screw	Mesh belt Furnace
A1-6		XHD005 screw	Mesh belt Furnace
A1-7	Bodycote Thermal Processing, Worcester, Massachusetts	Cylinder	Mesh belt Furnace
A1-8	American Heat Treating Inc. Monroe, Connecticut	Plate	Shaker Furnace
A1-9		Disc	Shaker Furnace
A1-10		Precision	Shaker Furnace
A1-11		Box type plate	Shaker Furnace
A1-12 A1-24	Caterpillar, Peoria, Illinois	Several studies	Pusher Furnace

VACUUM FURNACES

The case studies for vacuum furnace were done at three companies – American Heat Treating, Bodycote and Sousa Corporation. This section presents all the case studies grouped by company. The table below lists all the case studies that were done for vacuum furnaces.

S. No.	Company	Workpiece	Furnace type
A2-1	American Heat Treating Inc. Monroe, Connecticut	Handle	VFS Vacuum Furnace
A2-2		Blade	Vacuum furnace
A2-3		Standard	Vacuum furnace
A2-4		Geared Shaft	Vacuum furnace
A2-5		Geared Shaft II	Vacuum furnace
A2-6	Sousa Corporation, CT	4340 Plates & 4340 block	Bar Pressure Quench furnace
A2-7	Bodycote Thermal Processing,	Cylinder	Abar-Ipsen Turbo Treater

	Wisconsin		
A2-8	Bodycote Thermal Processing, Worcester, Massachusetts	SS-bar	Abar Vacuum Furnace
A2-9		Marver machine part, 243348	Vacuum furnace, 438
A2-10		Bourdon Forge Company part	Vacuum furnace, 438
A2-11		Blade	Abar Vacuum Furnace
A2-12	Bodycote Thermal Processing, Wisconsin		Ipsen Furnace
A2-13	Bodycote Thermal Processing, South Windsor, Connecticut	Robot	Abar Vacuum Furnace
A2-14		ST-11	Abar Vacuum Furnace

BATCH FURNACES

The case studies for batch furnace were done at four companies – American Heat Treating, Bodycote, Surface Combustion and Queen City Steel Treating. This section presents all the case studies grouped by company. The table below lists all the case studies that were done for batch furnaces.

S. No.	Company	Workpiece	Furnace type
A3-1	American Heat Treating Inc. Monroe, Connecticut	Diesel Tech	T3 Furnace
A3-2	Bodycote Thermal Processing, Worcester, Massachusetts		Pit Furnace
A3-3		Casco	Lindure Furnace
A3-4		R. H. Handles	Pit Furnace
A3-5		Numa part	Pit Furnace
A3-6		Hitchiner part no. 87296 & 87292	Pit Furnace
A3-7		Hitchiner part - 87191	Allcase Furnace
A3-8		Hitchiner part	Allcase Furnace
A3-9		Hitchiner part - 4140	Allcase Furnace
A3-10		Hitchiner 87056, Shift Lever	Allcase Furnace
A3-11		Hitchiner 243860	Allcase Furnace
A3-12		Rack	Temper, 466
A3-13		Washer	Lindure Furnace
A3-14	Surface Combustion Inc., Toledo, Ohio	Alumina Rods and metal chips	Allcase Furnace
A3-15	Queen City Steel Treating Company, Cincinnati, OH	Flat Ring	Box type HFC36-34-38 Furnace

